STELLAR DISTRIBUTIONS AT HIGH GALACTIC LATITUDES

by

Julian J. Schreur

A Dissertation Submitted to the Faculty of the

DEPARTMENT OF ASTRONOMY

In Partial Fulfillment of the Requirements
For the Degree of

DOCTOR OF PHILOSOPHY

In the Graduate College

THE UNIVERSITY OF ARIZONA

1 9 7 1

THE UNIVERSITY OF ARIZONA

GRADUATE COLLEGE

I hereby recommend that this dissertation prepared under my direction by Julian Jay Schreur

entitled Stellar Distributions at High Galactic Latitudes

be accepted as fulfilling the dissertation requirement of the degree of Doctor of Philosophy

Bart J. Bok — Dissertation Director — 19 Oct 1970 — Date

After inspection of the final copy of the dissertation, the following members of the Final Examination Committee concur in its approval and recommend its acceptance:*

David L. Crawford	19 October 1970
Raymond G. Wilson	19 October 1970
Bart J. Bok	19 Oct 1970
William G. Tifft	Oct 19, 1970
Bruce J. Lyons	Oct 19, 1970

*This approval and acceptance is contingent on the candidate's adequate performance and defense of this dissertation at the final oral examination. The inclusion of this sheet bound into the library copy of the dissertation is evidence of satisfactory performance at the final examination.

STATEMENT BY AUTHOR

This dissertation has been submitted in partial fulfillment of requirements for an advanced degree at The University of Arizona and is deposited in the University Library to be made available to borrowers under rules of the Library.

Brief quotations from this dissertation are allowable without special permission, provided that accurate acknowledgment of source is made. Requests for permission for extended quotation from or reproduction of this manuscript in whole or in part may be granted by the head of the major department or the Dean of the Graduate College when in his judgment the proposed use of the material is in the interests of scholarship. In all other instances, however, permission must be obtained from the author.

SIGNED: Julian J. Hebrew

ACKNOWLEDGMENTS

This work has been carried out under the direction of Dr. B. J. Bok, who originally proposed the subject. Dr. Bok's strong and diligent guidance, his frequent and helpful suggestions, his support, and his enthusiasm for this study are greatly appreciated. Thanks go to Dr. B. T. Lynds, Dr. D. L. Crawford, Dr. W. G. Tifft, and Dr. R. E. White for their many helpful suggestions and their willing assistance. Thanks are due, also, to Dr. A. F. Aveni for his assistance in the preparation of this manuscript.

Extensive use was made of the facilities of the Kitt Peak National Observatory. The assistance given, and the many kindnesses shown, by the staff of the Kitt Peak National Observatory are greatfully acknowledged.

The photoelectric and photographic data were reduced with the aid of the CDC 6400 computer of the Numerical Analysis Laboratory of The University of Arizona. Thanks go to Dr. W. S. Fitch for his assistance in altering the photoelectric reduction program originally written by him.

To my wife, Barbara, is owed the greatest debt of gratitude. Her patience, her moral support, her assistance, and willingness to sacrifice have made the past years most enjoyable.

TABLE OF CONTENTS

TABLE OF CONTENTS (Continued)

TABLE OF CONTENTS (Continued)

LIST OF TABLES

LIST OF TABLES (Continued)

LIST OF ILLUSTRATIONS

LIST OF ILLUSTRATIONS (Continued)

LIST OF ILLUSTRATIONS (Continued)

ABSTRACT

A system of four-color photographic photometry is presented which is very similar to the Strömgren photoelectric four-color (uvby) system. The small difference between the two systems is due to a less than ideal match of the photographic violet filter to the photoelectric violet filter. The photographic four-color system is described in detail, and the transformation between the photographic and photoelectric four-color systems is given.

The photographic four-color system is applied to a study of the stellar distributions in Selected Areas 56 ($l = 199^{o}$, $b = 79^{o}$), and 27 ($l = 175^{o}$, $b = 28^{o}$). It is found to be a significant improvement over the three-color (RGU) system, because the addition of the fourth color has made it possible to discriminate between giants and dwarfs of spectral types F, G and K. The four-color indices are used to separate the stars in each of the two survey fields into four groups; the halo giants and dwarfs, and the disk giants and dwarfs. Space densities at various distances from the sun are computed for each group.

The density gradient of the halo giants in SA 56 is found to be very similar to the r^{-3} density gradient

exhibited by the RR Lyrae variables near the north galactic pole. The space densities of the halo giants are found to be approximately 100 times those of the halo component of the RR Lyrae variables.

The space densities at a given z-distance in the direction of SA 27 are found to be 0.7 times those at the same z-distance in SA 56. This result has been obtained directly from the star counts by the use of the Oort-Vashakidse method of computing relative space densities, and also by the use of a modified Oort-Vashakidse method. The same result is obtained from a density analysis based on the four-color photometry.

The ratio of space densities found at a given z-distance in the two fields, when coupled with the r^{-3} density gradient found for SA 56, leads to the conclusion that the surfaces of equal space density are inclined to the galactic plane by five degrees, in the sense that the equidensity surfaces approach the galactic plane in the direction of the galactic anticenter.

CHAPTER I

INTRODUCTION

There are several reasons why a study of stellar distributions in regions of intermediate and high galactic latitude is of interest. A knowledge of stellar number densities at various distances from the galactic plane is necessary for the determination of the component of the galactic gravitational force in the direction perpendicular to the galactic plane. A determination of isodensity contours far from the galactic plane yields information about the general galactic force field and, therefore, about the distribution of matter throughout the galaxy. Finally, our knowledge of the distribution of stellar types in the galactic halo as well as the extent of the galactic halo is still incomplete.

In the past, a number of surveys of high latitude regions have been made utilizing several different techniques. This study applies the method of multicolor photographic photometry to a determination of the density distributions of various types of stars at high galactic latitudes, to a faint limiting magnitude. The photographic system, which was developed as a part of this study, mimics

very closely the four-color (uvby) system of photoelectric photometry as described by Strömgren (1963a).

The Value of High Latitude Surveys

Kinematical Mass Densities and the K_z Force Law

The detailed derivation of the equations presented in this section are to be found in Appendix I. The equation numbers in this chapter are those of Appendix I.

Two relationships can be found between the gravitational force perpendicular to the galactic plane and the distribution of matter near the galactic plane (Oort 1932). The first, generally known as the "hydrodynamical equation", is usually written in the form

$$\frac{\partial(\overline{Z^2}\Delta(z))}{\partial z} = \Delta(z)K_z \ , \qquad (6)$$

where z is the perpendicular distance from the galactic plane with north taken as positive, $\Delta(z)$ is the number density of an identifiable class of stars, $\overline{Z^2}$ is the average of the squares of the velocities in the z-direction for that class of stars, and K_z is the gravitational acceleration in the z-direction. In addition to the hydrodynamical equation, Poisson's equation must also be satisfied. When dealing with the K_z force law, Poisson's equation is usually written in the form

$$\frac{\partial K_z}{\partial z} = -4\pi\ G\ \rho(z)\ , \qquad (19)$$

where $\rho(z)$ refers to the total mass density at distance z.

If observations of the velocity dispersion in the z-direction, and of the stellar number density, are available for an identifiable class of stars, both in the galactic plane and at various distances from the galactic plane, the dependence of the K_z force on varying z can be determined. From the slope of the force law, $\frac{\partial K_z}{\partial z}$, evaluated in the galactic plane, the total mass density in the galactic plane, ρ_o, can be determined. This mass density is generally referred to as the "kinematical mass density".

In dealing with the hydrodynamical equation, it can be shown (Oort 1932) that if the distribution of Z-velocities at the galactic plane for a specific class of stars is Gaussian, then the velocity dispersion will be independent of z. This allows a simplification of the hydrodynamical equation to the form

$$K_z = \overline{Z^2}\ \frac{\partial(\ln\Delta(z))}{\partial z}\ , \qquad (18)$$

where $\overline{Z^2}$ can now be determined for stars in the galactic plane. The problem of determining the K_z force law then is reduced to the determination of $\overline{Z^2}$ for nearby bright stars and the determination of $\Delta(z)$ by means of star counts near the galactic pole.

It is also interesting to note that in the case of a Gaussian velocity distribution, the hydrodynamical equation integrates to yield the expression

$$\Delta(z) = \Delta_o \quad \exp \quad \left(\frac{1}{\overline{z_o^2}} \int_0^z K_z dz\right) , \qquad (16)$$

where Δ_o and $\overline{z_o^2}$ refer to the values in the galactic plane. If the Z-velocities of a class of stars can be represented by two or more Gaussian distributions, each with its own Z-velocity dispersion, the number density of the higher velocity subclass will decrease less rapidly than the number density of lower velocity subclass with increasing z, and this will result in a $\overline{z^2}$ which increases with z.

Thus, a determination of K_z and ρ_o requires either the selection of one homogeneous group of stars, that is one group of stars having similar age and physical parameters and therefore most likely belonging to one kinematical class, or the determination of the variation of $\overline{z^2}$ with z for the inhomogeneous but identifiable group of stars studied.

In the past, several approaches to the determination of K_z have been considered. The first reliable determination of K_z was that of Oort (1932). In his study, using stars of all spectral types, the density distribution $\Delta(z)$ was computed for four intervals of absolute visual magnitude. The radial velocities of stars observed near

the North Galactic Pole were used to determine the velocity distribution for each spectral type in his study. Oort found the values of $\overline{Z^2}$ for each absolute magnitude interval by combining the assumed Gaussian velocity distributions of each spectral type within the luminosity range, weighted by the relative density of that type in the galactic plane. The K_Z force law found by Oort, along with other determinations, is shown in Figure 1.

More recently other investigators have restricted themselves to using either the giant stars or early-type main-sequence stars. Such stars are ideal for studies of the K_Z force law because they are intrinsically bright, and therefore easily identifiable at distances up to one kiloparsec. Also their intrinsic luminosities are known, permitting an accurate determination of $\Delta(z)$. Moreover, they exist in great enough numbers to allow the solutions to be statistically meaningful.

Hill (1960) made counts of the stars classified in the Henry Draper Catalogue and the Bergedorfer Spectral-Durchmusterung as K giants. He used proper motion data to separate the main-sequence (dwarf) stars from the giant stars. The Z-velocities were determined both from the space motions of nearby stars, and from the radial velocities of faint stars at the galactic poles. The velocity distribution in the galactic plane was represented as the sum of

three Gaussian components, a strong line, a weak line, and a high velocity component. The variation of $\overline{Z^2}$ with z was computed from the assumed ratio of the densities of the three components.

The results of Hill's study showed a maximum value for K_z of 6×10^{-9} cm/sec^2 at a z distance of 400 pc, with a decrease to half that value for z > 1 kpc. Hill shows this result to be incompatible with Poisson's equation and any reasonable assumptions about mass distributions in the Galaxy, and for this reason he accepts the determination of K_z only to 500 pc. Oort (1960) showed that a K_z force law constructed from reasonable estimates of the distribution of mass in the Galaxy with the aid of Poisson's law was in full agreement with counts of K giant stars. In particular, Oort points out that the inclusion of a halo component of K giants, with a velocity dispersion much greater than that of Hill's high-velocity component, and with a density low enough that the Z-velocity distribution in the galactic plane would be virtually unaffected, would completely remove the discrepancy found by Hill. A more recent determination of the force law by Yasuda (1961) is quite similar to Oort's.

Perry (1969a) made an attempt to determine K_z from the density and velocity distributions of the A stars. The Z-motions in the galactic plane were determined from the

space velocities of nearby stars and the Z-velocities at various heights above the galactic plane were determined from radial velocities of stars near the north galactic pole. In this study, the space density and the velocity dispersion were determined for the same stars, thereby eliminating the possibility that the two sets of data might apply to different stellar groups, and thus be incompatible. Although Perry's analysis allowed for the variation of $\overline{Z^2}$ with z, his determination of K_z was found to violate Poisson's law, having a sharp maximum at z=250 pc. Perry concluded that the difficulty was probably due to the space distributions of the A stars, either because the system was not well enough mixed to allow a steady state treatment, or because there was a mixture of two populations of A stars at high galactic latitudes.

Turon (1968), also working with the K giants, applied a method suggested by King (1965) to a determination of K_z. Where the usual form of the hydrodynamical equation is formed by multiplying the equation of continuity by Z and integrating over all velocity space, King showed that if the continuity equation is multiplied instead by $\frac{1}{Z}$ and then integrated over all velocity space, the hydrodynamical equation takes the form

$$K_z \, \overline{Z^{-2}} = \frac{\partial(\ln \Delta(z))}{\partial z} \, ,$$

with

$$\overline{Z^{-2}} = -\frac{1}{\Delta(x,y,z)} \int_{-\infty}^{\infty}\int\int \frac{1}{Z} \frac{\partial f(x,y,z,X,Y,Z)}{\partial Z}\, dX\, dY\, dZ$$

where (x, y, z) are space coordinates, (X, Y, Z) are the corresponding velocities, f(x,y,z,X,Y,Z) is the distribution in phase space, and $\Delta(x,y,z)$ is the density in coordinate space.

Turon determined $\overline{Z^{-2}}$ numerically from histograms of the K giant velocities, and using Hill's density data arrived at a solution for K_Z very similar to that of Perry. Turon suggested that the difficulty may be due to the inhomogeneity of the sample of stars studied or to the system not being in a well mixed state.

Several determinations of K_Z are shown in Figure 1. Their variety demonstrates that the K_Z force law can not yet be considered well determined beyond a distance of a few hundred parsecs from the galactic plane.

As mentioned before, a solution for K_Z near the galactic plane allows a determination of the total mass density in the solar neighborhood, ρ_o. It is interesting to compare these kinematically determined values of ρ_o, listed in Table I, with estimates of the density of observable material found in the solar neighborhood. Luyten (1968) gives 0.064 $M_\odot/pc^3$ as the density of the luminous objects and Blaauw (1965) gives 0.025 $M_\odot/pc^3$ as the density

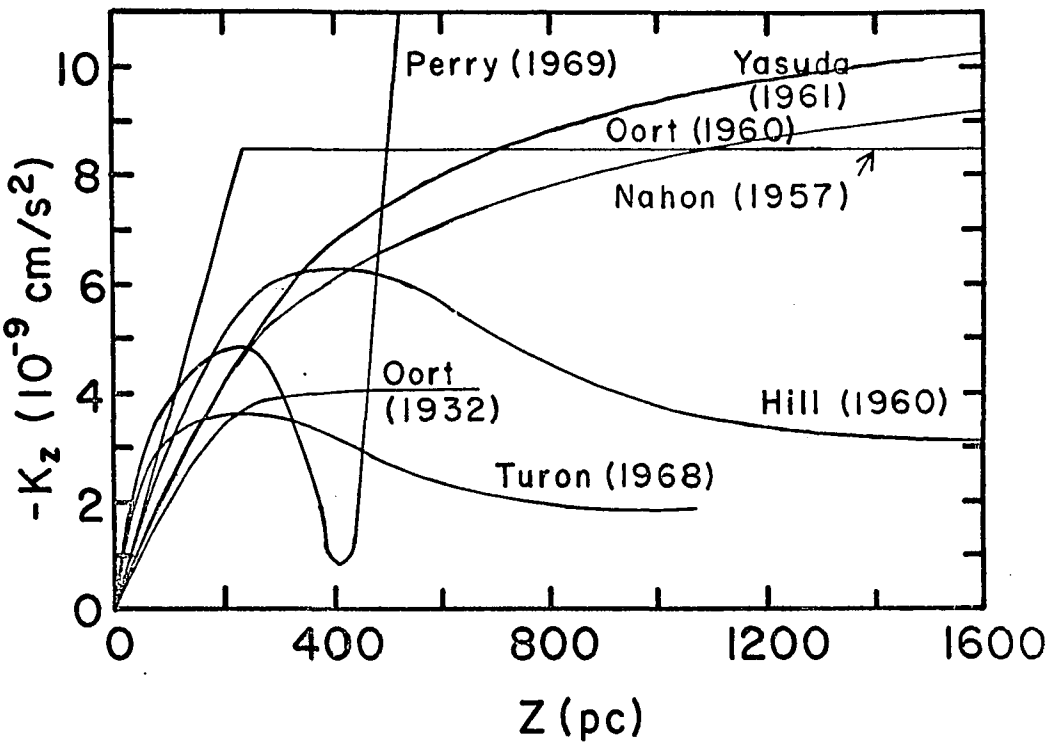

Figure 1. Several determinations of the galactic K_Z force law.

Table I. Determinations of ρ_o.

	ρ_o ($M_\odot/pc^3$)
Kinematical density	
Nahon	0.23
Woolley (1957)	0.18
Oort (1960)	0.15
Hill (1960)	0.13
Yasuda (1961)	0.15
Jones (1962)	0.14
Stothers and Tech (1963)	0.13
Woolley and Stewart (1967)	0.11
Turon (1968)	0.13
Density of Observable Material	0.09
(With Weidemann's W.D. density)	0.11

of the interstellar material, resulting in a total mass density of 0.089 $M_\odot/pc^3$. Weidemann (1967) would increase the density of white dwarfs by as much as 0.020 $M_\odot/pc^3$, thereby bringing the observed density to as much as 0.11 $M_\odot/pc^3$.

Some of the earlier kinematical determinations of ρ_o, coupled with the lower estimate of the observed mass density, prompted discussion about an "unseen" component of the local material. The more recent kinematical mass densities, along with Wiedeman's greater white dwarf density, would bring these values into close agreement. It is apparent, however, that some doubt remains not only

as to the best value for the kinematical mass density but also about the general nature of the K_z force law for $z > 500$ pc. Perhaps much of this doubt could be removed by the study of a truly homogeneous sample of stars, or by a careful treatment of an inhomogeneous sample when all constituent kinematical groups are positively identified.

The General Galactic Force Field

At distances greater than 1 kpc from the galactic plane, the total mass distribution in the galaxy, not just the mass density in the galactic plane, begins to play an important role in influencing the motions of stars. Galactic models such as Schmidt's (1956) can be used to compute the expected K_z force law to large z distances. These theoretical force laws can be used as a check on the models through a comparison with observationally determined K_z force laws. Two such observational determinations, extending to $z \approx 10$ kpc, were made by Oort and van Woerkom (1941) and by Parenago (1952), with both studies using a sample of RR Lyrae-type variable stars.

Both of the above observational determinations of K_z assumed that the RR Lyrae variables form one homogeneous group of stars. White (1967) has shown, however, that the RR Lyrae stars, when separated into two groups according to metal content, show different spatial distributions,

one a highly flattened spheroid and the other more spherical. According to White the group with the lower metal content, the more spherically distributed group, has a density four times lower than the other group in the galactic plane, yet it dominates the sample of RR Lyrae variables encountered beyond z = 2 kpc. One would expect a distinct change in $\overline{Z^2}$ as z approaches 2 kpc, and this was not allowed for in the determinations of K_Z.

A solution for K_Z is not the only check one has on a variety of galactic models. Homogeneous groups of stars which are well mixed and in a steady state will be distributed so that surfaces of equal number density are surfaces of equal gravitational potential. The configuration of these equidensity surfaces can be determined from star counts made at several galactic latitudes. The observed equidensity surfaces can then be compared with the equipotential surfaces predicted by a galactic model. The difficulty with this approach is the selection of a homogeneous group of stars at distances from 1 to 10 kpc. While RR Lyrae variables can be used, it would be preferable to isolate a more numerous group of stars.

The Galactic Halo

The stars in the galactic halo are among the oldest objects in the Galaxy (Blaauw 1965). They are generally considered to have formed during the Galaxy's initial

stages of evolution (Eggen, Lynden-Bell, and Sandage 1962). A study of the space distribution of the halo objects could tell much about star formation during the early history of the Galaxy, particularly if the study yielded information about the correlation of the average stellar metal content and the distribution of spectral types with the position in the galactic halo.

The metal-weak globular star clusters, and the metal-weak RR Lyrae-type variable stars are considered to be excellent tracers of the halo distribution because they are bright and easily recognizable. The globular clusters show the Galaxy to be very large. King (unpublished) claims that two clusters, which are nearly 100 kpc from the galactic center, have radii which appear to be tidally limited, as if the clusters were once within 20 kpc of the galactic center. A perigalacticon of 20 kpc indicates that the clusters are in orbit about the galactic center, and therefore belong to the Galaxy.

The system of globular clusters is roughly spherical, and it is centered on the galactic center. There is a marked concentration of clusters toward the galactic center with those clusters near the center showing higher average metal content than those farther out in the halo (Arp 1965).

Kinman, Wirtanen and Janes (1966) studied the distribution of the RR Lyrae stars in the direction of the north galactic pole. Their results show the density varies roughly as the inverse cube of the distance from the galactic center. The faint limit of this study was reached at a distance of about 20 kpc, and presumably a fainter limit would have resulted in stars being found at still greater distances.

The distribution of RR Lyrae stars is similar to the distribution found by Fenkart (1967) for the common stars in Selected Area 57, a field near the north galactic pole. Fenkart's work is a part of a larger program of mapping the distribution of common stars in the galactic halo (Becker 1965). In Selected Area 51, a field near the galactic anticenter, Becker (1967) has extended this study to $m_V = 21$, and reaches a distance of 35 kpc. He finds that the densities drop off somewhat slower than the inverse cube shown by the RR Lyrae variables. It can be said that the common stars of the halo, like the globular clusters, extend over a very large volume of space.

Although the majority of the halo objects have spectral types GO and later, a great deal of attention has recently been directed toward bluer objects which have been found at high latitudes. Finding lists of such objects by Feige (1958), Luyten, Anderson, and Sandage

(1967), Humason and Zwicky (1947), Haro and Luyten (1962), Iriarte and Chavira (1957), Slettebak and Stock (1959) and others have produced numerous objects which have merited further investigation.

Photoelectric and spectroscopic studies of a number of high latitude blue stars by Graham (1966), Kinman (1965), Philip (1968, 1969a,b), Slettebak, Bahner and Stock (1961), and Slettebak, Wright and Graham (1968) show most of the stars brighter than V = 11 to be normal young stars. Between V = 11 and V = 14, the majority are similar to stars which fall on the horizontal branch of the color-magnitude diagram of a globular cluster. Fainter than V = 14, the white dwarfs are prevalent. In addition, when the stars were selected on the basis of a negative U-B color-index alone, many of the objects proved to be type F and G subdwarfs. For V > 14 Sandage and Luyten (1969) have found that although the white dwarfs are the major constituent up to 25% of the objects may be quasi-stellar galaxies.

Although a picture of the galactic halo has emerged as a roughly spheroidal distribution of stars which has a diameter several times greater than that of the galactic disk, a number of questions remain either unanswered or only tentatively answered. Is the luminosity function the same throughout the halo? Does the metal content of the

stars change with distance from the galactic center? Does the blue end of the horizontal branch become more pronounced in any particular region of the halo? A deep survey of stellar distributions in several directions at high galactic latitudes, in a system which distinguishes between stars of different temperature, luminosity, and metal content, would provide answers to these questions.

Methods of High Latitude Survey Work

In a study of stellar distributions a systematic plan must be followed whereby all stars in certain directions are counted. Unless the sample of stars is complete, or unless a correction for incompleteness can be made effectively, a meaningful determination of the space distribution is not possible. On the other hand, a complete survey of the entire sky is not possible, therefore some plan restricting the regions to be studied must be followed. One such plan is Kapteyn's Plan of Selected Areas (e.g., Blaauw and Elvius 1965), and much of the work on stellar distributions is done in these Selected Areas.

Many authors have contributed to our knowledge of stellar distributions at intermediate and high galactic latitudes, and the results of their work have been summarized by Elvius (1965). A few studies are singled out here to present the overall picture of high latitude

distributions, and to demonstrate the different methods by which a high latitude survey may be carried out.

Monochromatic Star Counts

The most complete survey to date was performed by Oort (1938). He based his survey on monochromatic star counts made in all Selected Areas with a galactic latitude north of $+15^{\circ}$ or south of -15°.

Values of log A(m) were determined for each Selected Area, where A(m) is the number of stars with photographic magnitudes between $m-\frac{1}{2}$ and $m+\frac{1}{2}$. The values of log A(m) for latitudes other than 90° were compared with those at the galactic pole, and the relative densities at given z-distances were found. The determination of the relative densities was based on geometrical considerations alone, and was independent of any assumed luminosity function or density distribution at the pole. A geometrical treatment was necessary because the luminosity function at large z-distances was unknown, and the monochromatic magnitudes provided no information about the spectral types of stars being counted.

The general picture which emerged was one in which surfaces of equal star density for $z \geq 800$ pc were inclined 10° with respect to the galactic plane, corresponding to an increasing stellar number density in the direction of the galactic center.

Oort found that within 800 pc the densities for a particular z-distance were lower in the direction of the galactic pole than at other latitudes. This indicates that the sun is in an area of relatively low density which persists up to z = 800 pc. The general picture of the stellar density distribution has remained basically unchanged since Oort's initial survey.

Objective Prism Schmidt Surveys

Another classic type of high latitude survey makes use of objective prism spectra from Schmidt telescopes. Limiting magnitudes of surveys of this type are generally near V = 13, implying that the limits in distance are reached near 1 kpc.

The objective prism spectra are classified according to spectral type and, where possible, according to luminosity. Usually if a luminosity classification is not possible, reasonable assumptions are made about the ratio of giants to dwarfs in each apparent magnitude range for a given spectral type. The apparent magnitudes can be obtained from direct plates, or from the photographic density of the spectra on the objective prism plates. In this manner, it is possible to determine star counts, A(m), for stars of a given luminosity and spectral type. Since the luminosity is known, the distance for a given

apparent magnitude is also known, and thus it is a simple matter to convert the star counts into a density distribution.

A recent survey of this type was made by Upgren (1963). The principal features found by Upgren are that for the main sequence stars the earliest spectral types not only have lowest density in the galactic plane, but also have the sharpest fall off in density away from the galactic plane, and that the giant stars in general show a less steep density gradient than do the main-sequence A stars.

The differences in the density gradients result in changes in the general luminosity function at different heights above the galactic plane. The depletion of the bright main-sequence stars causes a distinct dip in the general luminosity function at $M_V \approx 3$ at heights of a few hundred parsecs. In fact, the general luminosity function at z = 400 pc closely resembles the luminosity function of the globular cluster M3. It is apparent that already at z = 400 pc a very old group of stars is encountered.

Multi-color Photographic Surveys

There are certain advantages that surveys of star fields based on direct photographic plates have over surveys based on objective prism spectra. With a given

telescope, the limiting magnitude on plates is significantly fainter with direct photography than with objective prism techniques. In crowded fields many overlapping spectra of faint stars appear on objective prism plates. Also the light from the star is spread out in wavelength and in the trail across dispersion. Moreover, because of practical difficulties in the manufacture and support of large lenses and prisms, objective prism spectroscopy is generally limited to telescopes of modest aperture, while direct photography with filters is possible with the largest telescopes. Thus, while the limit for most objective prism surveys is near V = 13, direct photographic surveys have been accomplished to V $\approx$ 21. This represents a gain of a factor of 40 in the distance which can be reached.

With a single direct plate, however, one may obtain only the apparent magnitude of a star, while with the spectroscopic technique one may determine the temperature and, to some extent, the intrinsic luminosity of a star. This advantage of the spectroscopic technique can be approached in direct photography by the addition of other magnitudes in different wavelength regions. Each additional magnitude allows one more physical stellar parameter to be determined.

A two-color survey using blue (B) and visual (V) plates was performed by Bok and Basinski (1964) in the

region of the south galactic pole. They used direct plates taken with the Uppsala Schmidt telescope (20/26 inches; f/3.5). The star images were measured with an iris photometer, and the measurements were converted to magnitudes with the aid of a photoelectrically determined three-color (UBV) sequence. V-magnitudes and (B-V) color-indices were determined photographically for 1432 stars in a 13.8 square degree field centered on Selected Area 141. The limiting magnitude of the survey was $V = 16^{m}.2$.

The stellar data were sorted into groups according to the (B-V) color-index which indicates temperature or spectral type. The run of densities at different z-distances was determined for the F stars ($0.3 < (B-V) < 0.6$), and in general the results are similar to those found by Upgren for the north galactic pole. The density distribution of stars with $(B-V) > 0.6$ was not determined because of uncertainties in the stellar luminosity distribution.

A three-color photographic survey in the RGU system (Becker 1963) has been undertaken by Becker and his associates (Becker 1965; Fenkart 1967). The (G-R) color-index allows a temperature (spectral type) determination, and the (U-G) color excess is used as an indicator of metal content. They separated the stars into a halo component

(low metal content) and a disk component (higher metal content) by the use of the (U-G) color excess. They assumed all stars to be on the main sequence, and they calculated density distributions for various absolute magnitude (spectral type) groups. This work, for which the photographic plates were obtained with the 48-inch Palomar Schmidt telescope, has a limiting magnitude of 19. A two-color (BV) extension in Selected Area 51, with plates from the 200-inch telescope, reached a limiting magnitude of 21 (Becker 1967).

Strömgren Four-color Photometry Applied to High Latitude Surveys

Becker's RGU photometry allowed a two dimensional (temperature, metal content) classification. A properly selected four-color system should make possible a three-dimensional classification of stars. One such system in which a large number of field stars and several nearby clusters have been observed (Strömgren and Perry unpublished; Perry 1969b; Crawford and Perry 1966; Crawford and Barnes 1969a, b) is the Strömgren uvby system (Strömgren 1963b; Crawford and Barnes 1970). The main characteristics of the filters of this system are listed in Table II.

Three indices can be formed from the four observed magnitudes. In the spectral range from AO to late G, the three indices allow a classification of stars according

Table II. The Strömgren four-color filter system.

Filter	Central Wavelength (A)	Half-width (A)
u (ultraviolet)	3500	300
v (violet)	4110	190
b (blue)	4670	180
y (yellow)	5470	230

to temperature, luminosity, and metal content. In addition, the y-magnitude can be transformed to the V-magnitude of the Johnson and Harris (1954) system, as is demonstrated in Chapter II.

The (b-y) color-index provides a measurement of the energy distribution in the stellar continuum, thus allowing a determination of the star's effective temperature. The b- and y-passbands are not completely free of line blocking; hence, the (b-y) color-index is not completely independent of metal content. Cayrel (1968), however, points out that the slight reddening effect of the spectral line blocking is partially compensated for by the blueing effect due to backwarming in the stellar atmosphere. Using Cayrel's estimates of the line blocking and backwarming, one finds

the total difference between the (b-y) color-indices of an extremely metal poor star and a normal star with the same effective temperature to be about $0^{m}.01$ at spectral type GO.

Toward shorter wavelengths, the blocking due to metallic absorption lines becomes more pronounced. The m_1-index, where

$$m_1 = (v-b) - (b-y),$$

was designed to measure the increased metallic line blocking in the violet, and differences in the m_1-index for two stars with the same (b-y) color-index can be used as a measure of relative metal content (Strömgren 1964).

The ultraviolet filter is located on the short wavelength side of the Balmer discontinuity. Therefore the c_1-index,

$$c_1 = (u-v) - (v-b),$$

is sensitive to the size of the Balmer discontinuity (Strömgren 1964). For normal A and F type stars, the size of the Balmer discontinuity is correlated with the intrinsic luminosity. The metallic line blocking can be large in the ultraviolet, however, it is approximately twice as great as that in the violet; therefore, the effects of line blocking in the violet and ultraviolet nearly cancel, and the c_1-index is fairly insensitive to metal abundance.

The parameter δm_1 is defined as the difference between the m_1-index of a star with a given (b-y) color-index, and the m_1-index of the Hyades main-sequence stars which have the same value of (b-y). The parameter δc_1 is defined as the difference between the c_1-index of a star with a given (b-y) color-index and the c_1-index of stars on the zero-age-main-sequence (Strömgren 1963a) with the same (b-y). Strömgren (1964) has determined that, for stars with spectral type GO,

$$\left[\frac{Fe}{H}\right] = 0.3 - 12\delta m_1,$$

where

$$\left[\frac{Fe}{H}\right] = \log\left\{\frac{(Fe/H)\,star}{(Fe/H)\,sun}\right\} .$$

Wallerstein and Carlson (1960) found the relation

$$\left[\frac{Metals}{H}\right] = 0.1 - 7\ E(U-B)$$

for the F and G dwarfs. This means that δm_1 is about half as sensitive a metal abundance parameter as is an indicator of the ultraviolet excess. On the other hand δm_1 is insensitive to the stellar luminosity where the (U-B) color-index is quite luminosity sensitive. It is difficult to disentangle the effects of high luminosity and high metal abundance on the (U-B) color-index of a star.

In summary, as has been shown by Strömgren (1963a, 1964), the four-color system has three fairly, although not

totally, independent indices. The (b-y) color-index is a temperature index, the m_1-index is a measure of metal content, and the c_1-index is a measure of luminosity. The four-color system does in fact provide a three dimensional classification of stars.

For stars later than type G5 little work has been done in the four-color system, and the calibrations of c_1 and m_1 in terms of M_V and $\left[\frac{Fe}{H}\right]$ have not been made. The work by Bond (1970) indicates that the m_1-index becomes increasingly sensitive to metal content as later spectral types are reached, and that the c_1-index is able to separate late-type giants from late-type dwarfs. Because of the scarcity of data, a number of late-type stars with galactic orbits of eccentricity greater than 0.60 (Roman 1955) were observed as a part of this investigation. The four-color observations of these stars are listed in Table III.

The four-color data from Bond (1970) and from Table III are plotted in diagrams of m_1 versus (b-y), and of c_1 versus (b-y). Figures 2 and 3 are the (m_1, b-y)-diagram and the (c_1, b-y)-diagram respectively. The high velocity stars from Table III, and Bond's metal poor stars are plotted as triangles. The circles represent bright stars from the list of four-color standard stars of the Kitt Peak National Observatory (Crawford and Barnes 1970), which have normal

Table III. Photoelectric observations of late-type high-velocity stars on the Strömgren four-color system.

Star Name (HD, BD)	Sp	(b-y)	m_1	c_1	e
16 Vir.	K1III	0.72	0.49	0.50	0.61
108754	G8V	0.44	0.21	0.26	0.82
108910	K4III	0.88	0.69	0.45	0.63
114703	K2V	0.54	0.45	0.28	0.61
84 Vir.	K2III	0.69	0.56	0.42	0.67
126778	K0III	0.58	0.32	0.41	0.90
32 Boo.	G8III	0.58	0.35	0.40	0.79
+6° 2932	G6V	0.44	0.18	0.30	1.19
+30° 2611	G8III	0.80	0.33	0.59	0.77
134063	G8III	0.58	0.28	0.39	0.67
135204	G6V	0.46	0.18	0.30	0.61
-3° 3746	K4V	0.66	0.56	0.00	0.71
143291	K0V	0.46	0.30	0.24	0.62
144515	G8V	0.49	0.26	0.25	0.60
150275	K1III	0.61	0.34	0.42	0.70
152391	G6V	0.46	0.27	0.30	0.80
154276	G2V	0.40	0.17	0.32	0.77
154733	K4III	0.79	0.55	0.44	0.75
+31° 3025	G8V	0.38	0.15	0.30	0.73
161848	K1V	0.48	0.34	0.28	0.78

metal content. Two known Population II stars (HR4550, HR5270) in the K.P.N.O. list have been plotted as triangles. The giants are represented by open figures, and the dwarfs are represented by solid figures. The solid lines in the diagrams are the (m_1, b-y)-relationship shown by the Hyades dwarfs (Crawford and Perry 1966), and the (c_1, b-y)-relationship for dwarf stars given by Strömgren (1963a). The

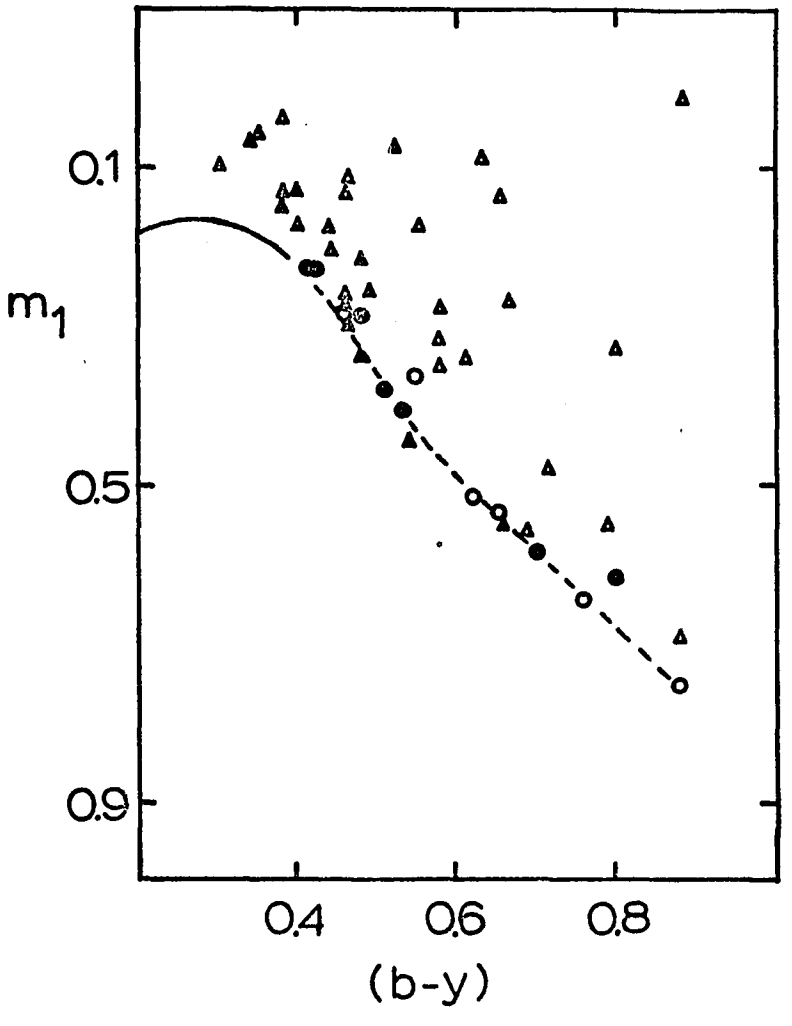

Figure 2. The (m_1, b-y)-diagram for late-type stars.

The triangles refer to stars suspected of being metal poor, and the circles refer to stars with a normal metal abundance. The solid line is the Hyades main-sequence relation of Crawford and Perry (1966). The broken line is this writer's extrapolation to later spectral types.

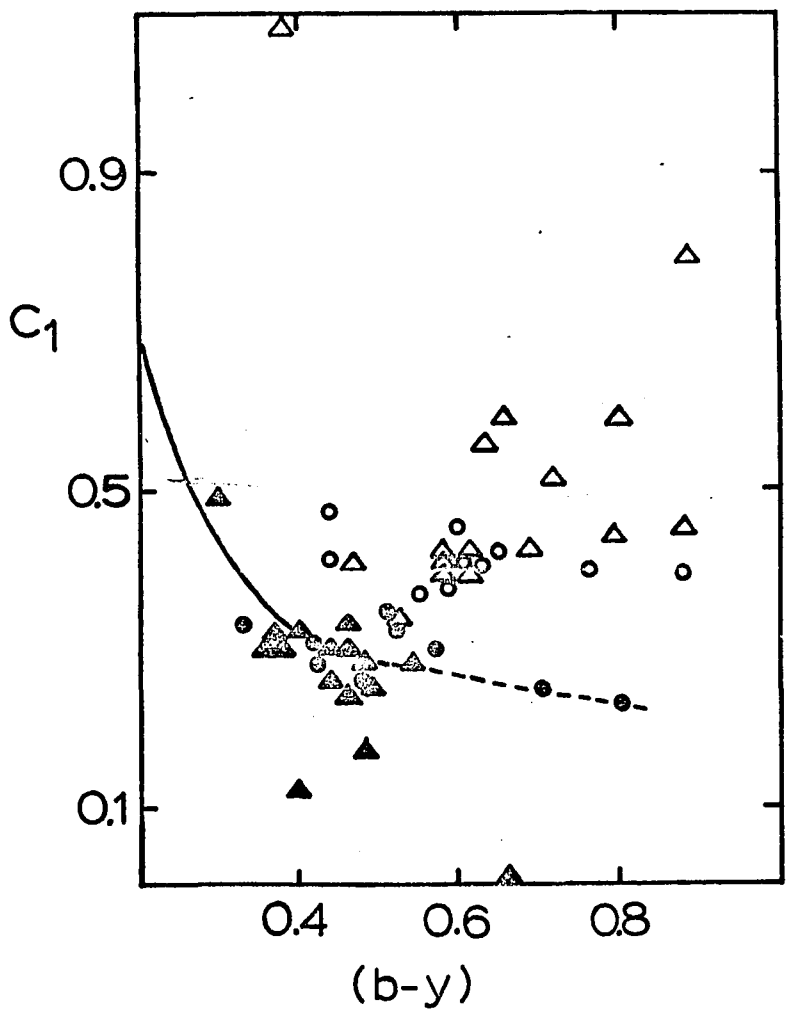

Figure 3. The (c_1, b-y)-diagram for late-type stars.

The triangles refer to stars suspected of being metal poor, and the circles refer to stars with a normal metal abundance. The solid line is the main-sequence relation given by Strömgren (1963a). The broken line is this writer's extrapolation to later spectral types.

broken line is this writer's extrapolation to later spectral types.

The differences between m_1-indices of the late type Population I and II stars, that is stars with normal metal content and the metal deficient stars, are shown in Figure 2. The differences between the Population I and II dwarfs are not as large as are the differences between the giants, but the high velocity stars with more normal m_1-indices may have normal metal content, and therefore may actually not be Population II stars. Those high velocity stars with the highest eccentricities show the largest differences in the m_1-index. The separation of the dwarfs, particularly the metal poor dwarfs, from the giants is also quite apparent in Figure 3.

It is not immediately clear why the c_1-index allows a luminosity separation in late type stars. It does not seem reasonable that Balmer continuum absorption would cause this separation; rather it seems more plausible that the late type giants have an increased metallic line blanketing in the ultraviolet.

Since blocking by spectral lines is extreme in late type stars, it does not seem unreasonable to attribute the differences in the m_1-index to differences in line blocking. That the m_1-index is not overly sensitive to luminosity is indicated by the small separation of the MK

giants and dwarfs in Figure 2. It should be possible to separate the late type stars according to metal content, at least into extreme groups. After sorting according to metal content, the c_1-index may be used to separate the sample into high and low luminosity stars.

In the previous discussion of the four-color system it was assumed that the stars studied were free of interstellar extinction and reddening. If this is not the case corrections to the observed indices must be made. Crawford and Barnes (1970) give the following differential extinction ratios for the four-color system:

$$E(b-y) = 0.7\ E(B-V)$$

$$E(m_1) = -0.3\ E(b-y)$$

$$E(c_1) = 0.2\ E(b-y)$$

$$E(u-b) = 1.7\ E(b-y)$$

If the extinction in (b-y) or (B-V) is known, the reddening corrections can be made.

Often an Hβ index, a photoelectric measurement of the Hβ line-strength, is used to supplement the four-color system (Strömgren 1966). This index is essentially reddening free, and has been found to be a good temperature indicator in A and F stars. Since (b-y) is also a temperature index, an unreddened (Hβ, b-y)-relation can be found (Crawford and Barnes 1969c) and the observed Hβ and (b-y) values for a star are sufficient to determine the quantity E(b-y).

Four-color Photometry of Halo Stars

Eggen, Lynden-Bell, and Sandage (1962) have found evidence that the oldest stars were formed in the galactic halo during a period in which the Galaxy was rapidly collapsing. They have shown that stars with the highest ultraviolet excess, that is stars with the lowest metallic line blanketing, have the highest dispersion in Z-velocities, and therefore are able to reach the greatest distances from the galactic plane. They also find that stars with the greatest ultraviolet excess have galactic orbits with the highest eccentricities. Roman (1955) has also found that stars with the weakest metal lines have the highest space velocities. Because metal content is correlated with the dispersion in Z-velocity, and since the fall off of density with z is also dependent upon the Z-velocity dispersion, it is clear that the average metal content must change with z-distance.

Strömgren (1964) found that the stars in Roman's (1955) catalogue of high velocity stars, for which four-color photometry was available, show a definite increase in their average absolute velocity, $\overline{|Z|}$, with increasing values of δm_1. The stars with $\Delta m_1 > 0^m.08$ have a value $\overline{|Z|}$ = 49 km/sec. The m_1-index is apparently quite effective in sorting stars into kinematical groups. In general, the

G and F subdwarfs have ultraviolet excesses, $\delta(U-B) \simeq 0^m.2$ (Wallerstein and Carlson 1960) which implies that δm_1 for the halo population dwarfs would be of the order of a tenth of a magnitude. This implication is borne out by the observations of a few subdwarfs (Cayrel 1968; Bond 1970) which have $0^m.10 < \delta m_1 < 0^m.15$.

Slettebak, Wright and Graham (1968) and Philip (1969a, b) have shown that a number of the blue objects at high galactic latitudes have photometric properties very much like those of the blue horizontal-branch stars. These stars have δm_1 near $+0^m.05$ and values of δc_1 near $+0^m.3$; therefore, they are quite easily recognized as a distinct class of stars.

Spectroscopic analysis of several of the faint high latitude blue stars by Wallerstein and Hunziker (1964), Kodaira (1964) and Kodaira, Greenstein and Oke (1969) shows the class to be deficient in metals by at least a factor of 10. Moreover, Philip (1970) finds $\overline{|Z|}$ for the class to be 118 km/sec. The identification of these stars as blue horizontal-branch stars, and thus true halo objects, seems quite well established. The blue horizontal-branch stars point out very clearly the extreme metal deficiencies and high velocity dispersions shown by the halo stars.

A Photographic Four-color High Latitude Survey

The Strömgren four-color system, which is able to sort stars according to age (metal content) with the m_1-index, luminosity with the c_1-index, and temperature with the (b-y) color-index, seems to be an ideal system to apply to the study of high latitude stellar distributions. Since photoelectric photometry of a large number of faint stars is not practical, the application of photographic techniques is necessary. Photographic photometry can yield colors accurate to $\pm 0^{m}.04$ (Bok and Basinski 1964). Because values of δm_1 and δc_1 several times this large are found in the high latitude stars, the use of photographic techniques will not severely limit the ability of the four-color system to discriminate between stars of different types.

In this study an attempt has been made to develop a four-color photographic system, and to apply it in a survey of stellar distributions at high galactic latitudes.

CHAPTER II

THE FILTER SYSTEM

While four-color photographic photometry on the Strömgren uvby system offers distinct advantages for survey work at high galactic latitudes, filters suitable for photographic photometry which isolate the four passbands are not generally available. One aspect of this study has been to devise a photographic filter system which mimics the Strömgren four-color system used in photoelectric photometry.

The Filters Selected

A set of filters which isolates the four passbands has been found. Two of these were constructed by the writer and the others were purchased. The filters and the passbands they isolate are discussed below.

Ultraviolet

The ultraviolet passband has been isolated for photography by a 6 mm thickness of Schott UG 1 glass. The transmission profiles of the photographic and photoelectric u filters used in this study are shown in Figure 4. The filter used in photoelectric photometry is a

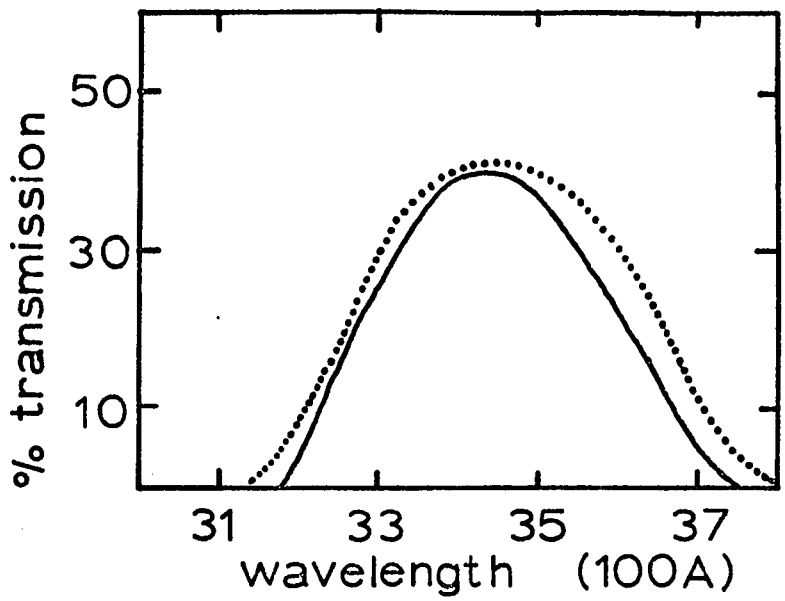

Figure 4. The ultraviolet passband.

The dotted line represents the filter used for photoelectric photometry, and the solid line represents the photographic filter.

sandwich of an 8 mm thickness of Schott UG 11 glass and a 1 mm thickness of Schott WG 3 glass.

As was pointed out by Strömgren (1963a), for most stars later than spectral type A2, the observed intensity is usually lower in the u-band than in the other three bands. The exposure times needed to reach faint F and G stars are likely to be longest in the u passband. The long exposure times cannot be shortened by using a broader passband. This is well demonstrated in Figure 5, where the difference between the intermediate band and broad-band ultraviolet magnitudes (u-U) is plotted as a function of the (b-y) color-index. The peak near (b-y) = 0 is due to a greater sensitivity of the narrower filter to the Balmer discontinuity, and the height of the peak indicates the importance of using the narrow ultraviolet passband.

Violet

The violet filter is a critical filter in the Stromgren system since it is used for both the m_1- and c_1-indices. It must be located to the red side of the spectral region in which the lines of the Balmer series crowd together, and yet it should not extend beyond the region where the metal lines show a concentration. This requires a filter with a central wavelength near 4100A and a width at 50% of the peak transmission (hereinafter referred to as the half-width) near 200A.

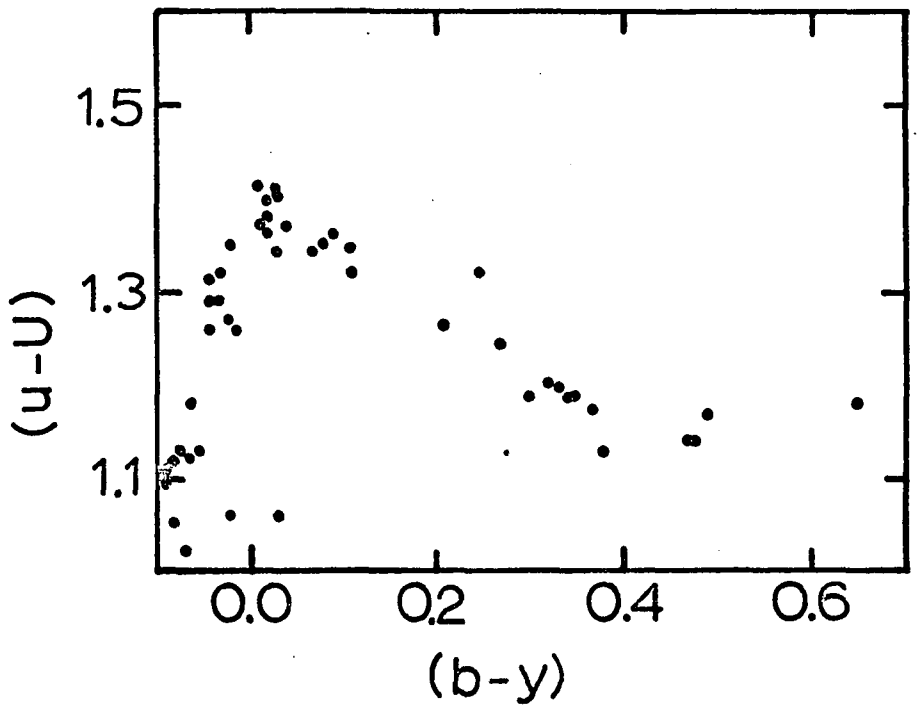

Figure 5. Broad- and intermediate-band ultraviolet magnitude differences for main-sequence stars.

The stars are main-sequence stars from the Kitt Peak National Observatory list of four-color standard stars (Crawford and Barnes 1970). The intermediate-band magnitudes and the (b-y) color-indices are the standard values. The broad-band magnitudes are from Johnson, Mitchell, Iriarte, and Wisniewski (1966).

The violet filter used in this study consists of two layers of colored gelatin cemented between layers of glass. This filter and a similarly constructed blue filter were cemented by the writer. A description of the method used to cement the filters can be found in Appendix II.

The colored sheets of gelatin used in the construction of the violet filter were Eastman Kodak Wratten filters 2c and 36. Together they form a filter with a central wavelength of 4200A, a half-width of about 300A, and a maximum transmission of 33%. This filter will hereinafter be referred to as the 4200-filter, and the passband it defines will be referred to as the v' passband.

Since the Strömgren filter is somewhat narrower than the 4200-filter, and since it is centered nearly 100A to the blue of the 4200-filter, the fit is not as good as had been desired. An inquiry was made to Eastman Kodak and the reply was that they cannot change the characteristics of the dye in the direction needed to improve the 4200-filter without causing it to be highly unstable. As it is, the stability of the 4200-filter is barely acceptable. A test of the stability will be discussed in a later section.

The transmission of the 4200-filter and the photoelectric violet (v) filter used in this study are shown in Figure 6. The photoelectric violet (v) filter is an

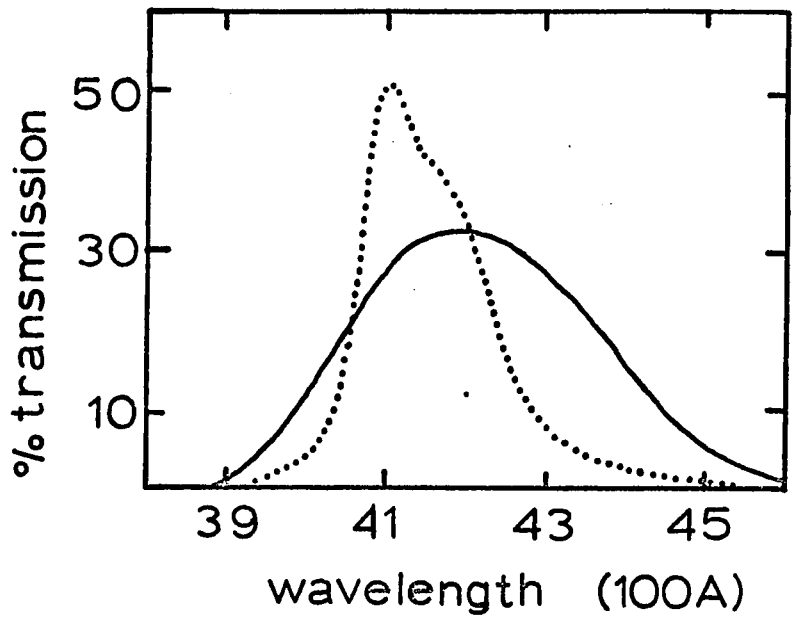

Figure 6. The violet passband.

The dotted line represents the interference filter used for photoelectric photometry. The solid line represents the photographic filter.

interference filter, as are the blue (b) and yellow (y) filters of the Strömgren system.

The 4200-filter has 65% of its peak transmission at Hγ, and 85% of its peak transmission at Hδ, while the v-filter is centered nearly on Hδ. The two filters, however, have the same sensitivity to the strength of the hydrogen lines. This is because the addition of Hγ to the passband of the 4200-filter is compensated for by the inclusion of a wider range of the continuum.

Since the effective wavelengths of the 4200- and v-filters differ by nearly 100A, the difference in response of the two filters was checked by making photoelectric observations of bright stars through each filter. In order to use the 4200-filter photoelectrically it was necessary to block its red leak with a 2 mm thickness of Schott BG 12 glass. The addition of the blocking filter did not appreciably change the 4200-filter profile, as is shown by Figure 7.

The difference in response between the 4200-filter and the v-filter, given as a (v' - v) magnitude difference, is shown in Figure 8. The solid and the open figures represent main-sequence and higher luminosity stars respectively. Circles refer to normal field stars and triangles refer to the high velocity stars listed in Table III. The scatter is about that expected from the random errors in

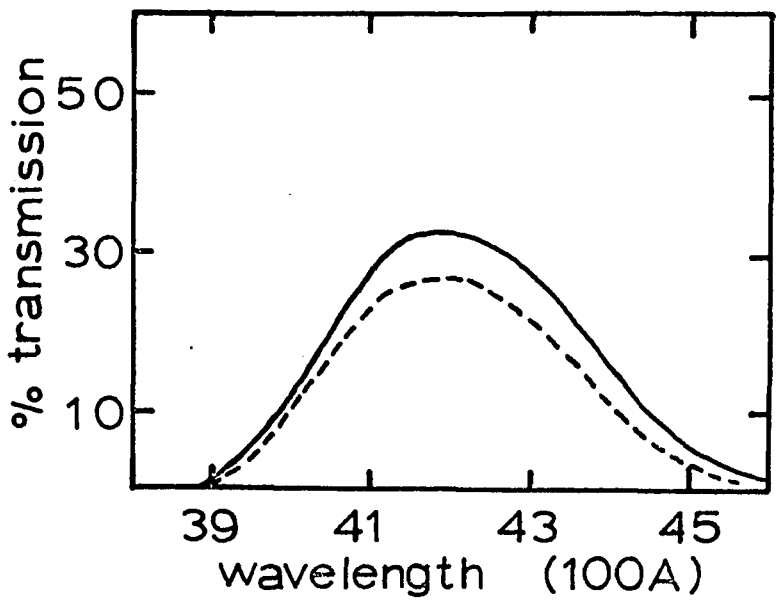

Figure 7. The change in the transmission of the 4200-filter due to the addition of a blocking filter.

The solid line refers to the normal photographic filter. The broken line refers to the photographic filter with the red leak blocked by the addition of a BG 12 glass filter.

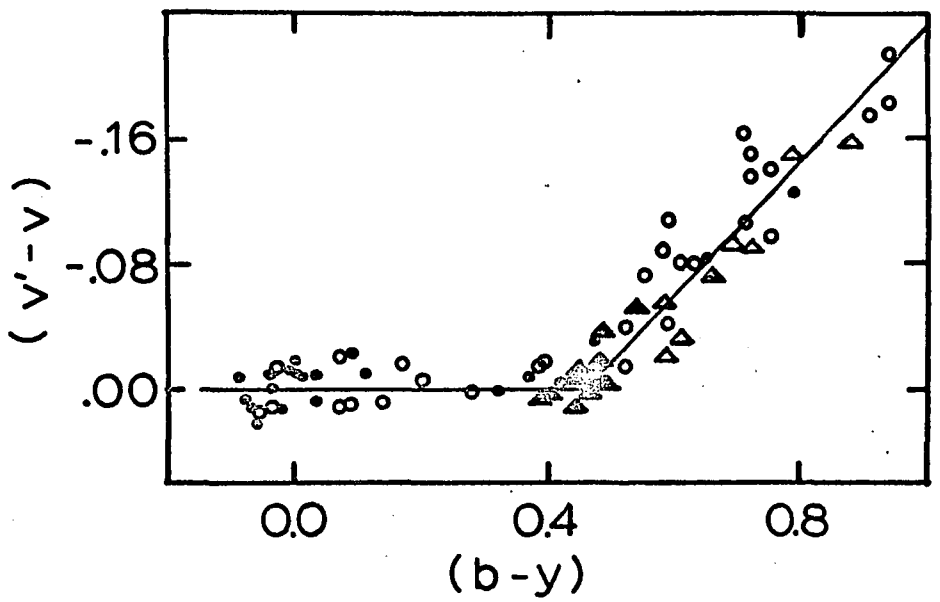

Figure 8. The difference in response between the photographic and photoelectric violet filters.

The solid and the open figures represent main-sequence and giant stars respectively, circles refer to normal field stars and triangles refer to high velocity stars listed in Table III.

the photoelectric photometry. The relation,

$$v' = v \quad ; \ (b-y) \leq 0.45$$

$$v' = v - 0.425\ (b-y) + 0.19 \quad ; \ (b-y) > 0.45$$

is drawn as a solid line in Figure 8. This relation has been used to transform the photoelectric v magnitudes of the standard sequence stars to the photographic v' magnitude system.

Because it does not match the v-filter well, the 4200-filter cannot be considered an established filter in the four-color photographic system. It should be replaced as soon as a more appropriate filter can be found. Presumably high quality interference filters with sizes up to 8 or 10 inches square will be available in the future.

Blue

In the blue wavelength region there are few spectral features. A measurement of the b-magnitude is essentially a measurement of the brightness of the continuum in this wavelength region. For this reason, the restrictions on the bandwidth of the b-filter are not as stringent, and a broader passband may be used in order to shorten the exposure times.

A blue filter, hereinafter called the 4700-filter, has been constructed using Eastman Kodak Wratten filters 3 and 32. When used with an Eastman Kodak 103a-0 emulsion,

which shortens the red end of the passband by 100A, this filter is nearly identical in half-width and central wavelength to the Strömgren interference filter. Were it not for the fact that a broader passband can be used in the blue, it would have been ideal for use in the four-color photographic system.

Another excellent match in effective wavelength, with a slightly broader passband, is provided by a 3 mm thickness of Schott GG 455 glass (previously listed by Schott as GG 5) used with the 103a-0 emulsion. Figure 9 shows the profiles of the two photographic filters when used with the 103a-0 emulsion, and of the Strömgren b-filter (interference) used in this study.

Differences in blue magnitudes of stars, determined with the use of the two photographic filters, are plotted in Figure 10 as a function of the (b-y) color-indices of the stars in question. It can be seen that there are no systematic differences in the magnitudes determined by the two filters. The GG 455 filter was chosen for the photographic four-color system because it allows much shorter exposure times.

Yellow

In the yellow passband, as in the blue there is no loss in the efficiency of the four-color system if a broader passband is used. In fact, observations of bright stars

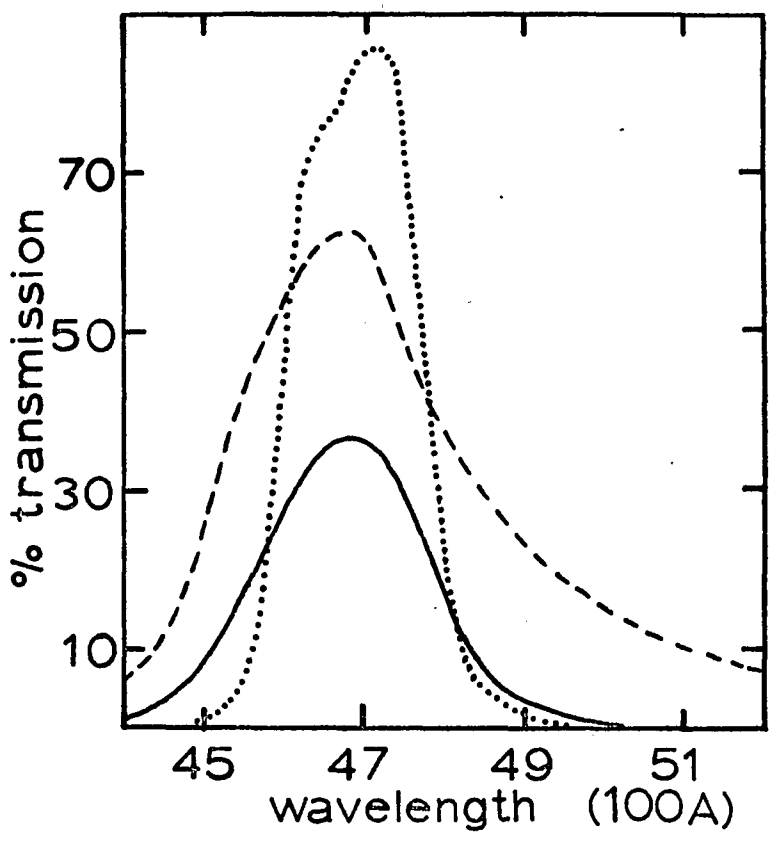

Figure 9. The blue passband.

The dotted line refers to the interference filter used for photoelectric photometry. The broken line and solid line refer to the response of the OG 455 glass filter and the 4700-filter respectively, when used with the 103a-0 emulsion.

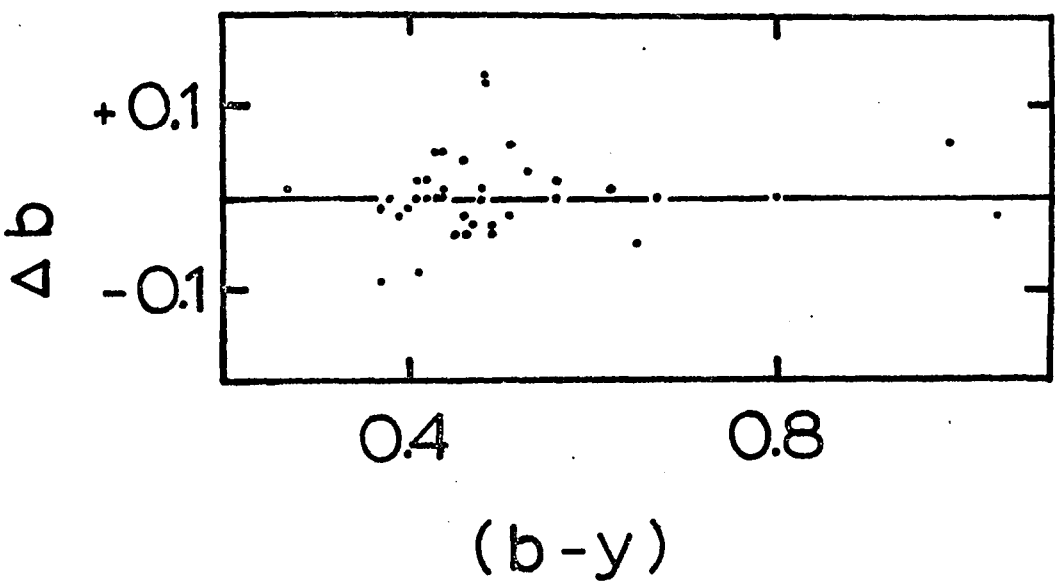

Figure 10. Differences in b-magnitudes obtained through the use of the two photographic b-filters.

indicate that there is very little difference between the broad-band V-magnitude of the UBV system and the narrow-band y-magnitude of the four-color system.

In Figure 11, the (y-V) magnitude difference is plotted as a function of the (b-y) color-index. Although there appears to be a weak dependence on (b-y), the systematic differences are nearly lost in the random errors of the observations. For photographic photometry, with its inherently greater random errors, the broad-band V-magnitude can be taken to be equal to the narrow-band y-magnitude. Therefore, when used with an Eastman Kodak 103a-D emulsion, the Schott GG 495 filter (previously listed as GG 14) will yield photographic y magnitudes with sufficient accuracy.

Although it should not be needed when observing normal objects, a narrower yellow passband is available. A 3 mm thickness of Schott OG 515 glass (previously listed as OG-4), used with an Eastman Kodak 103a-G emulsion, yields a passband with a half-width of 550A, and the combination has the same central wavelength as the Strömgren y-filter. The profiles of the narrower photographic y-passband, and of the y-filter used for photoelectric photometry are shown in Figure 12.

Tests of the Gelatin Filters

After their construction, the total transmission of the gelatin filters was measured with a microdensitometer.

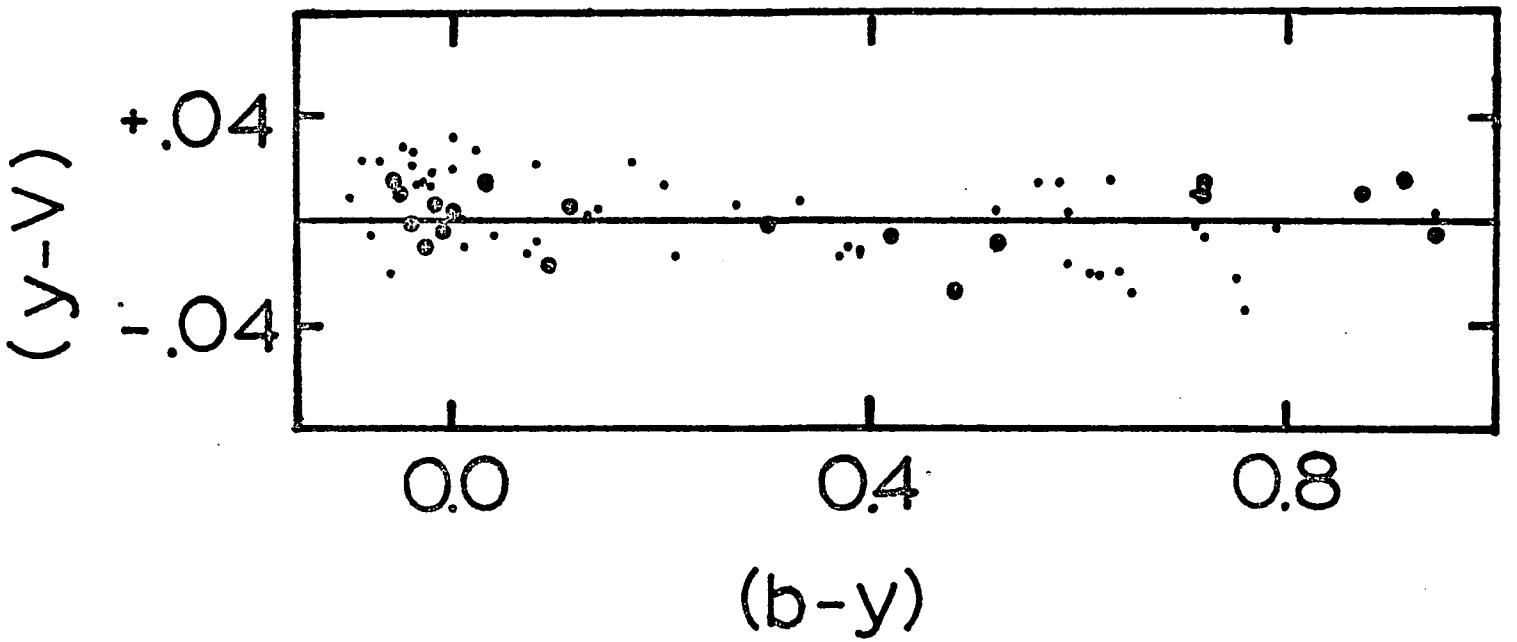

Figure 11. Broad-band visual and intermediate-band yellow magnitude differences.

The yellow magnitudes are the average y-magnitudes found by the writer for the four-color standard stars used in this study. The visual magnitudes are those of Johnson, Mitchell, Iriarte, and Wisniewski (1966). The large filled circles refer to stars with three or more observations.

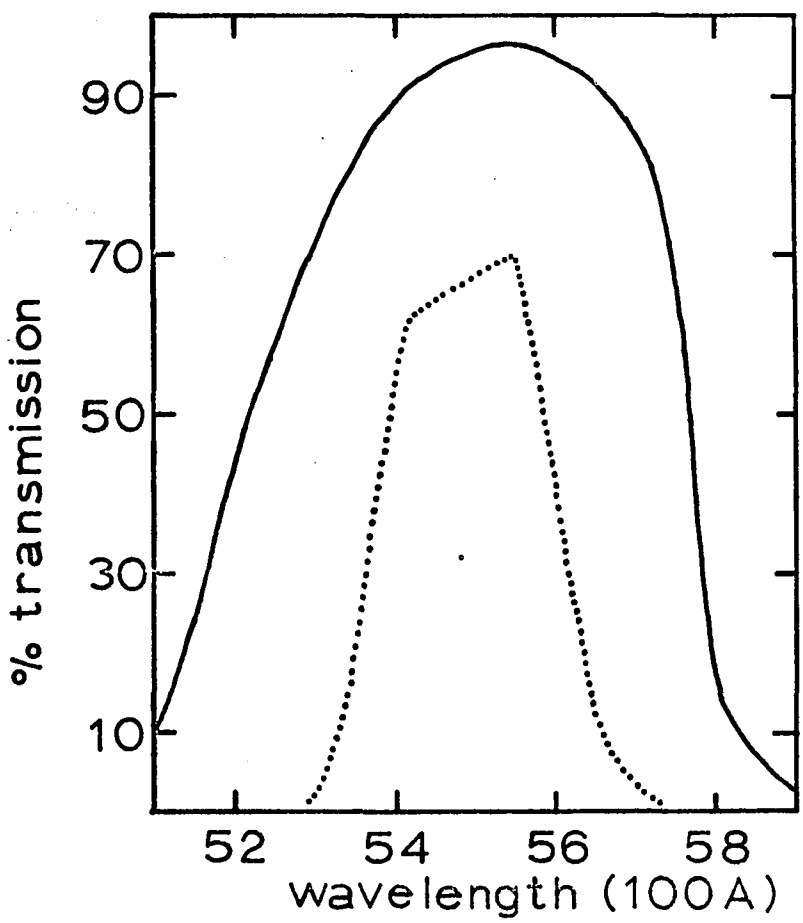

Figure 12. The yellow passband.

The response of the combination of the 103a-G emulsion and the OG 515 filter is represented by the solid line. The dotted line represents the transmission of the yellow interference filter used in this study for photoelectric photometry.

Several scans were made across the eight-inch face of each filter. The filters proved to be quite uniform, with the total transmission varying by ±1% or less. Therefore, no significant errors in the photographic photometry will be introduced by non-uniformities in these filters.

Since three out of the four pieces of gelatin used to make the filters were given "C" stability ratings by the Eastman Kodak Company, meaning that direct exposure to sunlight for a period of two weeks would produce up to a 10% change in transmission, it was necessary to test the completed filters for photometric stability. Both the 4200- and the 4700-filters were subjected to direct sunlight for periods of time ranging from 30 seconds to three days. The results of this test, which are shown in Figures 13 and 14, indicate that the 4200-filter is extremely sensitive to bright light. Since several weeks of exposure to incandescent room lighting produced no change in filter characteristics, the changes resulting from exposure to direct sunlight are most likely due to a sensitivity to ultraviolet light.

A 30 second exposure to direct sunlight is a great deal more severe than any exposure the filters would receive during normal use in astronomical photography. With the filters stored in the dark there was no change in the filter characteristics after a period of about one year.

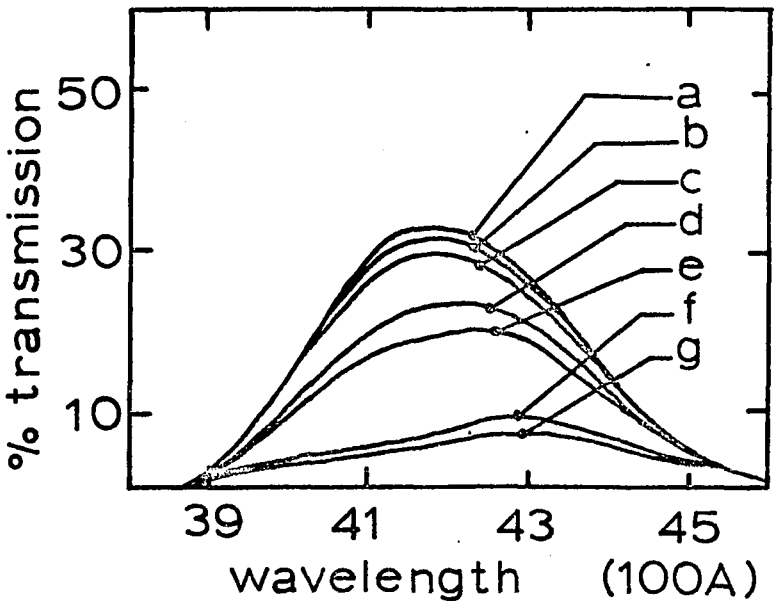

Figure 13. Changes in the 4200-filter profile resulting from exposure to direct sunlight.

Curves a, b, c, d, e, f, and g refer to no exposure, 30 seconds, two minutes, five minutes, ten minutes, one hour and one day of exposure to sunlight respectively.

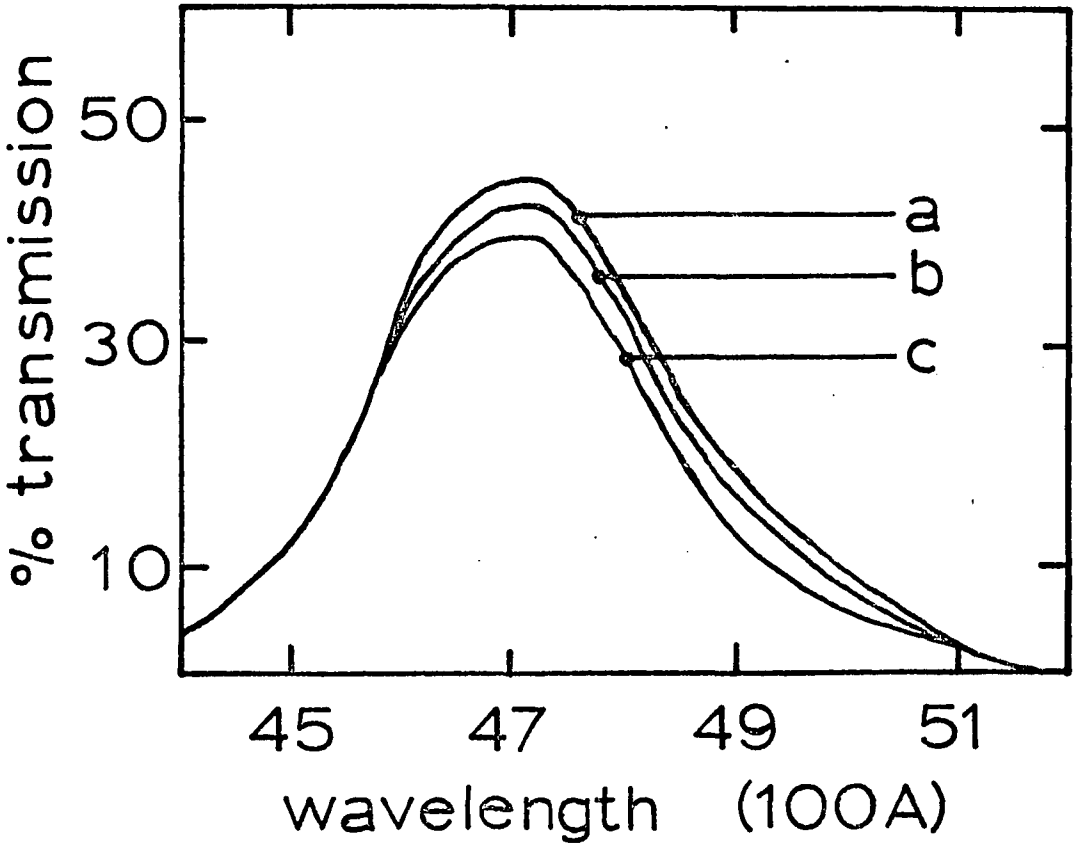

Figure 14. Changes in the 4700-filter profile resulting from exposure to direct sunlight.

Curves a, b, and c refer to no exposure, one day and three days of exposure to sunlight respectively.

Therefore, if care is taken not to expose the filters to bright light, they should provide several years of service.

Photography with Interference Filters

It is clear that interference filters can be constructed which will isolate the passbands of the four-color system. In order to determine whether an interference filter was suitable for photographic photometry of large fields, a four-inch square interference filter with a passband matching that of the Stromgren v-filter was purchased.

The largest filter which could be obtained at the time was six inches square; even so, its uniformity could be guaranteed over only a four-inch square field. Since it was desired to use fields eight inches square, the four-inch size of the interference filter was held to be a serious disadvantage. However, photography of several adjacent fields was still possible, therefore further tests were made.

The passbands of several areas distributed across the face of the filter were determined by the use of the Cary spectrophotometer of the Kitt Peak National Observatory. Both the half-width and the central wavelength of the filter proved to be quite uniform, unlike similar tests of a slightly narrower Hα filter made by Wurm (1963). Wurm

found both variations in effective wavelength and in bandwidth with his filter.

The profiles of the interference filter tested for this study did show slight differences in maximum transmission from point to point along the face of the filter. Because of these differences, the changes in the total transmission across the face of the filter were measured with a microdensitometer. The filter showed a 10% to 15% variation in total transmission across its face, with a sharp change occuring near the center of the filter. Figure 15 is a reproduction of a representative sample of the microdensitometer tracings.

Although the variation in total transmission ruled out the use of this interference filter for photographic photometry of star fields, it was also tested at the telescope. Direct plates using the interference filter were obtained at both the 84-inch telescope of the Kitt Peak National Observatory and the 36-inch telescope of the Steward Observatory. These plates showed that the interference filter produced strong ghost images of all bright stars, which is still another reason why interference filters are unsuitable for photographic photometry. In order to provide a comparison, the 4200- and 4700-filters were also tested at these telescopes and they showed no signs of ghost images. The ghost image problem might be

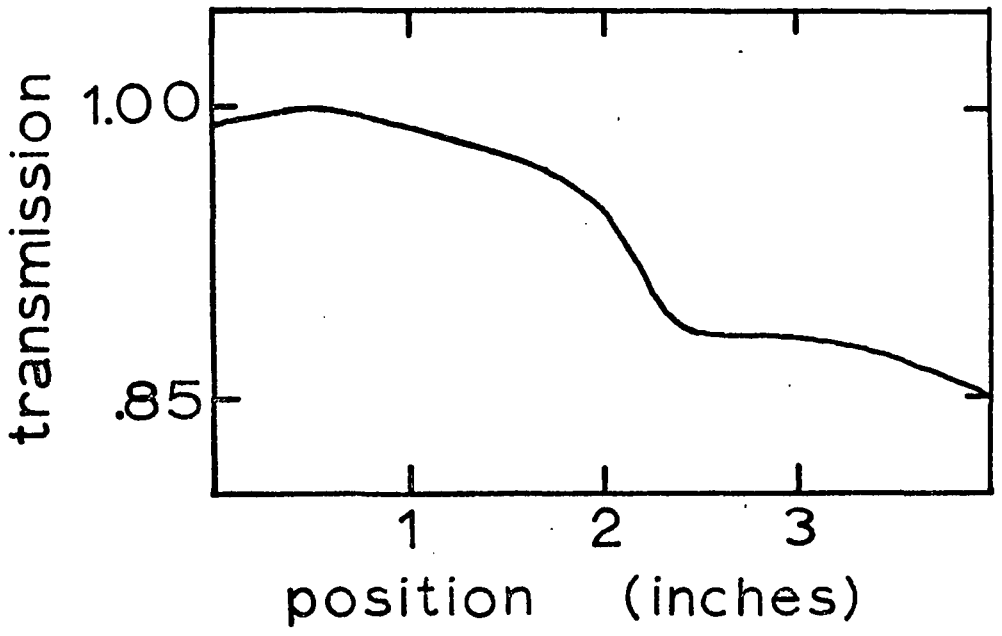

Figure 15. Changes in the total transmission across the face of the four-inch square interference filter.

The maximum value of the total transmission of the filter is normalized to one.

reduced by the use of non-reflection coatings on the surfaces of the interference filter, but large filters with coated surfaces would make normal handling and cleaning difficult.

From the results of the tests of the violet interference filter, and Wurm's tests of his Hα filter, it appears that interference filters, which are of high enough quality for photographic photometry over large fields, are not yet available. This does not mean that hopes of using large interference filters must be completely abandoned. High quality, large-sized interference filters would still be the best filters to use for the violet passband of the photographic four-color system. It is quite conceivable that future developments will provide the high quality filters desired.

Liquid Dye Filters

Wurm (1963) has reported on his work with liquid dye filters, and the results look very promising. Liquid dye filters offer a high degree of uniformity, limited only by the accuracy with which the cells can be constructed. Their size is also limited only by the construction of the cell, and presumably cells of any reasonable size can be built.

Not only can liquid dye filters be large and uniform, but also they offer very narrow passbands. Some of Wurm's filters have half-widths of less than 100A. On the other hand, the liquid dye filters suffer from the same shortcomings as the gelatin filters. The dyes which form the red side of the passband do not have cuts as sharp as those which form the blue side, often resulting in an assymetric passband, and the dyes which form the red cutoff are not available at as many wavelengths. The dyes which would isolate the v-passband of the four-color system are not known to this writer. Finding the correct dye, if indeed one does exist, could require a great deal of chemical experimentation.

Summary

For the present, the photographic four-color filter system is taken to consist of the filters and filter and emulsion combinations shown in Table IV.

A transformation between the photoelectric and the photographic four-color system is possible. For stars with $(b-y) \leq 0.45$, the two systems are the same, while stars with $(b-y) > 0.45$ require a small adjustment to their violet magnitudes.

Table IV. Filters of the photographic four-color system.

Color	Filter	Emulsion
ultraviolet	6 mm UG 1	103a-O
violet	4200	103a-O
blue	3 mm GG 455	103a-O
yellow	2 mm GG 495	103a-D

CHAPTER III

THE OBSERVATIONS

The four-color photographic filter system described in Chapter II has been applied to a photographic survey of stars in two fields at high galactic latitudes. This survey was accomplished by obtaining several plates of each field in each color of the four-color system, and then measuring all star images on each plate with an iris photometer. The iris photometer measurements were calibrated by photoelectrically determined magnitude sequences in all four colors for each field. Magnitudes and four-color indices were found for all stars which were bright enough to allow the determination of a magnitude in each of the four colors.

The Star Fields of Interest

Selection of the Star Fields

The selection of the fields to be studied was based on three criteria. First, the fields were restricted to those of the Kapteyn Selected Areas (e.g., Blaauw and Elvius 1965) which lie near a plane perpendicular to the galactic plane, which passes through the galactic center

and the galactic anticenter. Second, only fields in which no obscuration was apparent on the National Geographic Society and Palomar Observatory Sky Survey (POSS) prints were considered. Third, an effort was made to pick fields in which very little work has been done previously.

The two fields chosen for this study are the Kapteyn Selected Areas (henceforth abbreviated as SA) 27 and 56. The coordinates and central stars of these fields are given in Table V. The galactic coordinates are on the new system (Blaauw, Gum, Pawsey, and Westerhout 1960).

Table V. The fields studied.

Field	Equatorial Coordinates (1950) α	δ	Galactic Coordinates l	b	Central Star
SA 27	7 41.6	+44 43	174.5	+27.9	HD 62300
SA 56	12 00.6	+29 23	199.6	+79.2	HD 104688

Other Investigations in the Selected Fields

Two monochromatic surveys of photographic magnitudes of stars in the Kapteyn Selected Areas have been published. The "Durchmusterung of Selected Areas" by Pickering,

Kapteyn and van Rhijn (1918) covers a field 80 minutes of arc on a side in SA 56 and 60 minutes of arc on a side in SA 27. The limiting magnitudes of this survey are 15.30 in SA 27 and 16.18 in SA 56.

The "Mount Wilson Catalog of Photographic Magnitudes in Selected Areas 1-139" by Seares, Kapteyn and van Rhijn (1930) covers a circular field 23 minutes of arc in diameter in both SA 57 and SA 27. The limiting magnitudes are 18.36 in SA 56 and 19.00 in SA 27.

Two surveys of objective prism spectral types for stars in the northern Selected Areas have been made. These are the survey by Humason (1932) and the "Bergedorfer Spektral-Durchmusterung der 115 Nordlicher Kapteynschen Eichfelder" by Schwassman and van Rhijn (1935). Both surveys reach some thirteenth magnitude stars in SA 27 and SA 56.

A survey of several Selected Areas, in which photographic colors and magnitudes in the UBV system are found, has been undertaken at the Engelhart Observatory (Elvius 1964). Observations of 4,000 stars, with a limiting visual magnitude near 15, have already been published by Urassin (1969) for SA 25.

A number of stars in SA 56, reaching $V \approx 13$, have been observed by Bok and Hoxie (unpublished). Their

observations were made in the UBV system. Most of the stars they observed were incorporated into the standard sequence determined for use in this work. A comparison between the Bok and Hoxie V-magnitudes and the y-magnitudes of this study shows no serious disagreement.

The Photographic Observations

The photographic material used in this study was obtained at the Cassegrain focus of the 90-inch telescope of the Steward Observatory. One plate was provided by Dr. B. J. Bok. The remainder were obtained by the author. The majority of the plates were taken with the aid of an automatic guider. The plates used for the photographic survey are listed in Table VI.

The Processing of the Plates

All plates were processed in Eastman Kodak developer D-19 for five minutes at a temperature of 68° Farenheit. A tray rocker was used during the developing in order to insure uniform agitation. Care was taken so that no standing waves would form in the developer, and so that the plate would remain totally covered with developer at all times.

The development was followed by an acid stop bath, hypo, water rinse, and hypo clear. The plates were washed

Table VI. The photographic survey plates.

Field	S.O. Plate No.	Emulsion	Filter	Exposure (min.)
SA 27	149	103a-D	GG 495	24
	150	"	GG 495	30
	151	"	GG 495	37
	292	103a-O	GG 455	60
	323	"	GG 455	60
	324	"	GG 455	60
	185	"	4200	240
	293	"	4200	150
	184	"	UG 1	170
	317	"	UG 1	97
SA 56	187	103a-D	GG 495	30
	188	"	GG 495	30
	189	"	GG 495	45
	194	"	GG 495	45
	162	103a-O	GG 455	75
	190	"	GG 455	120
	191	"	GG 455	120
	192	"	4200	240
	202	"	4200	120
	203	"	4200	120
	320	"	4200	100
	199	"	UG 1	227
	204	"	UG 1	135
	224	"	UG 1	150
	331	"	4700	62

in running water and rinsed in a weak detergent solution before drying.

Field Corrections

The 90-inch telescope was installed during the early stages of this investigation. The telescope was

intended to have an unvignetted field eight inches in diameter. A number of plates were taken in order to determine the amount of any field corrections which might be present. The plates used in the field correction determination are listed in Table VII.

Table VII. Field correction test plates.

S.O. Plate No.	Offset of Plate Center from SA 56	Filter	Emulsion	Exposure
326	1000 arc sec. South	None	103a-O	20
327	None	None	"	20
191	None	GG 455	"	120
372	500 arc sec. North	GG 455	"	45
373	500 arc sec. South	GG 455	"	45

Two sets of plates were used, one taken without a filter, and the other making use of the Schott GG 455 glass filter. Of the unfiltered plates, one was centered on SA 56 and the other was centered 10 cm, about 1000 seconds of arc, to the south of SA 56. One of the filtered, blue, plates was centered on SA 56 while the other two were displaced five centimeters to the North and South respectively.

The set of filtered plates was measured and reduced by the method explained in later sections of this work.

The blue magnitude difference between the offset plates and the plate centered on SA 56 was found for each star. The differences between the blue magnitudes determined from the offset plates and the blue magnitudes determined from the plate centered on SA 56 were found for each star.

The unfiltered plates were calibrated using the blue magnitudes determined for the stars in the survey, a procedure which yielded a good determination of the slope of the calibration curve despite the inevitable scatter caused by the use of different spectral passbands. The difference in the iris readings of a star on each of the two plates was plotted against the iris reading of the star on one plate. This was done for all stars in the field of the general survey. A curve was drawn through the plotted points. The displacement of any point from the curve was converted to a magnitude difference by using the slope of the magnitude-iris reading relation. Magnitude differences were then found for images common to the two unfiltered plates.

The distance of each star image from the center of the offset plates was measured. Also the distance of the same star image from the center of the reference plate, which was centered on SA 56, was measured. The difference between the radial distance of a star image on an offset plate and on the reference plate was found for each star.

If this difference was greater than one half inch, the difference between the measured magnitudes of the two images was plotted against the greater of the two distances from the respective plate centers. The sign of the magnitude difference was taken to be positive if the image farthest from its plate center was faintest.

In Figure 16 the magnitude differences are shown as a function of distance from the plate center. The filled circles represent the blue plates and the open circles the unfiltered plates. No field corrections are indicated within a radius of 3.75 inches, which is the radius of the two areas studied in the survey. Strong vignetting sets in near 4.25 inches.

The Measurement of the Photographic Plates

The Identification of Stars to be Measured

A long exposure visual plate of each of the two fields was examined carefully in order to identify the stars to be measured. Normal galaxies were easily excluded, even near the faint limit of the plate, because their images were noticeably larger and less dense than the stellar images. All star images on the plate were marked.

The marked images were measured on the iris photometer. The stars which were significantly (about 0.2

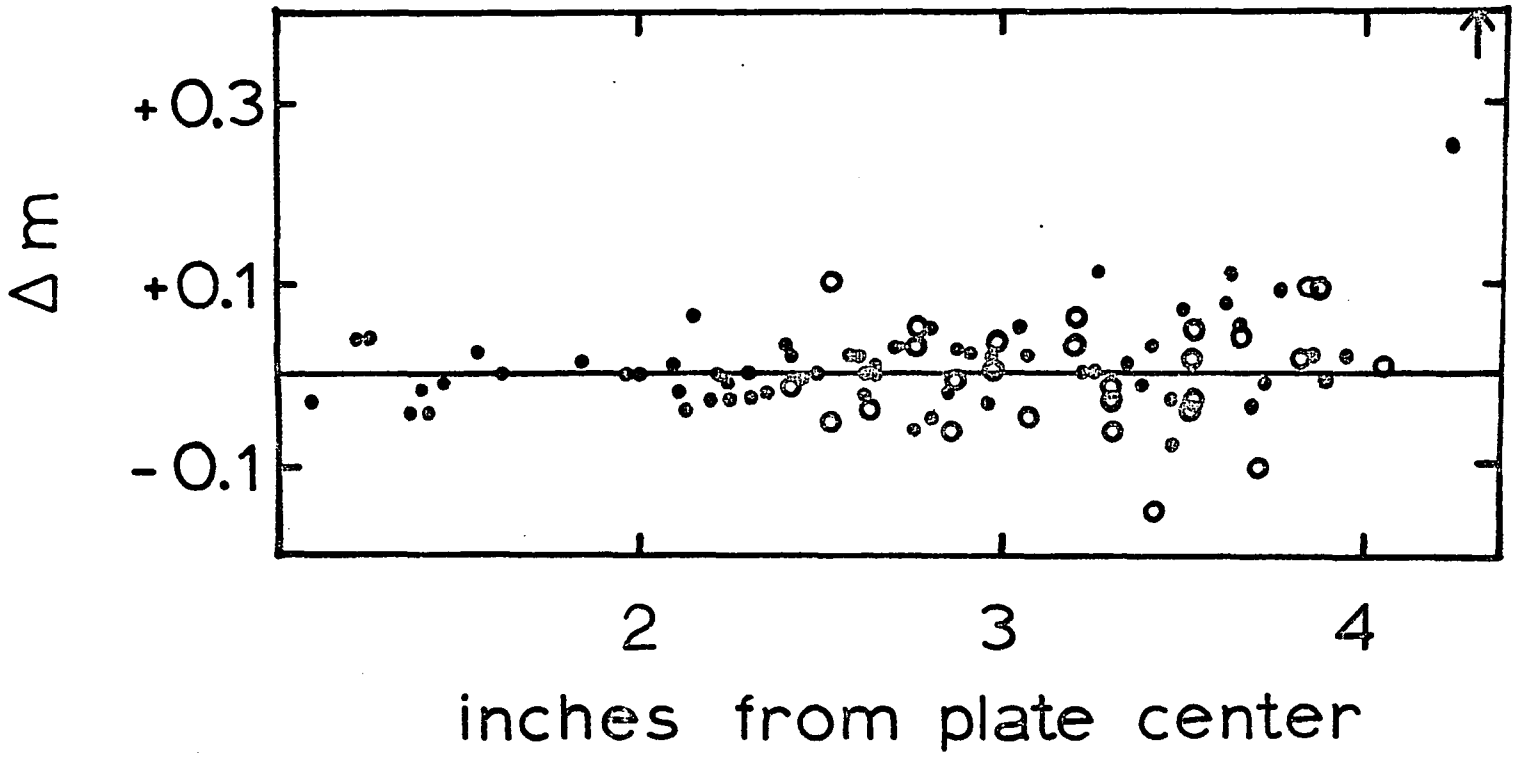

Figure 16. Field corrections for the 90-inch telescope.

The filled circles represent magnitude differences found from the set of blue plates. The open circles are from the unfiltered plates.

magnitudes) fainter than the faintest photoelectric standard were eliminated from the list to be measured.

The radius of the field to be investigated was set at 3.75 inches. The stars which fell outside of this limit were rejected. In addition, the guide probe of the 90-inch telescope extended into the field being photographed. Those star images which suffered vignetting by the guide probe were rejected.

The stars not rejected were given identification numbers. An identification chart of the numbered stars was made up. All stars on the identification chart were measured for each plate of the survey on which they had measurable images.

The Iris Photometer

The stars were measured on the Cuffey-model iris photometer of the Steward Observatory. The iris photometer, originally of conventional design as described by Cuffey (1956), has been modified to provide automatic setting of the iris and automatic data recording on punched paper tape.

A peak holding circuit, which allows the iris to open only, was incorporated into the automatic iris setting circuitry (Tifft, Fannin, Hanzi, and Bowers 1969). All plates were measured with the use of the peak holding circuit.

In order to make a measurement, the star was centered in the diaphragm. The diaphragm was closed and then allowed to open under the control of the peak holding circuit. After the iris had come to a stop, the star was moved slowly across the iris in several directions. The iris opened an additional slight amount if there had been an error in the initial centering of the star. Using this method, the scatter in the measurements caused by centering errors was effectively eliminated.

One star was picked to be measured at the beginning and end of each measuring session, and also between every set of 25 star measurements. This was done in order to determine whether there was any zero-point drift in the measuring system. No zero-point drift was found.

In order to insure the homogeneity of the measurements, all stars on one plate were measured in one measuring session. Slight changes in the focus of the system, caused by departures of the photographic plates from flatness, proved capable of producing systematic errors of up to a tenth of a magnitude for large sections of a plate. These systematic errors were eliminated, at the expense of slightly increased scatter in the measurements, by mechanically moving the plate into the focal plane of the optical system before each individual measurement.

Once the measurement was made, the iris reading and star number were recorded manually. The data for each plate were punched on computer cards, and the cards were checked against the hand tabulated data. The iris readings were converted to magnitudes by the method described in the next chapter.

The Photoelectric Observations

The photoelectric observations of the standard sequence stars were carried out at the 36-inch and 90-inch telescopes of the Steward Observatory. The observations made with the 36-inch telescope reached $V \approx 15$ and the observations on the 90-inch telescope extended the sequences to $V \approx 18.5$. In addition, a number of cool, high velocity stars were observed with the 90-inch telescope.

Observations at the 36-inch Telescope

The stars chosen for observation were picked to be well distributed over the region of the survey. An examination of the POSS prints was made to be certain no stars brighter than the survey limit were within one minutes of arc of the sequence stars. One large clear area near the center of each field was chosen to serve as a suitable area for the measurement of the flux from the sky.

A diaphragm with a diameter of 23 seconds of arc was used. The stars observed on the 36-inch telescope were bright enough to be easily centered in the diaphragm.

The general observing procedure for bright standard stars was to first measure the flux from the sky in all colors. The star was then observed in all colors, going through the filters from yellow to ultraviolet. The star was measured a second time passing through the filters in reverse order, and if the sky signal was a significant fraction of the star signal, another measurement of the sky was made. Fifteen second integration times were used on the bright stars.

The observing procedure for the program stars was somewhat different than for the standard stars. The measurement of each program star in all passbands was followed by a sky measurement in all passbands. In several instances, the sky was measured about two minutes of arc from a program star, and those sky measurements varied neither appreciably nor systematically from the measurements of the centrally located sky position.

Sixty second integration times were used for the faint program stars. The brighter program stars were observed using both 15 and 60 second integration times. No systematic differences were found between measurements made using the two different integration times.

Observations at the 90-inch Telescope

Only stars for which no neighbors within one minute of arc were visible on the POSS prints were chosen to comprise the faint end of the standard sequences. A further search for faint neighboring stars was made on sky limited blue plates obtained with the aid of a Carnegie image tube. These plates show considerably more faint stars than the POSS prints, yet no faint stars were found in the immediate vicinity of the sequence stars.

The sky brightness was always measured at a point 20 arc seconds to the North or to the South of the program stars. The diaphragm used had a diameter of 10 seconds of arc, so the sky was measured at a point four diaphragm radii away from the star. Because of the small diaphragm size, the photoelectric observations were limited to nights of good seeing.

The general method of observation was to set on the star and integrate for 20 seconds. The telescope was then offset to the sky position and the sky was measured. A series of alternate observations of the star and the sky was made in each color. Up to 15 integrations on the star were made in each color for the faintest stars. On the bright stars ($m_V < 16$) at least two integrations were made on the star.

In each field a red and a blue star, that had been observed on the 36-inch telescope, were used as regional standard stars. On all nights, these stars were supplemented by observations of a few of the K.P.N.O. four-color standards.

The Offsetting Technique

Photographic sequences reaching $m_V \approx 19$ were needed in both survey fields. In order to reach these faint stars it was necessary to use an offsetting technique: the telescope was guided on neighboring bright stars while observations of the faint stars were being made. The tailpiece of the 90-inch telescope is equipped with an offset guider. The guider is equipped with accurate screws, and is intended to be capable of offsetting to a fraction of a second of arc over distances of several minutes of arc.

One of the brighter stars in the field was selected as a guide star. A number of bright stars were centered in the diaphragm, the offset reticle was centered on the guide star each time and the coordinate of the offset guider was recorded to 0.01 millimeters. Finally, the guide star was centered in the diaphragm of the photometer, the reticle of the offset guider was set on it, and the coordinate of the offset guider was recorded. These measurements could be repeated to a fraction of a second of arc.

The positions of all sequence stars, and the bright stars for which the offset coordinates had been determined, were measured from direct plates of the two fields. The two screw D. W. Mann comparator of the Steward Observatory was used for the measurements.

Because the direct plate had been taken with the field flattener in place, there was a difference in the scale of the positions measured from the plates and by the offset guider. Some care was taken to place the plate on the measuring table so that there would be no rotation between the two sets of coordinates. The scale factor between the direct measurements with the offset guider, and the measurements of the photographic plate was found to be 0.985, and all positions measured from the plates were multiplied by this constant to obtain offset coordinates for the program stars.

The telescope was set on a program star by adjusting the guider to the offset coordinate of the star and then placing the guide star on the reticle of the guider. This would place the program star well within the 10 second of arc diaphragm of the photometer. Offsetting could be done over distances of 1,000 seconds of arc (four inches), but it was noticed that over such distances the program stars were not well centered in the diaphragm.

In order to insure that the faint program stars were well centered in the diaphragm of the photometer, the telescope was first set on a bright star in the vicinity of the faint star. The centering of the bright star was checked and adjusted if necessary, and a correction to the offset coordinate was determined. The correction was applied to the offset coordinate of the faint star. In actual practice, then, it was necessary to do all offsetting from nearby bright stars. In order to insure uniformity in the observations, the regional standard stars were positioned in the diaphragm of the photometer by offsetting.

It was found that the corrections to the offset coordinates would change from night to night, in a sense that implied slight changes in the scale of the telescope. Such an effect could be caused by a change in the focal length of the telescope, i.e., by thermal variations in the figure of the primary.

CHAPTER IV

THE REDUCTIONS

The photographic and photoelectric data were reduced to magnitudes and colors on the CDC 6400 computer of The University of Arizona.

Reduction of the Photoelectric Data

The purpose of the photoelectric observations was to provide u-, v-, b- and y-magnitude sequences to be used for the calibration of the photographic plates. The normal procedure is to find the four-color indices directly from the observed instrumental magnitudes. However, combining the indices in the appropriate manner to obtain the u- and v-magnitudes would have resulted in an unnecessary propagation of observational errors into the magnitude sequences. In this study the photoelectric data were reduced to a y-magnitude and the (b-y), (v-y) and (u-y) color-indices.

The reductions were done by the PEPHOT 1 photoelectric reduction program of the Steward Observatory. The program, orinally written by Dr. W. S. Fitch, was modified by the writer to transform the observations to the system of the K.P.N.O. list of standard stars by the following equations.

$$y = y_I + Z_1 + k_1X + Rt$$

$$(b-y) = S_2(b_I-y_I) + Z_2 + k_2X$$

$$(v-y) = S_3(v_I-y_I) + Z_2 + k_3X$$

$$(u-y) = S_4(u_I-y_I) + Z_4 + k_4X$$

The values u_I, v_I, b_I, and y_I are the instrumental u-, v-, b-, and y-magnitudes. The values Z_1, Z_2, Z_3, and Z_4 are zero-point values of the magnitude or colors. The values k_1, k_2, k_3, and k_4 are the extinction coefficients and X is the air mass at which the star was observed. The term Rt makes allowance for any linear time dependent drift in the value of Z_1.

The catalog values of the colors of the standard stars were computed from the indices given in the K.P.N.O. list of four-color standards. The y-magnitudes of the standard stars were taken to be equal to the V-magnitudes given by Johnson et al. (1966).

The values of the zero-point (Z_i), slope (S_i), extinction (k_i), and rate (R) were determined by the method of least squares from the observations of the standard stars. Table VIII lists the extinction and slope coefficients found for the various nights during which the observations were made. The adopted photoelectric magnitudes of the sequence stars are listed in Appendix III.

The solution for the y-magnitude makes no allowance for a color dependence in the transformation to the

Table VIII. Photoelectric reduction coefficients.

Telescope	Date	k_1	k_2	k_3	k_4	S_2	S_3	S_4
36-inch	3/23/69	.217	.062	.176	.473	1.003	1.015	1.006
	4/15/69	.277	.052	.169	.473	1.040	1.035	1.002
	4/16/69	.208	.061	.185	.486	1.033	1.020	1.044
	4/19/69	.180	.069	.189	.487	1.037	1.013	1.055
	4/20/69	.209	.065	.175	.471	1.022	1.016	1.040
	4/21/69	.186	.062	.171	.465	1.031	1.010	1.047
	4/22/69	.175	.061	.170	.466	1.035	1.016	1.047
	4/23/69	.192	.058	.163	.465	1.035	1.009	1.052
	5/15/69	.193	.059	.167	.475	1.029	0.998	1.047
	5/16/69	.176	.055	.158	.461	1.029	0.995	1.049
	5/18/69	.195	.064	.159	.450	1.026	0.995	1.034
	5/19/69	.150	.059	.163	.466	1.041	1.000	1.049
	6/16/69	.127	.057	.168	.457	1.031	0.998	1.043
	6/17/69	.165	.053	.160	.450	1.034	1.007	1.049
	6/18/69	.161	.058	.173	.463	1.026	1.004	1.050
	6/19/69	.139	.065	.186	.477	1.019	1.005	1.048
90-inch	12/20/69	.112	.067	.184	.492	1.021	1.060	1.032
	3/25/70	.206	.055	.161	.490	1.005	1.048	1.008
	4/01/70	.166	.055	.178	.480	1.005	1.047	1.005
	4/11/70	.341	.070	.168	.463	1.001	1.046	1.003
	4/29/70	.154	.059	.177	.493	1.020	1.057	1.008
	5/03/70	.096	.014	.140	.467	1.021	1.056	1.004

V-magnitude system of the standard stars. This means that the y-magnitude is a natural magnitude which has been forced to fit only the zero-point of the standard system. In Figure 11 of Chapter II it is shown that there are no appreciable systematic differences between the natural y-magnitudes and the V-magnitudes of the UBV system.

Differences in the instrumental magnitudes measured with the v- and 4200-filters were corrected graphically for atmospheric extinction. The (v'-v) magnitude differences were plotted against the (b-y) color-index; from the plot a (v'-v) magnitude difference was assigned to a number of standard stars. The standard values were then used for a machine reduction of the (v'-v) data.

Reduction of the Photographic Data

A number of the stars chosen to be photoelectric sequence stars proved to have (b-y) color-indices greater than $0^{m}.45$. It was necessary to add a correction to the v-magnitudes of these stars to put them on the photographic v'-magnitude system. The corrections were taken from Figure 8. Most of these corrections were less than 0.1 magnitudes. The standard magnitudes of the sequence stars in the other spectral passbands of the photographic system were taken directly from the photoelectric photometry.

The iris photometer measurements of each plate were reduced independently. In order to perform the reductions, the standard magnitudes in the appropriate passbands were plotted against the iris readings of the sequence stars. A calibration curve, consisting of a series of straight line segments, was then drawn through the plotted points.

The magnitudes and iris readings of the ends of the line segments were placed in a table. The iris readings for all stars were then converted to magnitudes by a linear interpolation within the table. The magnitudes from all plates in a passband were averaged, and the (b-y)-color, and m_1-, and c_1-indices were found from the average magnitudes. The computed four-color magnitudes and indices of the program stars are listed in Appendix III.

Errors

The photoelectric observations are based on the K.P.N.O. four-color standard system. The faint stars were observed quite carefully and the offsetting was done with high enough precision to insure that the star being observed was well within the diaphragm at the time of the observation. In addition, the filters used for the photoelectric observations very closely matched the four-color filters used at the Kitt Peak National Observatory, resulting in good transformations of the observations to the

system of the K.P.N.O. four-color standard stars. There should be, therefore, no systematic errors in the photoelectric observations.

The photographic plates were calibrated by a photoelectric sequence in each field. Since the sequence stars are spread over a wide region in each field, errors caused by local irregularities in the photographic plates are incorporated in the random errors of the photographic photometry. In addition, the photographic and photoelectric systems are closely matched; therefore, the photographic observations also should be free of systematic errors.

One source of error which could be termed systematic results from inaccuracies in the drawing of the calibration curves. Although the errors at any given apparent magnitude may be systematic in character, these errors are produced by random errors in the photoelectric photometry and iris measurements. The systematic errors in the calibration curves will be discussed later.

Random Errors in the Photoelectric Photometry

The random errors in the photoelectric observations can be estimated from repeated independent observations of the same stars. They can also be estimated from the scatter in the plate calibration curves.

In general, five measures were made for each star observed with the 36-inch telescope. Because available time on the 90-inch telescope was limited, only a few of the fainter stars were observed twice. The probable errors expected for a single observation are listed in Table IX. The probable errors were determined from the data for the stars which were observed two or more times. The data for $y \leq 15$ and b, v, $u \leq 16$ refer to observations made with the 36-inch telescope and the data for fainter stars refer to observations made with the 90-inch telescope.

The scatter in the plate calibration curves is in general agreement with the data contained in Table IX. The scatter is somewhat lower than the expected errors at the faint end of the sequence, which is not surprising since the sequences were drawn in such a way that the scatter was minimized. If a greater number of faint standard stars had been observed, the freedom to draw the smooth curve close to all plotted points would have been more restricted, and it is likely that the scatter about the smooth curve would have been greater.

At the bright half of the sequence the scatter indicates errors of around $\pm$ 0.03 to $\pm$ 0.05 magnitudes. These errors are attributed to random errors in the photographic data.

Table IX. Random errors in the photoelectric observations.

Apparent Magnitude	Probable Error in Magnitudes			
	y	b	v	u
11	±.01	±.01	±.01	±.01
12	.01	.01	.01	.01
13	.02	.01	.01	.01
14	.03	.02	.02	.02
15	.06	.04	.04	.04
16	.07	.07	.07	.07
17	.10	.10	.10	.10
18	.14	.14	.14	.14
19	.17	.17	.17	.17
20		.20	.20	.20

Random Errors in the Iris Photometry

In order to evaluate the quality of the iris photometry, the iris readings for one plate in each color were plotted against the iris readings for the other plates in the same color. An envelope with a width of 20 units (arbitrary iris reading units) would contain well over half of the points in a plot of iris reading versus iris reading. There is a great deal of variation in the slope

of the calibration curves (iris reading versus magnitude), however, for most plates a scatter of ±10 iris reading units means a scatter of ±0.03 magnitudes. In general the slope of the calibration curve is greater at the faint end, which means the errors in the computed magnitudes are about $\pm 0^{m}.05$ for stars fainter than apparent magnitude 18.

The slope of the calibration curve depends strongly on the seeing conditions at the time the plate is exposed. Poor seeing produces large images; therefore, small differences in apparent magnitude result in large differences in the iris readings. The plates taken when the seeing was best have errors 1.5 times the size of those given above, which apply to average or poor seeing.

The errors in the iris photometry were almost entirely due to inhomogeneities in the photographic plates. The average error for a measurement with the iris photometer is less than ±0.01 magnitudes.

Since the plates were reduced independently, the scatter in the computed magnitudes could also be used to determine the internal accuracy of the measurements. The probable error of a single magnitude determination is about ±0.03 magnitudes even at the faint limit of the observations. The probable error of the final magnitudes is about $\pm 0^{m}.02$. This means that the probable errors in the computed y-magnitude, (b-y) color-index, m_1-index, and

c_1-index are expected to be $\pm 0^m.02$, $\pm 0^m.03$, $\pm 0^m.04$, and $\pm 0^m.04$, respectively. It must be emphasized that these are the probable errors computed from the internal scatter in the reduced data only.

Errors in Drawing the Calibration Curves

As mentioned before, the calibration curves are drawn by eye through a plot of the magnitudes versus the iris readings of the sequence stars in such a way that the scatter of points about the curve is a minimum. The expected error in the curve where it passes through a tight group of points would be approximately equal to the mean deviation of the points off of the curve, divided by the square root of the number of points in the group.

When the points representing the sequence stars are more evenly distributed along the calibration curve the errors are more difficult to estimate. If the calibration curve is a fairly straight line a number of points will influence the position of the curve near any single point. The probable error in the calibration curve would then be substantially lower than the probable error of a single plotted point. On the other hand, if the calibration curve is not straight, the curvature along it can be varied in such a way that it passes very close to, or through, each of a series of well distributed points.

In this case the probable errors in the curve would be equal to the probable errors of the individual points. At the ends of a sequence the uncertainty is somewhat larger than at other points because the direction in which the curve should continue is not known.

The errors in drawing the calibration curve result from random errors in the photographic and photoelectric photometry; however, they produce errors in the final data which are systematic in nature. An error of + ε magnitudes in a limited range of the calibration curve will result in every star within that range being given a magnitude too faint by the amount ε.

Systematic errors in the magnitudes result in still larger systematic errors in the colors and indices computed from the magnitudes. In this study the systematic errors in the computed (b-y) color-index and c_1- and m_1-indices could be as large as the random photometric errors listed in Table IX.

Large systematic errors do not rule out a comparison of the indices for the stars under investigation. The comparison can only be made, however, for stars with similar apparent magnitudes. On a plot of the (b-y) color-index against the m_1- or c_1-index, any scatter greater than the expected internal errors in the indices can be attributed to intrinsic differences between stars, providing the

range in apparent magnitudes for the stars plotted is not large.

Summary

Photoelectric u-, v-, b-, and y-magnitude sequences have been established in SA 27 and SA 56. These sequences have been reduced to the system of the K.P.N.O. four-color standard stars.

Photographic plates in each of the four colors have been measured on an iris photometer. The photoelectric sequences were used in converting the iris measurements to magnitudes.

The internal probable errors in the y-magnitudes, (b-y) color-indices, and m_1- and c_1-indices for the stars under investigation are ±0.02, ±0.03, ±0.04, and ±0.04 magnitudes respectively. These errors are caused almost entirely by inhomogeneities in the photographic plates, and are independent of the apparent magnitudes of the stars in question.

The external probable errors in the y-magnitudes, (b-y) color-indices, and m_1-, and c_1-indices are listed in Table X. These errors refer to the expected errors for stars with a spectral type of G5 III. The errors for stars brighter than y=16 are due primarily to the random errors

Table X. External probable errors in the photographic photometry.

y mag.	Probable Errors in Magnitudes			
	y	(b-y)	m_1	c_1
≤13	±.03	±.04	±.05	±.05
14	.03	.04	.05	.05
15	.03	.04	.05	.06
16	.04	.06	.08	.11
17	.06	.08	.14	.15
18	.09	.12	.18	.25
18.5	.11	.15	.20	.30

in the photographic measurements. For stars with $y \geq 17$, the errors are due primarily to the random errors in the photoelectric magnitudes of the sequence stars.

CHAPTER V

THE RESULTS

This chapter describes the method used to separate the stars in the survey into four groups, the halo giants and dwarfs, and the disk giants and dwarfs. Density distributions are determined from star counts in SA 56 and SA 27. The density distributions are then compared with those found by Becker and Fenkart; the agreement is found to be good.

The Correction for Interstellar Reddening

There have been many recent determinations of the interstellar reddening near the north galactic pole, some of which have included the region of SA 56. These determinations result from photoelectric observations in several photometric systems, of a variety of types of objects.

Bidelman and Westerlund (1960) and Westerlund (1963) have determined (B-V) color excesses of 110 early-type stars within 15° of the north galactic pole. They find the reddening to be negligible. McNamara and Langford (1969), from a study of the color-indices of the RR Lyrae-type variable stars, find $E(B-V) \leq 0^{m}.01$ near the north galactic

pole. McClure and Racine (1969) determined the (B-V) color excess in the direction of the globular clusters M3 ($b=78^{o}$) and M13 ($b=41^{o}$) from narrow-band photometry of late-type stars, and Crawford and Barnes (1969c) determined the reddening in the direction of the same clusters from four-color and Hβ photometry of A and F stars; both determinations show the reddening to be negligible. Peterson (1970) finds a total visual absorption, A_V, of 0.06 ± 0.07 magnitudes at the north galactic pole from his study of the magnitudes and colors of external galaxies. FitzGerald (1968), and Gottlieb and Upson (1969) find that the (B-V) color excess, E(B-V), is less than 0.1 magnitudes for all regions which have a galactic latitude greater than 20^{o}, except for a few clouds in the Ophiuchus region which extend up to a latitude of 40^{o}.

This wealth of information, from several independent sources, is taken as a justification for the assumption that the reddening in the direction of SA 56 is negligible. FitzGerald (1968) finds the reddening in the direction of SA 27 to be less than 0.1 magnitudes, but, since a more precise value was desired, a more careful analysis of the reddening in this direction was made.

The Bright Star Catalogue (Hoffleit 1964) and the photoelectric catalogue of Blanco, Demers, Douglass, and FitzGerald (1968) were searched for stars within 15^{o} of

SA 27 for which both UBV photometry and spectral classifications on the MK system were available. The intrinsic (B-V) color-indices for the various spectral types were taken from Gottlieb and Upson (1969), and the absolute magnitudes were taken from Schmidt-Kaler (1965).

The difference between a star's observed (B-V) color-index and its intrinsic $(B-V)_o$ color-index is taken as the (B-V) color excess of the star. These color excesses, E(B-V), found for the stars in the direction of SA 27, are plotted in Figure 17 as a function of the distance from the sun.

There is no indication of interstellar reddening to a distance of 200 pc from the sun in the direction of SA 27. The luminosity of the one star at 300 pc (HR 3612) is not known with certainty, therefore, the value of its color-excess is a few hundredths of a magnitude more uncertain than the values of E(B-V) for the other stars.

FitzGerald (1968) finds that the material which causes the reddening has a half thickness in the range 40 to 100 pc. Since there is no indication of reddening in the direction of SA 27 to z distance of 100 pc it seems reasonable to assume that the reddening in that direction is negligible over all distances.

The validity of the assumption of low reddening at all distances in the direction of SA 27 is borne out by

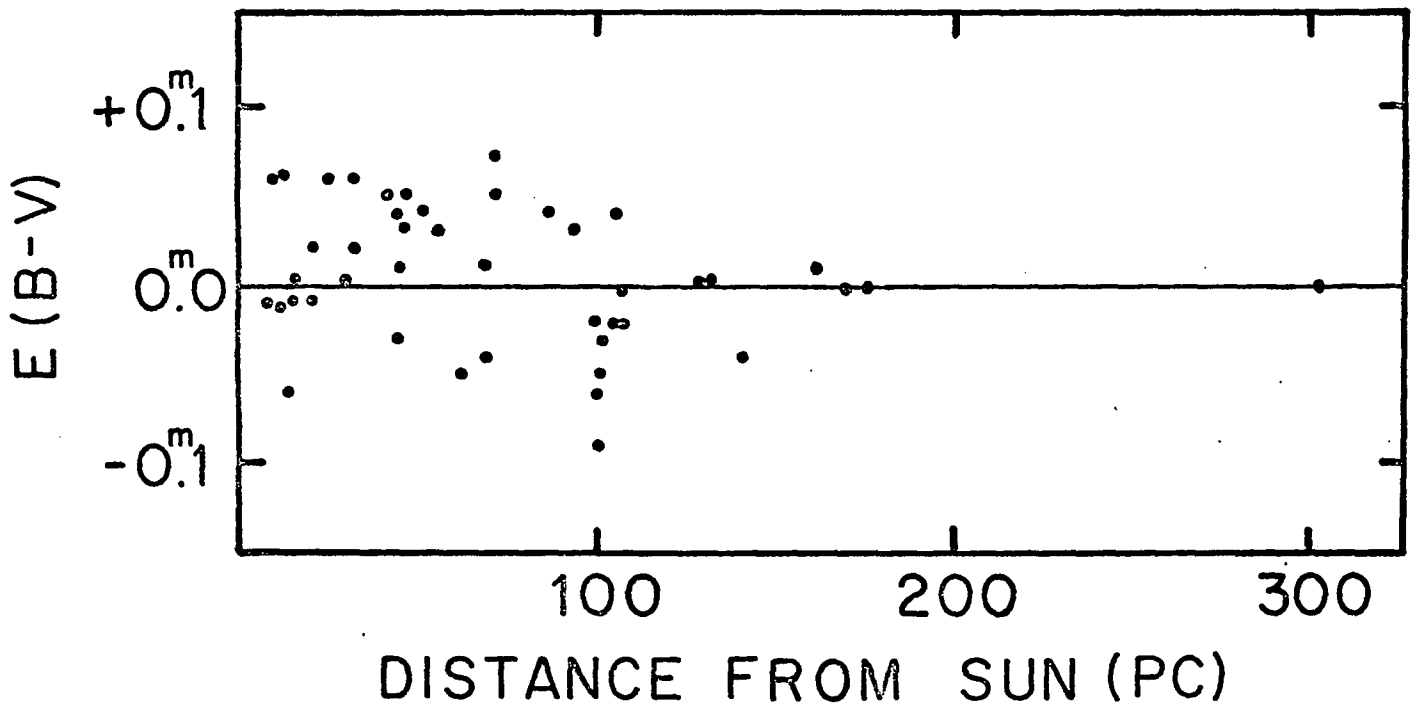

Figure 17. The interstellar reddening in the direction of SA 27.

the counts of galaxies in this region. Hubble (1934) finds the number of galaxies per square degree in the direction of SA 27 to be a few percent higher than that in the direction of the north galactic pole. The galaxy counts indicate that the negligible reddening observed at the galactic pole applies also to the direction of SA 27.

Hubble finds that the "zone of avoidance" where no galaxies are observed is narrowest in the direction of the galactic anticenter. This means that at the longitude of SA 27 ($l = 173^{o}$) the absorbing layer is very thin. The galaxy counts indicate that there is no interstellar absorption and reddening, in agreement with the results given from the negligible color excesses.

The Classification of the Stars

The stars in the survey were classified into four groups on the basis of their four-color indices. Stars with values of $\delta m_1 > 0.1$ are taken to be metal-poor stars, and are referred to as halo stars. The stars with lower values of δm_1 are referred to as disk stars. A few stars have δm_1 values characteristic of the disk group, but have an ultraviolet excess, $\delta(u-b) > 0.1$; these stars are taken to be members of the halo group.

The stars which have $\delta c_1 < 0.1$ are taken to be main-sequence stars. They are referred to as dwarfs. The

stars with $\delta c_1 > 0.1$ are referred to as giants. In Figure 3 there is an indication that the halo dwarfs with (b-y) > 0.6 have very low values of the c_1 index, with $\delta c_1 \lesssim -0.2$, and the (c_1, b-y)-diagrams for the survey stars show a similar result; therefore, halo stars which have (b-y) > 0.6 magnitudes, and δm_1 values as low as -0.1 magnitudes are classified as giants.

The classification of the stars has been made subject to one additional constraint. In Chapter IV it was pointed out that random errors in the photoelectric photometry of the sequence stars can result in systematic errors in the derived photographic magnitudes and indices of the program stars. The probable systematic errors in the photographic m_1- or c_1-indices, as indicated by Table X, are of the order of 0.05 magnitudes for stars brighter than y = 15, and may increase gradually to 0.2 magnitudes at y = 18.

Because these errors are due to errors in the drawing of the calibration curves, all stars within a limited range of apparent magnitude should exhibit the same errors in their indices; therefore, if data for the stars with $17.0 \leq y < 18$ are plotted in an (m_1, b-y) diagram, the plotted points may be shifted by 0.15 magnitudes with respect to the (m_1, b-y) relation of the Hyades main-sequence stars. The halo stars can still be separated

from the disk stars, in spite of the possible systematic errors in the m_1-index, because the halo stars will have higher values of δm_1 than the disk stars.

One case where such a systematic error is apparent is in the (m_1, b-y) diagram in Figure 26. The lower envelope of the plotted points is well defined, and is parallel to the main-sequence relation. Since these stars are bright it is likely that a number of them have normal metal abundance. In this case a star is considered a halo star if $\delta m_1 > 0.15$ magnitudes.

The four-color indices for the stars in the survey are plotted in (m_1, b-y)-, (c_1, b-y)-, and (u-b, b-y)-diagrams for several discrete ranges of the apparent y-magnitude. In SA 56 the ranges are, $y < 16$, $16 \leq y < 17$, $17 \leq y < 18$, and $y > 18$; the faint limit to the survey is reached at $y = 18.4$. More stars were observed in SA 27 than in SA 56 so it is possible to use a finer division of magnitude ranges. In SA 27 the divisions between the magnitude ranges fall at y = 14, 15, 15.5, 16.0, 16.5, 17.0, and 17.3; the faint limit to the survey is reached at $y = 17.6$.

The (m_1, b-y)-, (c_1, b-y)-, and (u-b, b-y)- diagrams for the two fields in the survey are shown in Figures 18 through 29. In these diagrams the triangles refer to halo stars and the circles refer to disk stars. The open

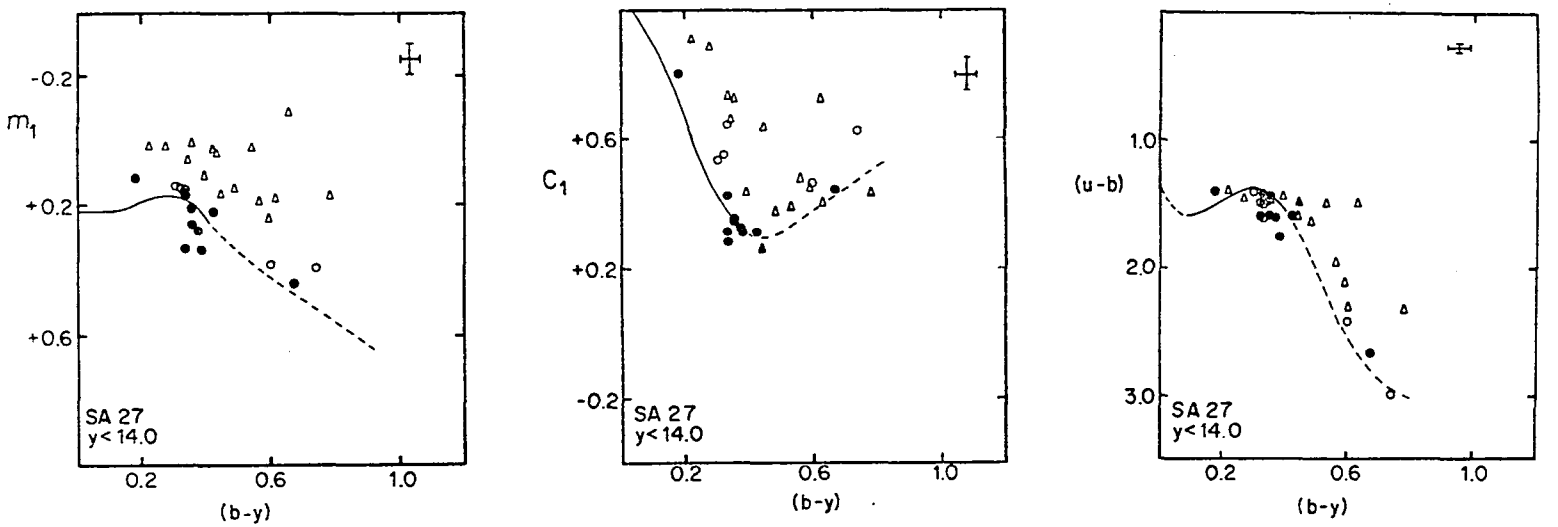

Figure 18. The (m_1, b-y)-, (c_1, b-y)-, and (u-b, b-y)-diagrams for the stars in the magnitude range y < 14.0 in SA 27.

The triangles refer to halo stars, and the circles refer to disk stars. The open figures indicate giants and the solid figures are for dwarfs. The cross in the upper right-hand corner of each diagram represents the probable internal errors in the photographic photometry. The solid lines are the Hyades and zero-age main-sequence relations as explained in the text. The broken lines are extrapolations of the main-sequence lines to later spectral types.

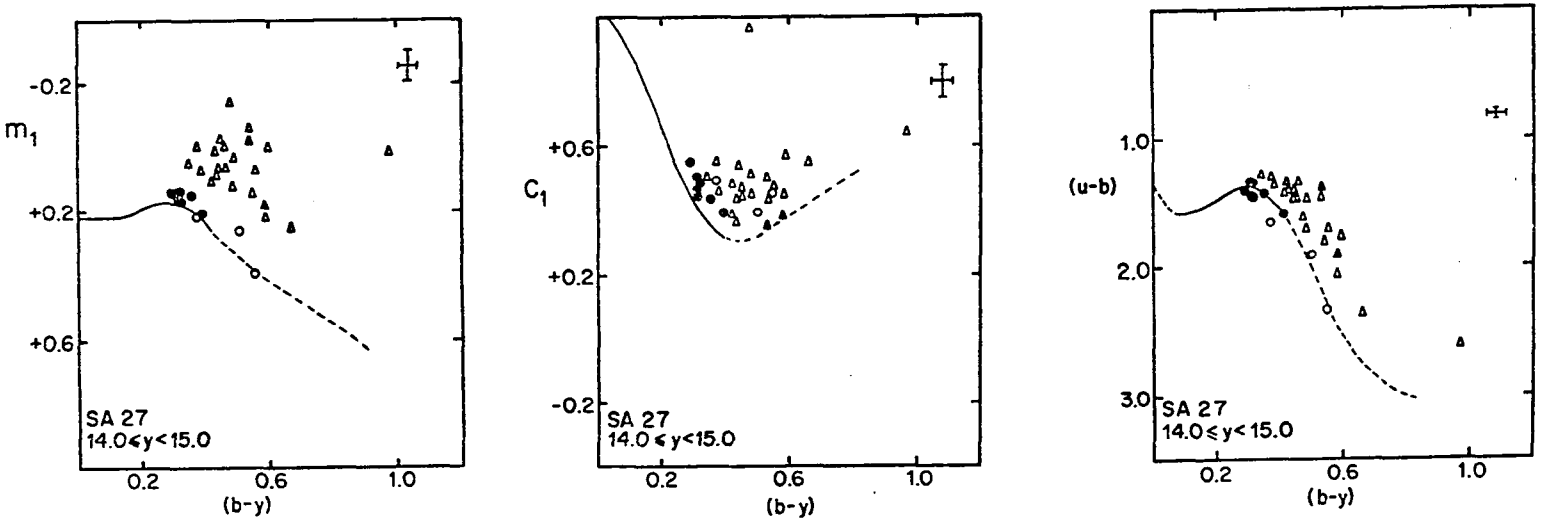

Figure 19. The (m_1, b-y)-, (c_1, b-y)-, and (u-b, b-y)-diagrams for the stars in the magnitude range $14.0 \leq y < 15.0$ in SA 27.

The symbols have the same meaning as those in Figure 18.

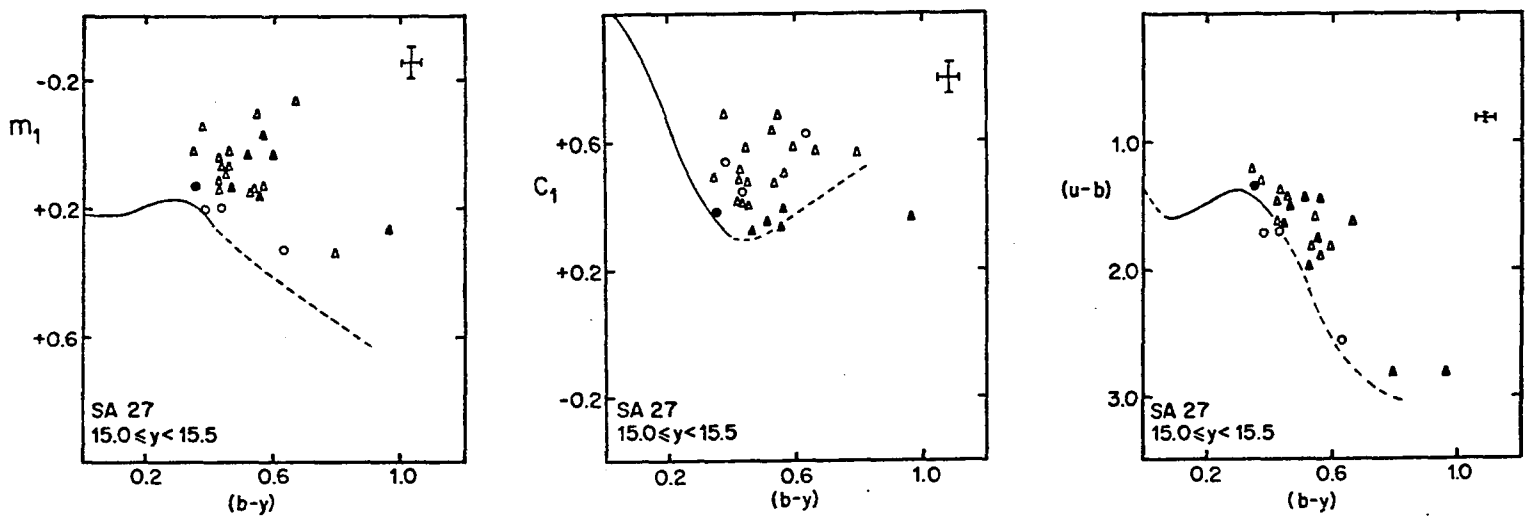

Figure 20. The (m_1, b-y)-, (c_1, b-y)-, and (u-b, b-y)-diagrams for the stars in the magnitude range $15.0 \leq y < 15.5$ in SA 27.

The symbols have the same meaning as those in Figure 18.

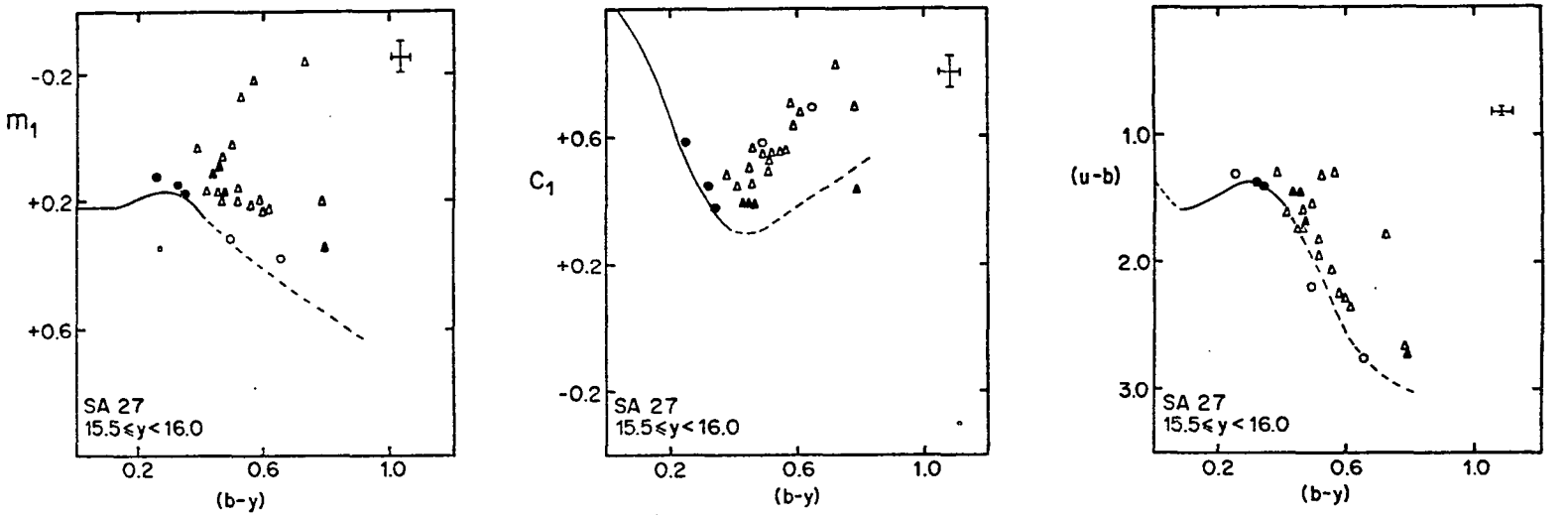

Figure 21. The (m_1, b-y)-, (c_1, b-y)-, and (u-b, b-y)-diagrams for the stars in the magnitude range $15.5 \leq y < 16.0$ in SA 27.

The symbols have the same meaning as those in Figure 18.

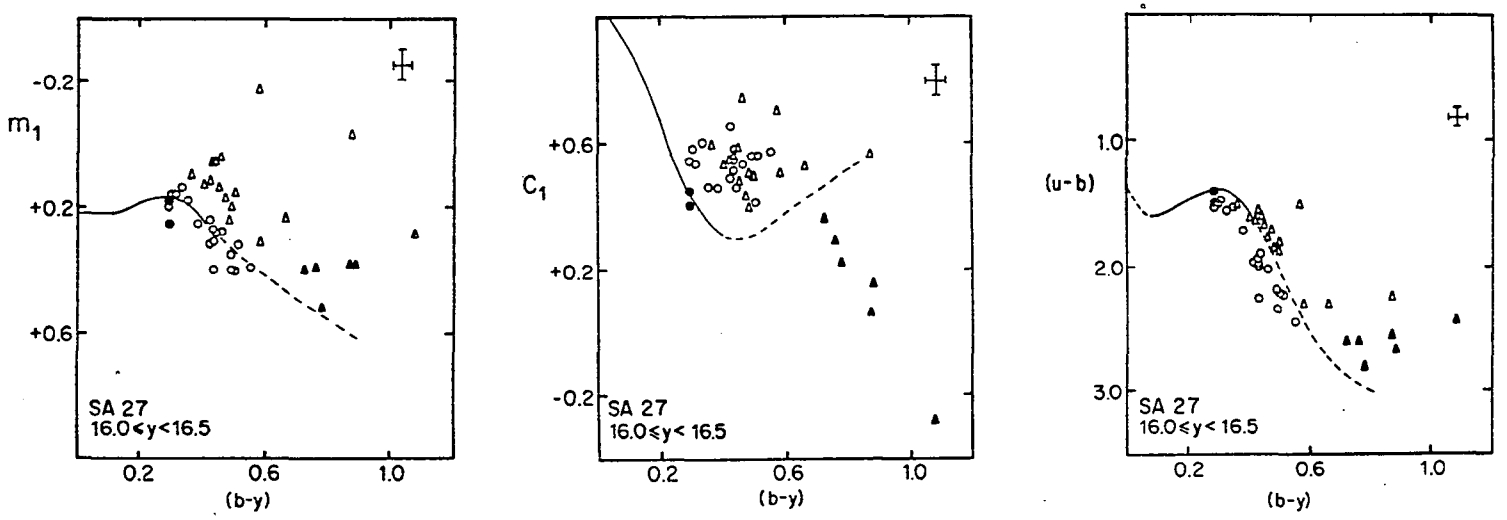

Figure 22. The (m_1, b-y)-, (c_1, b-y)-, and (u-b, b-y)-diagrams for the stars in the magnitude range 16.0 ≤ y < 16.5 in SA 27.

The symbols have the same meaning as those in Figure 18.

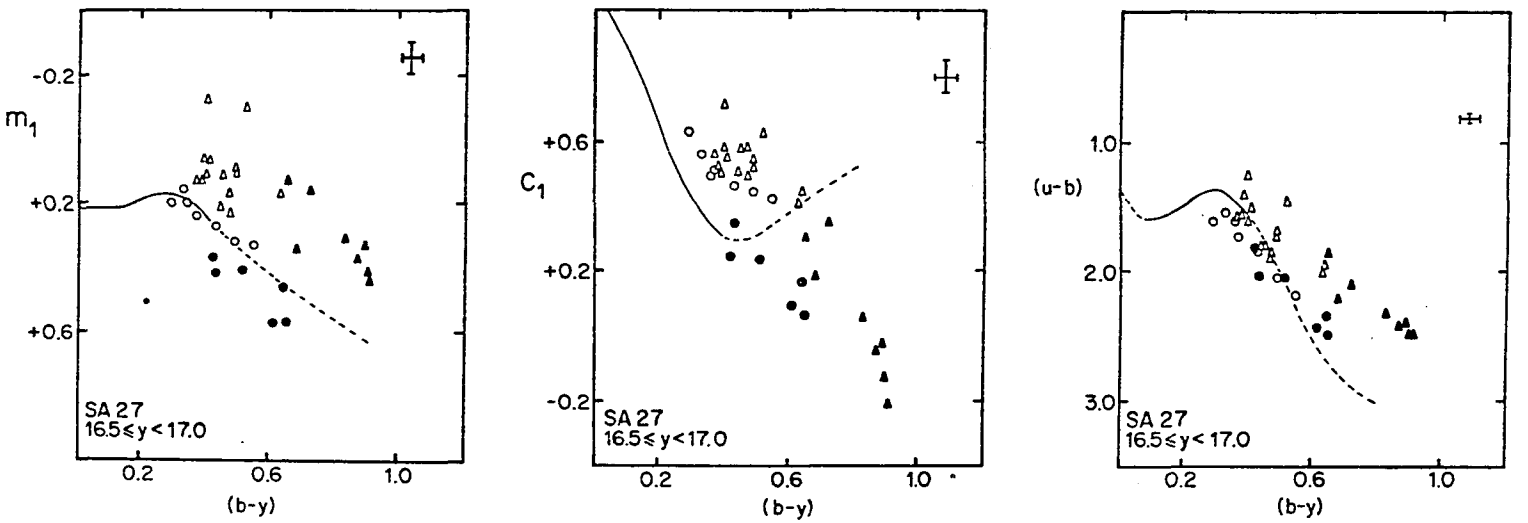

Figure 23. The (m_1, b-y)-, (c_1, b-y)-, and (u-b, b-y)-diagrams for the stars in the magnitude range 16.5 ≤ y < 17.0 in SA 27.

The symbols have the same meaning as those in Figure 18.

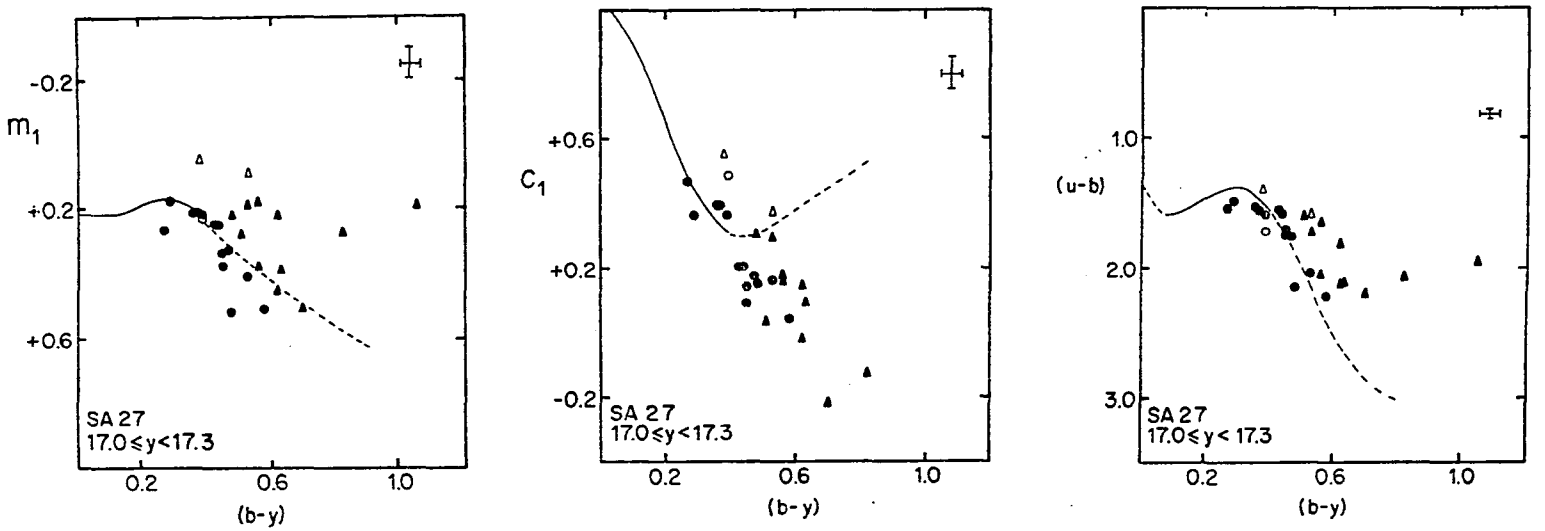

Figure 24. The (m_1, b-y)-, (c_1, b-y)-, and (u-b, b-y)- diagrams for the stars in the magnitude range $17.0 \leq y < 17.3$ in SA 27.

The symbols have the same meaning as those in Figure 18.

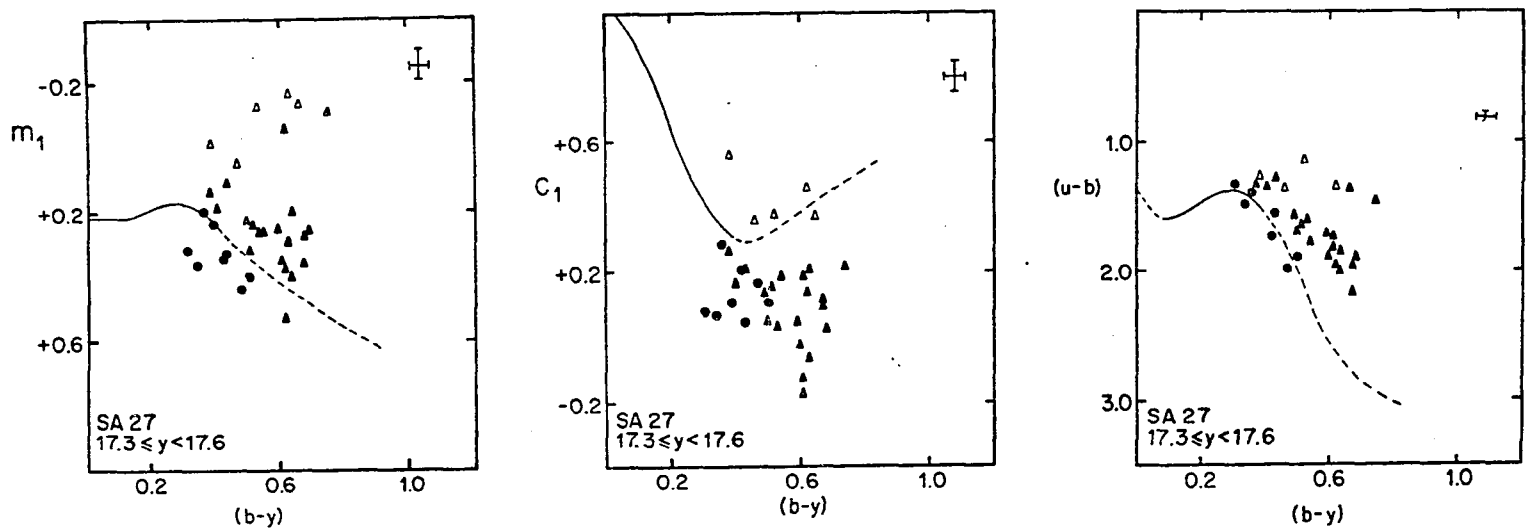

Figure 25. The (m_1, b-y)-, (c_1, b-y)-, and (u-b, b-y)-diagrams for the stars in the magnitude range $17.3 \leq y < 17.6$ in SA 27.

The symbols have the same meaning as those in Figure 18.

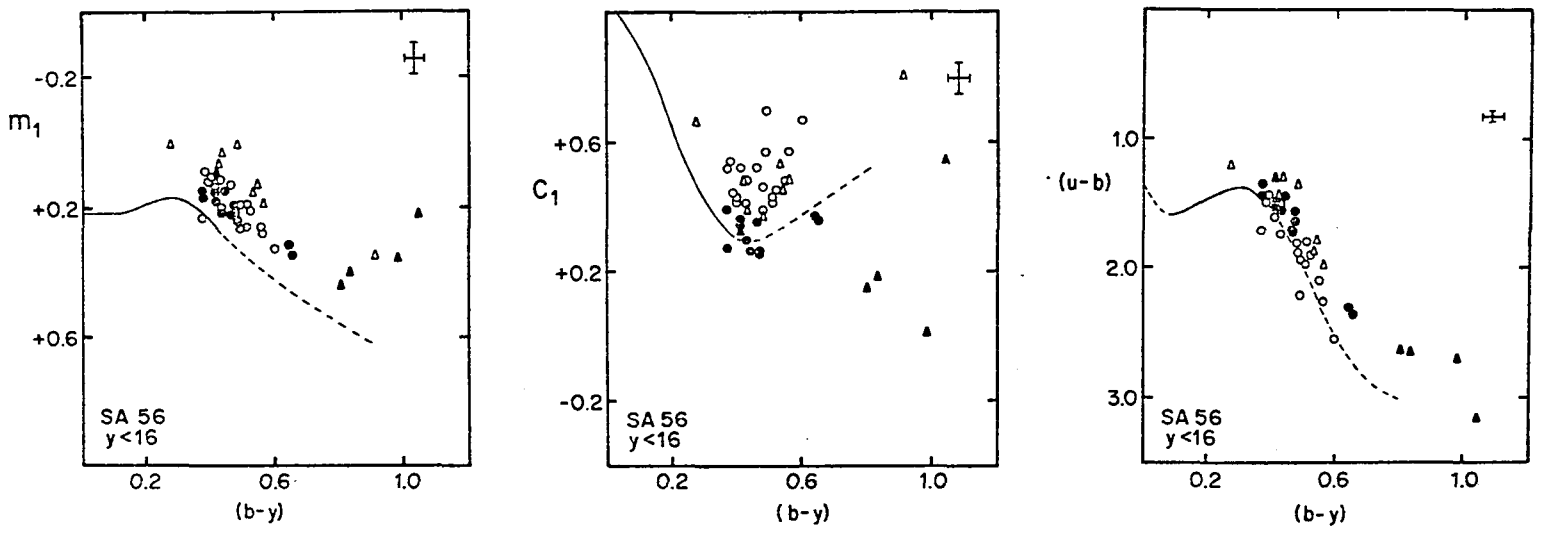

Figure 26. The (m_1, b-y)-, (c_1, b-y)-, and (u-b, b-y)-diagrams for the stars in the magnitude range y < 16 in SA 56.

The symbols have the same meaning as those in Figure 18.

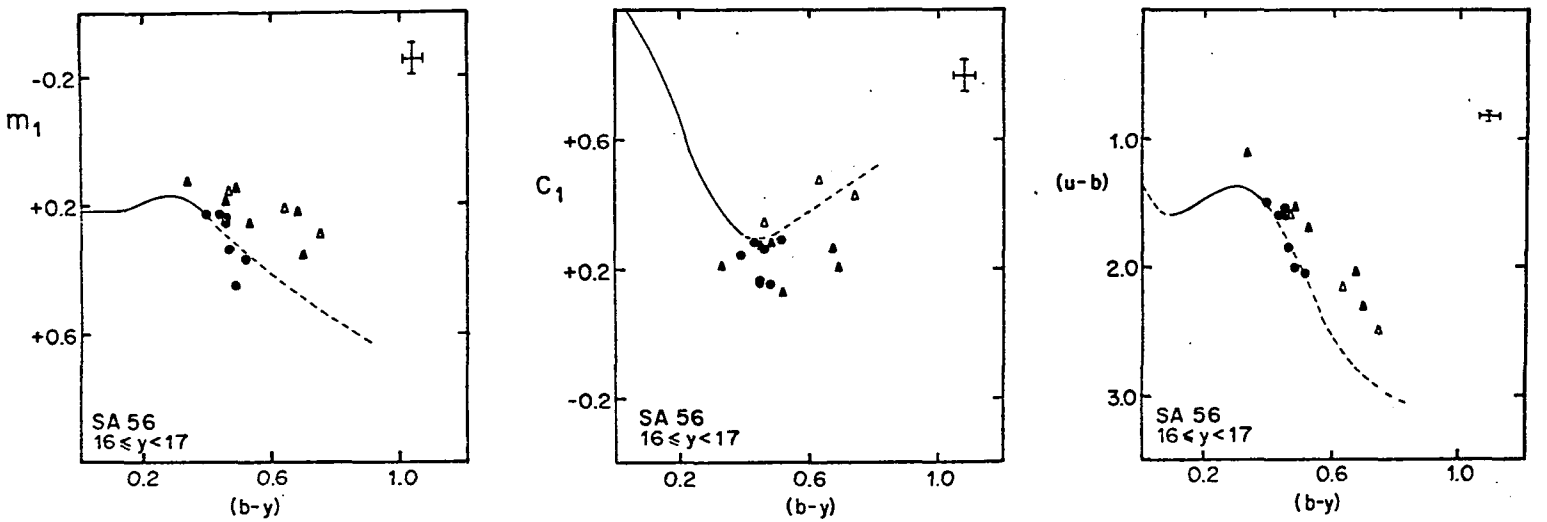

Figure 27. The (m_1, b-y)-, (c_1, b-y)-, and (u-b, b-y)-diagrams for the stars in the magnitude range $16 \leq y < 17$ in SA 56.

The symbols have the same meaning as those in Figure 18.

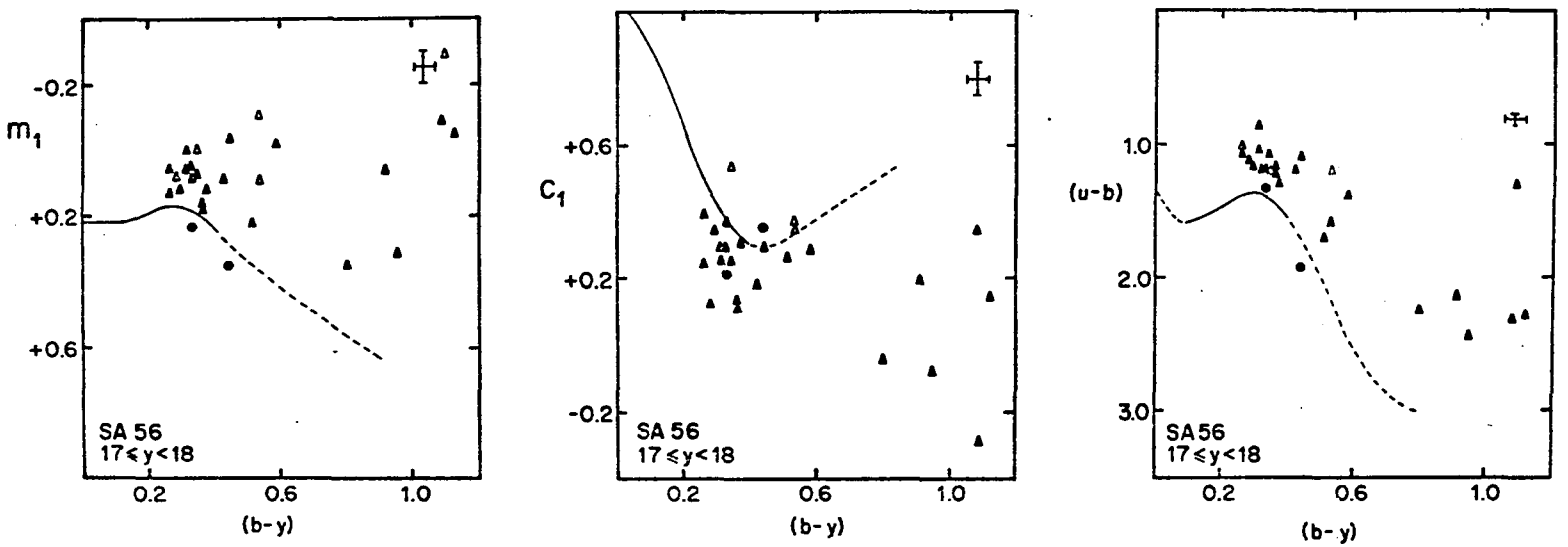

Figure 28. The (m_1, b-y)-, (c_1, b-y)-, and (u-b, b-y)-diagrams for the stars in the magnitude range $17 \leq y < 18$ in SA 56.

The symbols have the same meaning as those in Figure 18.

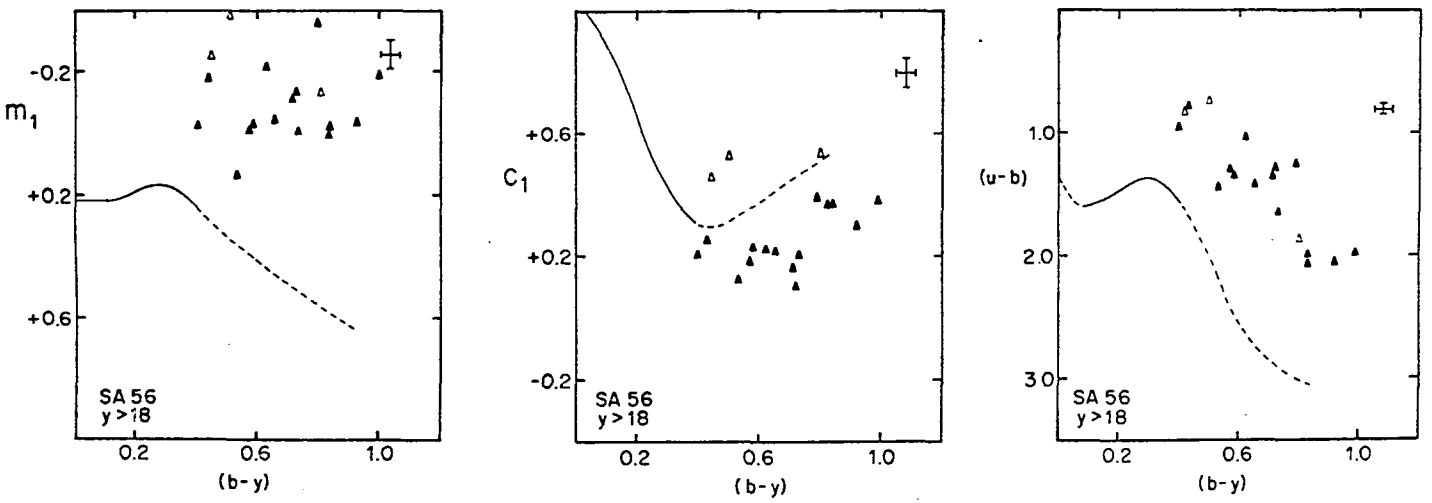

Figure 29. The (m_1, b-y)-, (c_1, b-y)-, and (u-b, b-y)-diagrams for the stars in the magnitude range y > 18 in SA 56.

The symbols have the same meaning as those in Figure 18.

figures indicate giants and the solid figures are for dwarfs. The probable errors shown by the cross in the upper right-hand corner of each diagram represent the internal errors in the photographic photometry. The solid lines in the (u-b, b-y)- and (m_1, b-y)-diagrams are the relations between those indices shown by the Hyades dwarfs (Crawford and Perry 1966), and the solid line in the (c_1, b-y)-diagram is the zero-age main-sequence relation given by Strömgren (1963a). The broken lines are extrapolations to later spectral types which have been corrected for the differences between the photographic and photoelectric four-color systems.

The General Star Counts

Two fields are included in the present survey in order to allow a comparison to be made between the stellar densities found in the direction of the north galactic pole (NGP) and the densities at a lower galactic latitude. The most direct comparison which can be made is based upon the numbers of stars observed in each direction. In the present study, the Oort-Vashakidse method (Oort 1938) and a modification of the Oort-Vashakidse method (Bok and MacRae 1941) are used to determine the ratio of the number densities of stars in SA 27 (at b = 28°) and SA 56 (near the NGP).

The Observational Limits of the Survey

The solid angle covered by the present survey is 0.21 square degrees for each field. The limiting y-magnitudes are 18.4 in SA 56 and 18.3 in SA 27. In order to insure the completeness of the star counts to the limiting magnitudes of the survey, images of all stars up to 0.25 magnitudes (100 iris reading units) fainter than the limiting magnitude were measured with the iris photometer. Magnitudes were determined only for those stars that have iris readings within the range of the calibration curves. In this way no images with iris readings that might have fallen within the range of the calibration curves were overlooked.

Although the limiting y-magnitude in SA 27 is 18.3, the stars fainter than y = 17.6 have not been classified according to their four-color indices. This is because the exposure time of blue plates of SA 27 was relatively short, and consequently they cannot be used with precision for stars fainter than $b \approx 18$.

The Oort-Vashakidse Method

The Oort-Vashakidse method makes use of certain geometrical considerations in order to compare star counts made in the direction of a galactic pole with star counts made at lower galactic latitudes. The star counts, A(m),

are defined here as the number of stars per 0.21 square degrees which have apparent magnitudes in the range $m-\frac{1}{2}$ to $m+\frac{1}{2}$.

Let us assume that there is a density gradient perpendicular to the galactic plane and that the surfaces are parallel to the galactic plane. If we define $\phi(M,z)$ as the number of stars per cubic kiloparsec at a height z above the galactic plane which have absolute magnitudes between M and M+dM, then, for a field at the NGP, we can write

$$A_{90}(m_{90}) = \omega \int_0^\infty \phi(M,z)dz \ ,$$

where

$$M = m_{90} + 5 - 5 \log z \ .$$

Now, since

$$z = r \sin b \ ,$$

the corresponding equation for a field at latitude b is,

$$A_b(m_b) = \frac{\omega}{\sin^3 b} \int_0^\infty z^2 \ \phi(M,z)dz \ ,$$

where

$$M = m_b + 5 - 5 \log z + 5 \log \sin b \ .$$

Therefore, if we define

$$m_{90} = m_b + 5 \log \sin b \ ,$$

we can write

$$A_b(m_b) = \frac{1}{\sin^3 b} \cdot A_{90}(m_{90}) \ .$$

This means that, if the surfaces of equal density are parallel to the galactic plane, we can predict the star counts expected for a field at latitude b from the star counts made in a field near the NGP. These predictions are totally independent of any assumptions about the luminosity function, $\phi(M,z)$, and the density gradient perpendicular to the galactic plane. All that is required is that the luminosity function $\phi(M,z)$ be applicable along the line of sight for galactic latitude b.

Therefore, the actual star counts made in a field at latitude b can be compared with the expected counts for that latitude, the latter derived from the star counts at the NGP. If the actual counts in a given field are lower than the expected counts for the latitude of the field, then the surfaces of equal density are presumably inclined toward the galactic plane in the directions of that field. If the actual counts are higher than the expected counts the surfaces equal density are inclined away from the galactic plane in that direction.

In the foregoing discussion no allowance is made for the effects of interstellar absorption. If the amount of absorption in each field is known its effects are easily taken into account by the Oort-Vashakidse method. However, as has been discussed previously, no appreciable amount of

interstellar absorption is observed in either SA 56 or SA 27; therefore, no corrections for absorption are necessary.

In this study the star counts made in SA 56 ($b=78^{o}$) are taken to represent the counts at the NGP. These counts are compared, by the method described above, with the counts obtained in SA 27 ($b=28^{o}$). For SA 27 the following values are found:

$$\sin^3 b = 0.10 ,$$

$$M_b = m_{90} + 1.65 .$$

The comparison of the star counts is made in Table XI. The columns headed by "m_{90}" and "M_b" give the values of the apparent magnitude in SA 56, and the corresponding magnitudes in SA 27 for which the values of A(m) were determined. The columns headed by "log $A_{90}(m_{90})$" and "log $A_b(M_b)$" give the logarithms of the observed star counts made in the two fields. The logarithms of the observed counts have been smoothed by a linear three-point formula, and the smoothed values are given in the columns headed by "[log $A_{90}(m_{90})$]" and "[log $A_b(M_b)$]", where the brackets are used to indicate that the data have been smoothed. The final column gives the value of $\delta(\log A)$, where

$$\delta(\log A) = [\log A_b(M_b)] - [\log A_{90}(m_{90})] - \log \sin^3 b.$$

The quantity $\delta(\log A)$ is the logarithm of the ratio of the

Table XI. The star counts in SA 27 compared with the star counts in SA 56 by the Oort-Vashakidse method.

m_{90}	log $A_{90}(m_{90})$	[log $A_{90}(m_{90})$]	m_b	log $A_b(m_b)$	[log $A_b(M_b)$]	δ(log A)
11	0.00	-0.15	12.65	0.85	0.91	+0.06
12	0.00	0.25	13.65	1.34	1.23	-0.02
13	1.00	0.62	14.65	1.52	1.50	-0.12
14	0.70	0.89	15.65	1.76	1.74	-0.15
15	1.15	1.09	16.65	1.91	1.95	-0.14
16	1.28	1.24	17.65	2.19	2.17	-0.07
17	1.36	1.41				
18	1.60:	1.57:				

actual value of $A_b(M_b)$ to the value predicted on the assumption of a plane parallel distribution of stars.

The last entry in the $A_{90}(m_{90})$ column is marked as being uncertain because the entire range from y=17.5 to y=18.5 is not covered by the survey. The number of stars (33) observed to the limiting magnitude of y=18.4 has been multiplied by the factor 1.21 in order to obtain the expected number of stars (40) if the limiting magnitude were y=18.5.

The negative values of δ(log A) in Table XI indicate that the surfaces of equal star density are inclined to the galactic plane in a pattern similar to the one given by Oort (1938). These values indicate that the densities at given z-distances in SA 27 are 0.75 times the densities at the same z-distances in SA 56.

The Modified Oort-Vashakidse Method

A modification of the Oort-Vashakidse method by Bok and MacRae (1941) makes use of (m, log π)-tables, to obtain information about the average distances of the stars in question. First, an (m, log π)-table is constructed, which represents the stellar distribution in the direction of the galactic pole. Star counts $A_b(M_b)$ are made in a field at latitude b. These star counts can be converted to the counts, $A'(m_{90})$, which would be obtained for an identical distribution of stars in the direction of the galactic pole by using the relations

$$A'(m_{90}) = \sin^3 b \; A_b(M_b)$$

and

$$m_{90} = M_b + 5 \log \sin b \; .$$

The (m, log π)-table for the galactic pole is then altered by adjusting the densities assumed for the various z-distances until the predicted counts agree with the values of $A'(m_{90})$. The densities at the various z-distances which yield the predicted counts in the closest agreement with the $A'(m_{90})$ values are taken to represent the distribution in z of the densities in the field at latitude b.

An (m, log π)-table has been constructed which predicts star counts in good agreement with those made in SA 56. This table, Table XII, is taken to represent the stellar distributions at the NGP. The first column of Table XII gives the volume in cubic kiloparsec of each unit range of distance modulus reached by the survey. The second column gives the distance in kiloparsec to the center of each volume element. The remaining columns give the number of stars in the apparent magnitude range $m_y - ½$ to $m_y + ½$ expected to be found in each volume element. The two rows at the bottoms of the table give the star counts predicted by the (m, log π)-table and the observed star counts in SA 56.

In the construction of Table XII we assumed the presence of a mixture of a halo and a disk component which,

Table XII. The (m, log π)-table for SA 56.

V(Kpc^3)	z(Kpc)	M_y	11	12	13	14	15	16	17	18
$4x10^{-7}$	.16		0.02	0.02	0.02	0.03	0.03	0.03	0.03	0.03
$1.6x10^{-6}$	.25		0.09	0.11	0.13	0.13	0.15	0.15	0.15	0.15
$6x10^{-6}$	.40		0.13	0.26	0.33	0.41	0.42	0.46	0.47	0.47
$2.5x10^{-5}$	.63		0.21	0.44	0.91	1.19	1.42	1.47	1.75	1.78
$1x10^{-4}$	1.0		0.45	0.52	1.06	2.21	2.97	3.62	3.80	4.20
$4x10^{-4}$	1.6		0.21	0.77	0.87	1.80	3.92	5.65	7.10	7.80
$1.6x10^{-3}$	2.5		0.07	0.23	0.69	0.69	1.54	3.94	6.93	9.56
$6x10^{-3}$	4.0			0.08	0.21	0.65	0.65	1.42	3.91	7.38
$2.5x10^{-2}$	6.3				0.11	0.29	0.85	0.76	1.81	5.21
$1x10^{-1}$	10					0.19	0.32	0.94	0.84	2.00
$4x10^{-1}$	16						0.19	0.32	0.94	0.84
1.6	25							0.12	0.31	0.91
6	40								0.12	0.29
A(m)	Predicted		1.2	2.4	4.3	7.6	12.5	18.9	28.2	40.6
A(m)	Observed		1	1	10	5	14	19	23	40:

together, would comprise the entire stellar distribution. The density distributions, $\nu(z)$, found by White (1967) for the disk- and halo-type RR Lyrae variables, are chosen to represent the density distributions of the two types of common stars. These density distributions, each normalized to unity in the galactic plane, are listed in Table XII.

Table XIII. The density distributions of the halo and disk stars.

Z(Kpc)	$\nu(z)/\nu(z=0)$	
	Halo	Disk
.16	1	1
.25	1	1
.40	1	0.85
.63	1	0.70
1.0	1	0.40
1.6	0.9	0.15
2.5	0.6	1.5×10^{-2}
4.0	0.2	1.5×10^{-3}
6.3	7×10^{-2}	10^{-4}
10	2×10^{-2}	
16	5×10^{-3}	
25	1.2×10^{-3}	
40	3×10^{-4}	

The luminosity function of the halo component is derived from the luminosity function of the globular cluster M3 (Sandage 1957) by multiplying that of M3 by the scale factor 0.53. The luminosity function of the disk component is derived from the van Rhijn (1936) luminosity function by multiplying it by a factor of 0.023.

These particular scale factors were used for two reasons. First, White (1967) finds that, in the galactic plane, the disk-type RR Lyrae variables are six times as numerous as the halo-type. The luminosity functions were scaled to achieve the same ratio of densities in the galactic plane for the disk and halo components of the common stars. Second, the scale factors used were subject to the constraint that the star counts predicted by Table XII agree with the observed counts in SA 56.

A final adjustment was made to the luminosity function derived for the halo stars, after an approximate agreement between the predicted and observed star counts was achieved. This adjustment was less than 25%, and it brought the predicted and observed star counts into close agreement.

The luminosity functions $\phi(M)$ so obtained were used in the construction of Table XII. These luminosity functions are listed in Table XIV. The entries in the

Table XIV. The luminosity functions of the disk and halo components.

M_y	$\phi(M)$ (#/Kpc^3 at z=0)	
	Disk	Halo
- 1	5×10^2	6.5×10^1
0	2.5×10^3	1.6×10^2
+ 1	1×10^4	4.7×10^2
2	1.2×10^4	4.2×10^2
3	2.4×10^4	1.0×10^3
4	4.8×10^4	2.9×10^3
5	6×10^4	5.7×10^3
6	7×10^4	8.2×10^3
7	7×10^4	1.0×10^4
8	8×10^4	1.0×10^4
9	8×10^4	1.1×10^4
+10	8×10^4	1.1×10^4

second and third columns give the number of stars per cubic kiloparsec with absolute magnitudes in the range M-½ to M+½.

The (m, log π)-table for SA 27 (Table XV) was constructed from the (m, log π)-table for SA 56 by changing the densities assumed for the various z-distances until the

Table XV. The (m, log π)-table which represents the stellar distribution as a function of z in SA 27.

$\nu(z)$ for SA 27 / $\nu(z)$ for SA 56	Z Kpc/M_{90}	11	12	13	14	15	16
1	.25	0.09	0.11	0.13	0.13	0.15	0.15
1	.40	0.13	0.26	0.33	0.41	0.42	0.46
.75	.63	0.26	0.33	0.68	0.89	1.07	1.10
.75	1.0	0.34	0.39	0.80	1.66	2.23	2.72
.75	1.6	0.15	0.59	0.74	1.35	2.94	4.25
.75	2.5	0.05	0.18	0.52	0.52	1.16	2.95
.75	4.0		0.06	0.15	0.49	0.49	1.06
.75	6.3			0.08	0.22	0.64	0.57
.75	10				0.15	0.24	0.71
.75	16					0.15	0.24
.75	25						0.09
.75	40						
	A'(m) Predicted	1.0	1.9	3.4	5.9	9.7	14.3
	A'(M_{90}) observed	0.7	2.2	3.3	5.8	8.2	15.5

predicted star counts agreed with the star counts $A'(m_{90})$ for SA 27. The stellar number densities in SA 27 are found to be 0.75 times those in SA 56 over a wide range of z-distance, which is the same value as we found by the simple Oort-Vashakidse procedure. Very few stars are expected to be observed within 0.5 kpc, or farther than 5 kpc from the sun. The results of the modified Oort-Vashakidse method are, therefore, insensitive to the densities assumed for those distances. Most of the stars contributing to the A(m) counts fall between 0.5 and 5 kpc, and over this distance interval the derived density ratio is meaningful.

The density ratio of 0.75, combined with the assumed density gradient in SA 56, results in surfaces of equal number density which are inclined about 5^{o} to the galactic plane, in the sense that the lower densities are found farther from the galactic center. A change in the density ratio of 0.05 would result in a change in the angle of inclination by one degree; therefore, a density ratio of 0.50 would mean that the surfaces of equal density are inclined by 10^{o}.

The Four-color Classifications Compared with the (m, log π) Data

A comparison can be made between the classification of the stars on the basis of their four-color indices and the number of stars of each type predicted by the

(m, log π)-table for SA 56. In Table XVI is given the number of stars classified as halo stars in each range of apparent magnitude, and the number predicted by the (m, log π)-table. The last entry in the observed A(m) column is uncertain because the observed count was made over an interval of 0.9 magnitudes, and it has been adjusted to give the expected count over a full magnitude interval. There is an excellent fit between the predicted and observed numbers of halo stars. This indicates that the density distributions and, to some extent, the luminosity functions used in the construction of the (m, log π)-table for SA 56 are appropriate and internally consistent.

Table XVI. The predicted and observed numbers of halo stars.

M_y	Predicted A(m)	Observed A(m)
11	0.2	0
12	0.5	0
13	1.1	3
14	2.3	2
15	4.7	2
16	9.3	9
17	17.2	18
18	28.8	30:

An additional check on the assumed luminosity functions can be made by comparing the percentages of giant stars predicted by the (m, log π)-table with the percentages of stars classified as giants. Those stars with absolute magnitudes $M_y \leq 3$ are taken to be giants. The observed and predicted percentages of giants are listed in Table XVII.

Table XVII. The predicted and observed percentages of giants.

M_y	% Predicted	% Observed
11	90	
		50 two stars
12	81	
13	68	40
14	48	80
15	20	86
16	19	26
17	17	9
18	10	20

Only 34 stars are classified as giants, and therefore, there are only a few in each range of apparent magnitude. The observed percentages, therefore, vary much less

smoothly than the predicted percentages. There is, however, a general agreement. Most stars brighter than y = 14 are found to be giants. For stars fainter than y = 14 the percentage drops off, reaching a value of about 10% at y = 18. The general agreement between the predicted and observed percentages gives additional evidence that the assumed luminosity functions are valid.

We are, therefore, able to reach a number of self consistent conclusions. The density distributions and luminosity functions used to construct Table XII result in predicted star counts very similar to those observed in SA 56. Moreover, they predict the observed counts of halo stars, and are in general agreement with the counts of giants which are observed in SA 56. The density distributions found for SA 27 by the Oort-Vashakidse method and the method of Bok and MacRae are also in close agreement. The surfaces of equal star density are found to be inclined 5° to the galactic plane.

A Comparison with the RGU Surveys by Becker and Fenkart

The three-color (RGU) surveys of common stars in the galactic halo by Becker (1965, 1967) and Fenkart (1967, 1968) have produced results very similar to those of this survey. Becker and Fenkart give the density distributions of dwarf stars as a function of distance from the sun in

direction of SA 57 ($b = 85^{\circ}$), SA 54 ($b = 59^{\circ}$, $l = 190^{\circ}$) and SA 51 ($b = 21^{\circ}$, $l = 189^{\circ}$). The galactic coordinates of the selected areas are on the new system (Blaauw et al. 1960).

Because the RGU system is not able to discriminate between dwarfs and giants, Becker and Fenkart assumed that all stars observed in their surveys were dwarfs. As has been shown in an earlier section of the present chapter, a considerable fraction of the stars brighter than $y = 15$ is likely to be composed of giants. The failure to recognize the large number of bright giants does not seriously affect the results of their surveys, however, because most of the stars they observe are fainter than fifteenth magnitude. The principal effect of the unrecognized giants is an overestimation by Becker's group of the derived densities in the vicinity of the sun, which results in a density gradient too steep within one or two kiloparsecs from the sun. At distances greater than two kiloparsecs the computed densities and density gradients should be substantially correct.

In the RGU system the (U-G) color excess is used to separate the stars according to metal content. Stars with large (U-G) excesses are taken to be halo stars while stars with normal (U-G) color-indices are referred to as disk stars. Fenkart finds that, at z-distances less than

5 kpc in the direction of SA 57 the densities of the disk stars are six times higher than those of the halo stars. This is similar to the ratio used in the present analysis for the construction of Table XII. The density gradient of the disk stars found by Fenkart is somewhat steeper than that given in Table XIII, and this may well be due in part to the presence of unrecognized giants.

The distributions of the halo stars found by Becker and Fenkart and those found in the present study agree quite well. This comparison is made for halo stars with absolute magnitudes in the range $5.0 \leq M(G) \leq 5.9$ because they have been observed by Becker and Fenkart to z-distances greater than 5 kpc in each of their fields, and because they are faint enough to avoid a serious contamination of the sample by giants.

Fenkart finds approximately 4×10^4 fifth magnitude halo stars per cubic kiloparsec at a z-distance of 1.6 kpc in the direction of SA 57. In the construction of Table XII a density of 5.4×10^4 stars per cubic kiloparsec was used. At $z = 4.0$ kpc a density of 1.2×10^4 stars per cubic kiloparsec was used, while Fenkart finds a density of 0.8×10^4 stars per cubic kiloparsec. The densities and the density gradient of the halo stars in SA 57 are very similar to those found in the present study for SA 56.

The densities Becker finds for the halo stars in SA 51, which have absolute G-magnitudes in the range 5.0 to 5.9, have been compared with the densities given by Fenkart for similar stars in SA 54 and SA 57. The results of this comparison are that the surfaces of equal density are inclined to the galactic plane by less than five degrees for z-distances greater than four kiloparsecs. The angle of inclination at a z-distance of 1.5 kpc is approximately 10°. This result is in general agreement with the inclination of five degrees found in the present study.

Summary

The results presented in this chapter are summarized as follows:

1) There is apparently no reddening in the direction of SA 27.

2) The photographic four-color system is shown to be capable of discriminating between stars of normal and low metal content, and between stars of high and low luminosity.

3) The star counts made in SA 56 are shown to be consistent with the density distributions and luminosity functions given in Tables XIII and XIV.

4) From the star counts in SA 56 and SA 27, the surfaces of equal star density are found to be inclined by 5° toward the galactic plane in the direction of the galactic anticenter.

5) The results of the RGU surveys of Becker and Fenkart are in general agreement with the density distributions found in this survey.

CHAPTER VI

ADDITIONAL RESULTS AND DESIDERATA

The Stellar Number Densities Found from the Four-color Photometry

It is possible to determine a distance for each star in the survey on the basis of its four-color indices. With a distance computed for every star, the density distributions for various types of stars can be found.

The Adopted Absolute Magnitudes

A star's absolute magnitude must be known before its distance can be determined. The absolute magnitudes adopted here are based on the color-magnitude diagrams for nearby stars (Parenago 1958), which certainly form a heterogeneous group and which probably represent the disk component, and for the globular cluster M3 (Sandage 1962) which is taken to represent the halo component.

The (B-V) color-indices of the (M_V, B-V)-diagram for the nearby stars are converted to (b-y) color-indices by the relationship given by Crawford, Barnes, and Golson (1970). The points representing the main sequence stars in the resulting (M_y, b-y)-diagram are divided into several ranges of the (b-y) color-index. The absolute magnitude

at the center of each range of (b-y) is taken to be the absolute magnitude of the disk dwarfs which have (b-y) color-indices within that range. The disk giants are assigned the absolute magnitude $M_V=0$ which is the average absolute magnitude of the nearby giants.

The relationship between (B-V) and (b-y) of Crawford et al. (1970) has been determined from observations of stars with normal metal content. The halo stars, however, are presumably highly deficient in metals. Since a (B-V) color-index is affected by line blocking, while a (b-y) color-index is relatively insensitive to metal content, the observed (B-V) of a metal-poor star must be corrected for the lack of line blocking before it can be converted to a (b-y) color-index.

Sandage (1962) gives a color-magnitude diagram for M3 in which the effects of line blocking have been added to the observed data. This corrected (M_V, B-V)-diagram is converted to an (M_y, b-y) diagram by the relationship given by Crawford et al. (1970). The absolute magnitudes appropriate to the halo giants and halo dwarfs in various ranges of (b-y) are determined in a similar manner to those of the disk dwarfs. The absolute magnitudes adopted for the halo dwarfs and giants and the disk dwarfs and giants are given in Table XVIII.

Table XVIII. The adopted absolute magnitudes.

Group	(b-y)	M_y
Normal Giants	all values	0.0
Normal Dwarfs	$0.15 \leq (b-y) < 0.25$	+3.0
	$0.25 \leq (b-y) < 0.35$	+4.0
	$0.35 \leq (b-y) < 0.45$	+5.0
	$0.45 \leq (b-y) < 0.65$	+6.0
Halo Giants	$(b-y) < 0.45$	+1.0
	$0.45 \leq (b-y) < 0.55$	+3.0
	$0.55 \leq (b-y) < 0.65$	+1.5
	$0.65 \leq (b-y) < 0.75$	0.0
	$0.75 \leq (b-y)$	-1.0
Halo Dwarfs	$0.35 \leq (b-y) < 0.45$	+4.0
	$0.45 \leq (b-y) < 0.60$	+6.0
	$0.60 \leq (b-y) < 0.75$	+7.0
	$0.75 \leq (b-y) < 0.90$	+8.0
	$0.90 \leq (b-y) < 1.00$	+9.0

A distance modulus (apparent minus absolute magnitude) is found for each star which is classified into one of the four groups, halo giants or dwarfs or disk giants or dwarfs. The number of stars in each group which have a distance modulus within the range $(m-M)-\frac{1}{2}$ to $(m-M)+\frac{1}{2}$

is determined for each value of the adopted absolute magnitude. Stellar number densities are computed from the counts of stars within each distance modulus interval by dividing the observed number of stars by the volume contained in the distance modulus interval.

The observed numbers of stars (n) and the corresponding density (ν), expressed in stars per cubic kiloparsec, are given in Tables XIX through XXII. The first column gives the distance (D) to the center of a distance modulus interval, and the second column gives the corresponding value of the distance modulus. The remaining columns give the observed numbers of stars in each interval and the corresponding densities.

In Table XIX the counts marked with a semicolon are made for a 0.9 magnitude interval in distance modulus. This is because the limit of the survey was reached at $y = 18.4$, while the unit distance modulus interval terminated at $y = 18.5$. The densities in the table are corrected for the ratio of the volumes of the partial interval of distance modulus and the complete interval.

The number densities given in Tables XIX through XXII lead to several interesting conclusions. A comparison of the densities of the halo giants observed in SA 56, and those observed in SA 27, shows that the densities at a given z-distance in SA 27 are about 0.7 times those at

Table XIX. The observed numbers of halo stars in SA 56.

A) Dwarfs

D Kpc	m-M	M_y = 4 n	log ν (#/Kpc^3)	6 n	log ν	7 n	log ν	8 n	log ν	9 n	log ν
0.16	6									1	6.40
0.25	7									0	<5.8
0.40	8							2	5.50	1	5.20
0.63	9	1	4.60			2	4.90	1	4.60	2:	4.98:
1.0	10	0	<4.0	2	4.30	0	<4.0	2:	4.38:		
1.6	11	0	<3.4	2	3.70	5:	4.18:				
2.5	12	0	<2.8	4:	3.48:						
4.0	13	11	3.24								
6.3	14	6:	2.46:								

Table XIX. (Continued)

B) Giants

D Kpc	m-M	$M_y = 0$ n	$M_y = 0$ ν (#/Kpc^3)	1 n	1 ν	1.5 n	1.5 ν	3 n	3 ν
0.63	9	1							
1.0	10							1	4.00
1.6	11					1	3.40	2	3.70
2.5	12					0	<2.8	1	2.80
4.0	13					0	<2.2	2	2.50
6.3	14					0	<1.6	0	<1.60
10	15			1	1.00	1	1.00	4:	1.68:
16	16			0	<0.4				
25	17	1	-0.20	1	-0.20				
40	18								

Table XX. The observed numbers of disk stars in SA 56.

D Kpc	m-M	Dwarfs M_y = 4		5		6		Giants 0	
0.16	6			1	6.40				
0.25	7			1	5.80	1	5.80		
0.40	8			3	5.68	0	<5.2		
0.63	9			1	4.60	1	4.60		
1.0	10			0	<4.0	5	4.70		
1.6	11			2	3.70	2	3.70	1	3.40
2.5	12			1	2.80			0	<2.8
4.0	13	1	2.20					2	2.50
6.3	14							2	1.90
10	15							11	2.04
16	16							2	0.70
25	17							0	<-0.2

Table XXI. The observed numbers of halo stars in SA 27.

A) Dwarfs

D		M_y = 4		6		7		8		9	
Kpc	m-M	n	ν (#/Kpc^3)	n	ν (#/Kpc^3)	n	ν	n	ν	n	ν
0.16	6									1	6.40
0.25	7									0	<5.8
0.40	8			1	5.20			4	5.80	3	5.68
0.63	9			5	5.30	1	4.60	4	5.20		
1.0	10	1	4.00	2	4.30	13	5.11				
1.6	11	0	<3.4	10	4.40						
2.5	12	1	2.80								
4.0	13	0	<2.2								
6.3	14										

Table XXI. (Continued)

B) Giants

D Kpc	m-M	M_y = -1 n	M_y = -1 ν (#/Kpc^3)	0 n	0 ν	.1 n	.1 ν	1.5 n	1.5 ν	3 n	3 ν
0.40	8										
0.63	9										
1.0	10					2	4.30	1	4.0	0	<4.0
1.6	11	1	3.46			2	3.70	0	<3.4	10	4.40
2.5	12	0	<2.8			1	2.80	1	2.8	12	3.88
4.0	13	0	<2.2			3	2.68	3	2.68	18	3.46
6.3	14	0	<1.6	1	1.60	3	1.90	7	2.45	12	2.68
10	15	1	1.00	0	<1.00	2	1.30	2	1.30		
16	16	1	0.40	3	0.88	4	1.00				
25	17	2	0.10	1	-0.20						
40	18	0	<-0.8								

Table XXII. The observed numbers of disk stars in SA 27.

D Kpc	m-M	Dwarfs $M_4 = 4$ n	Dwarfs $M_4 = 4$ ν (#/Kpc^3)	Dwarfs 5 n	Dwarfs 5 ν	Dwarfs 6 n	Dwarfs 6 ν	Giants 0 n	Giants 0 ν
0.16	6								
0.25	7								
0.40	8			4	5.80	1	5.20		
0.63	9	3	5.08	2	4.90	0	<4.6	1	4.60
1.0	10	2	4.30	2	4.30	0	<4.0	0	<4.0
1.6	11	3	3.88	0	<3.4	11	4.44	1	3.40
2.5	12	5	3.50	9	3.75			4	3.40
4.0	13	3	2.68					0	<2.2
6.3	14							4	2.20
10	15							6	1.78
16	16							20	1.70
25	17							8	0.70

the same z-distance in SA 56. This result is very close to that found from the star counts by the Oort-Vashakidse method.

A comparison between the densities of the halo dwarfs in SA 27 and SA 56 is not inconsistent with a plane parallel density distribution in which the densities decrease with increasing distance from the galactic plane. This comparison is not easily made, because the range in distance where the dwarfs of a given absolute magnitude are found is quite small.

It is surprising that the halo dwarfs in both fields show a definite density gradient within a z-distance of 1 kpc. Such an observed density gradient can be interpreted in one of two ways. Either the density gradient of the metal-poor dwarfs is real, in which case there would have to be a subgroup of metal-poor stars which has a low dispersion in their z-velocities, or a number of K dwarfs which have normal metal abundance are mistakenly classified as halo dwarfs.

No disk dwarfs having (b-y) >0.65 were found, either in SA 27, or in SA 56. The luminosity function of the nearby stars indicates that the disk dwarfs with (b-y) >0.65 should have higher space densities, higher than those of the bluer disk dwarfs. This means that a number of the redder disk dwarfs should have been found.

Many stars identified as halo dwarfs have (b-y) color-indices in the range 0.65 to 1.00, and since these are the very stars which show a density gradient within 1 kpc of the galactic plane, it seems likely that a number of them are disk stars incorrectly classified as halo dwarfs.

Although too few stars are observed to allow a determination of a luminosity function for the halo or disk stars, it is possible to make some comparisons between the densities found for stars with different absolute magnitudes. The brightest halo giants, those with $M_y \leq 0$, have space densities considerably lower than those of the horizontal branch stars ($M_y = 1$), or those of the halo subgiants ($M_y = 3, 1.5$). The halo subgiants, which are classified as giants, have densities at least a factor of 10 lower than those of the halo dwarfs. The halo dwarfs with $M_y = 4$ have densities somewhat lower than those of the fainter dwarfs. The densities of the disk giants are also found to be at least a factor of 10 lower than those of the disk dwarfs. While these comparisons would not allow a choice to be made between several possible luminosity functions, they are consistent with the luminosity functions adopted in Chapter V for the disk and halo components.

The density gradient for the halo giants in SA 56 is found to be very similar to the gradient found by

Kinman et al. (1966) for the RR Lyrae variables. The densities vary roughly as r^{-3} from a distance of 1 kpc to beyond 10 kpc. The densities of the halo giants are found to be 100 times higher than those found by White (1967) and Kinman et al. (1966) for the RR Lyrae variables.

In summary, the analysis of the star counts in Chapter V is to a great extent borne out by the density analysis for which the results are shown in Tables XIX through XXII. The density gradients of the halo and disk stars are similar to those used in the construction of Table XII, the (m, log π)-table for SA 56. The densities given in this chapter are consistent with the luminosity functions used in the construction of Table XII. Finally, the ratio of densities found in SA 56 and in SA 27 is the same as that found by the Oort-Vashakidse method. At a given height above the galactic plane, for $z > 1$ kpc, the space densities in SA 27 are about 0.7 times those at the same z-distance in SA 56.

Summary of Results

A set of filters has been developed, which can be used for photographic four-color photometry in a system similar to the photoelectric four-color system of Strömgren (1963a). The filters, and filter plus emulsion combinations,

which constitute the photographic four-color system are listed in Table IV.

The transformations between the photographic and photoelectric four-color systems have been determined. The only difference between the two systems is due to a less than ideal match of the photographic violet filter to the photoelectric violet filter. The amount of the correction to be applied to the violet magnitudes is shown in Figure 8.

The photographic four-color system has been applied to a study of the stellar distributions in Selected Areas 56 and 27. It is found to be a significant improvement over the three-color RGU system of Becker (1965), because the addition of the fourth color has made possible a discrimination between late type (spectral types F, G, and K) giants and dwarfs.

The photographic four-color data have been used to separate the stars in each of the two survey fields into four groups; the halo giants and dwarfs, and the disk giants and dwarfs. Space densities at various distances from the sun have been computed for each group.

The density gradient of the halo giants in SA 56 is found to be very similar to the r^{-3} density gradient found by Kinman et al. (1966) for the RR Lyrae variables near the north galactic pole. The space densities of the

halo giants are found to be approximately 100 times those given by White (1967), and Kinman et al. (1966) for the halo component of the RR Lyrae variables.

The space densities at given z-distances in the direction of SA 27 are found to be 0.7 times those at the same z-distances in SA 56. This result has been obtained directly from the star counts in the two fields by the use of the Oort-Vashakidse method of computing relative space densities for fields at different latitudes (Oort 1938), and also by the use of a modified Oort-Vashakidse method (Bok and MacRae 1941). The same result was obtained from the density analysis which was based on the four-color photometry.

The ratio of space densities found at a given z-distance in the two fields, when coupled with the r^{-3} density gradient found for SA 56, leads to the conclusion that the surfaces of equal space density are inclined to the galactic plane by five degrees, in the sense that the equidensity surfaces approach the galactic plane in the direction of the galactic anticenter. A comparison of the space densities given by Becker (1965, 1967) with those given by Fenkart (1967, 1968) leads to a similar inclination of the isodensity surfaces.

Suggestions for Future Research

As work on this program progressed, several areas which would prove fruitful for further research came to mind. Some of these are prompted by the deficiencies of the present study, and some are prompted by the results of this study.

One of the greatest limitations of the present survey is that the area covered in each field is only 0.21 square degrees. Only about 100 stars are included in the survey in SA 56, and just three times as many are observed in SA 27. The space densities derived from the four-color photometry, and those derived directly from the star counts, have presented a self-consistent picture of the stellar distributions in SA 56 and SA 27. However, statistical uncertainties in the star counts, and in the densities derived from the four-color photometry, are large enough that little information has been gained about the luminosity function of either the halo or the disk components. Moreover, since few of the survey stars are observed within 0.5 Kpc of the galactic plane, the density gradients of both components are poorly determined within that distance.

The obvious suggestion is to use a telescope like the 48-inch Schmidt telescope of the Hale Observatories, with the eight-inch square filters developed for use at the Steward Observatory, in order to extend the survey in

SA 56 to a larger area of the sky. The 48-inch Schmidt telescope, when used with eight-inch square filters, would cover an area approximately 50 times that covered in the present survey. The coverage of such a large area would decrease by a factor of seven, the statistical uncertainties in the star counts, and in the densities derived from the four-color data. It would, also, make possible the determination of space densities for the four groups of stars to distances much closer to the galactic plane than was possible in the present survey. These improved data should lead to a reliable determination of the luminosity functions of the disk and halo components, and to a direct determination of the relative densities of the disk and halo objects in the vicinity of the galactic plane.

If the 48-inch Schmidt telescope were available, the observing program would be as follows. Three plates of SA 56 would be taken in each of the four colors. The exposure times would be four hours in the ultraviolet and violet passbands, two hours in the blue passband, and 30 minutes in the yellow passband. A total of five nights would be required to complete the photographic observations. The faint end of the photoelectric sequence in SA 56 shows somewhat more scatter than is desirable. Two additional nights of photoelectric observations would give the calibration of the photographic plates the desired

accuracy. The photoelectric observations would have to be made with a telescope having an operture of at least 84 inches, preferably 90 inches or greater.

Plaut (1966) describes a program in which the space densities of the RR Lyrae variables have been determined in three fields, with galactic longitudes in the new system near zero, and with galactic latitudes near $+30^{\circ}$, $+12^{\circ}$, and -10°, respectively. Plaut finds that the RR Lyrae variables in these fields show a maximum space density at a distance of about 6 kpc from the sun, indicating that the galactic center may be considerably closer than the previously accepted value of 10 kpc. It would be very helpful if the four-color survey could be extended to include one or more of Plaut's fields.

A four-color survey in the direction of SA 108 ($l = 16^{\circ}$, $b = 29^{\circ}$) would be expected to show a distribution of stars similar to that found by Plaut in his first survey field. A survey of the common stars in SA 108 would also allow the isodensity contours determined in the present study to be extended in the direction of the galactic center. Such a survey could be carried out successfully with the use of the 90-inch telescope of the Steward Observatory. In order to complete the survey, five nights would have to be spent gathering the photographic material, and an additional four nights would be required to establish

the faint end of a photoelectric sequence. Some 12 stars in SA 108, with y-magnitudes ranging from 9 to 15, have already been observed photoelectrically during the course of the present survey.

One of the more interesting results of this study is the indication that the isodensity contours of the halo stars are inclined by only five degrees to the galactic plane. This is an important result because it has a direct bearing on the construction of models of the galaxy. Theoretical models of the galaxy are subject to several constraints. They must reproduce the observed curve of galactic rotation, the observed mass density in the solar neighborhood, and the observed distribution of stars at high galactic latitudes.

One of the most widely accepted galactic models, the Schmidt (1956) model, assumes an ellipsoidal distribution of halo stars in which the ratio of the minor axis to the major axis is 0.16. Such a distribution would lead to an inclination of the isodensity contours at a z-distance of 4 kpc of approximately five degrees. While this agrees well with the inclination found in the present study, and also with the results of Becker's group, it does not agree with the observed distribution of the globular clusters (Schmidt 1956) or the RR Lyrae variables (White

1967), both of which have ratios of the minor to major axis on the order of 0.5 (for distances greater than 10 kpc from the galactic center).

The inclination of the isodensity surfaces derived from the space density determinations of Becker and Fenkart, and that found in this study, depend on the densities found in the direction of the galactic anticenter. It is possible that there is an anomalous stellar distribution in that direction, and that, in general, the isodensity contours have a higher inclination. The importance of the low inclination found in the present survey makes a confirmation of this result desirable.

A verification of the low angle of inclination of the isodensity contours could come from a four-color survey of one or more fields with a galactic latitude of $+30^{\circ}$ and with longitudes well away from the anticenter direction. Two fields in which such a survey might be carried out are SA 77 ($l = 216^{\circ}$, $b = +38^{\circ}$) and SA 4 ($l = 140^{\circ}$, $b = +32^{\circ}$). In order to reach large enough z-distances these surveys would have to be made with a telescope having a large aperture, such as the 90-inch telescope of the Steward Observatory. The observing program would require nine nights of observing time per field, with the time being divided equally between the photographic program and the photoelectric observations of sequence stars. An additional

three nights of photoelectric observations with a telescope of moderate aperture would be required to establish the bright end of each photoelectric sequence.

A somewhat different, but equally desirable, program would be a detailed study of a globular cluster using the photographic four-color system. The type of each star would be known from its position in a color-magnitude diagram for the cluster. The dependence of the c_1- and m_1-indices on the stellar type could, therefore, be clearly established. A suggestion has been made by Dr. S. Strom (private communication) that there may be an enrichment of metals in the atmospheres of some evolved cluster members, due to a mixing of heavy elements from the interior of the star. Such an enrichment could be detected with the aid of the m_1-index.

The c_1-index is sensitive to differences in surface gravity between stars, at least to the extent that dwarfs can be separated from giants. If there are regions of a color-magnitude diagram of a globular cluster where the points representing stars which have undergone a significant loss of mass are found, then these regions may be indicated by variations in the c_1-index. A four-color study of a globular cluster might; therefore, provide information about the evolution of cluster members.

The value of the photographic four-color system, when applied to a study of stellar distributions at high galactic latitudes, has been established. There are, however, a number of other possible uses for this system. It could be used with a small Schmidt telescope in a search for stars of special interest, such as blue horizontal-branch stars, white dwarfs, or subdwarfs. The photographic methods could also be used as an alternative to photoelectric photometry in a study of open clusters. One must, however, seriously consider the advantages and disadvantages of the photographic methods before they are applied to a specific study. In general, the uses mentioned above could significantly reduce the observing time, although in a search for widely-scattered objects such as the blue horizontal-branch stars even this is doubtful. The reduction in observing time would, however, be obtained at the expense of a decrease in accuracy and a probable increase in the time needed to measure and reduce the data. Moreover, the equivalent, but more accurate, photoelectric observations would not require the use of a large telescope, and observing time is more readily available on telescopes with apertures up to 40 inches than it is on larger instruments.

The photographic four-color system is well suited to a study of stellar distributions at intermediate and high galactic latitudes. It is probable that its greatest application will be in this area of astronomical research.

APPENDIX I

THE GALACTIC FORCE LAW

The material presented in this section is compiled from several sources, including articles by Oort (1932, 1965), and Jeans (1915). Most of the material was taken from Bok (1970) and Mihalas and Routly (1968).

The Barometric Equation

Assume that at time t a group of stars is distributed according to the function

$$dN = f(x,y,z,U,V,W,t)\,dx\,dy\,dz\,dU\,dV\,dW\ ,$$

where x, y, z are space coordinates and U, V, W are the corresponding velocity components. It can be shown (Liouville's Theorem) that the density of points (stars) in the phase space remains constant:

$$\frac{dN}{dx\,dy\,dz\,dU\,dV\,dW} = f(x,y,z,U,V,W,t) = \text{Const.};$$

that is, if we follow a group of stars around in phase space, they will be found to always occupy the same total volume of phase space. We have,

$$f(x,y,z,U,V,W,t) = f(x+\delta x, y+\delta y, z+\delta z, U+\delta U, V+\delta V, W+\delta W, t+\delta t).$$

Therefore,

$$0 = \frac{Df}{dt} = \frac{\partial f}{\partial x}\frac{\partial x}{\partial t} + \frac{\partial f}{\partial y}\frac{\partial y}{\partial t} + \frac{\partial f}{\partial z}\frac{\partial z}{\partial t} + \frac{\partial f}{\partial U}\frac{\partial U}{\partial t} + \frac{\partial f}{\partial V}\frac{\partial V}{\partial t} + \frac{\partial f}{\partial W}\frac{\partial W}{\partial t} + \frac{\partial f}{\partial t}$$

or

$$U\frac{\partial f}{\partial x} + V\frac{\partial f}{\partial y} + W\frac{\partial f}{\partial z} + X\frac{\partial f}{\partial U} + Y\frac{\partial f}{\partial V} + Z\frac{\partial f}{\partial W} + \frac{\partial f}{\partial t} = 0, \qquad (1)$$

where (X, Y, Z) are accelerations in the (x, y, z) directions respectively.

Equation (1) is known either as the Collisionless Boltzmann Equation or as the equation of continuity. It is often called the "Fundamental Equation of Stellar Dynamics".

Because the Galaxy is roughly disk shaped, and it is useful to take advantage of this symmetry, the Boltzmann equation is written in cylindrical coordinates:

$$\frac{\partial f}{\partial t} + \Pi\frac{\partial f}{\partial r} + \frac{\Theta}{r}\frac{\partial f}{\partial \Theta} + Z\frac{\partial f}{\partial z} + \frac{\partial \Pi}{\partial t}\frac{\partial f}{\partial \Pi} + \frac{\partial \Theta}{\partial t}\frac{\partial f}{\partial \Theta} + \frac{\partial Z}{\partial t}\frac{\partial f}{\partial Z} = 0, \qquad (2)$$

where,

$$\Pi = \dot{r}\ , \quad \Theta = r\dot{\theta}\ , \quad Z = \dot{z}\ .$$

In cylindrical coordinates, if Φ is the potential energy per unit mass,

$$\text{a)} \quad \ddot{r} - r\dot{\theta}^2 = -\frac{\partial \Phi}{\partial r}$$

$$\frac{\partial \Pi}{\partial t} = \ddot{r} = \frac{\theta^2}{r} - \frac{\partial \Phi}{\partial r}$$

$$\text{b)} \quad r\ddot{\theta} + 2\dot{r}\dot{\theta} = -\frac{\partial \Phi}{\partial \theta}$$

$$\frac{\partial \Theta}{\partial t} = \dot{r}\dot{\theta} + r\ddot{\theta}$$

$$= -\frac{\partial \Phi}{\partial \theta} - \dot{r}\dot{\theta}$$

$$= -\frac{\partial \Phi}{\partial \theta} - \frac{\Pi\Theta}{r}$$

c) $$\frac{\partial Z}{\partial t} = \ddot{z} = -\frac{\partial \Phi}{\partial z} .$$

These relationships, substituted into (2) yield

$$\frac{\partial f}{\partial t} + \Pi\frac{\partial f}{\partial r} + \frac{\Theta}{r}\frac{\partial f}{\partial \theta} + Z\frac{\partial f}{\partial z} + (\frac{\theta^2}{r} - \frac{\partial \Phi}{\partial r})\frac{\partial f}{\partial \Pi} - (\frac{\pi\Theta}{r} + \frac{\partial \Phi}{\partial \theta})\frac{\partial f}{\partial \Theta} - \frac{\partial \Phi}{\partial z}\frac{\partial f}{\partial Z} = 0. \quad (3)$$

If it is assumed that the Galaxy is in a steady state, then

$$\frac{\partial f}{\partial t} = 0 .$$

The important equations of stellar dynamics are velocity moment equations obtained by multiplying the Boltzmann equation by $d\Pi\ d\theta\ dZ$, $\Pi d\Pi d\,\theta\, dZ$, $\Theta d\Pi d\Theta dZ$, or $Z d\Pi d\Theta dZ$, and integrating over all velocity space. The equation of interest for high latitude work is the one obtained by multiplying by $Z d\Pi d\Theta dZ$ and integrating. By performing the operation, and letting $\Delta = \Delta(r,\theta,z)$ be the number density of stars at a given point in the Galaxy, one obtains

$$\frac{\partial}{\partial r}(\Delta\ \overline{\Pi Z}) + \frac{1}{r}\frac{\partial}{\partial \theta}(\Delta\ \overline{\Theta Z}) + \frac{\partial}{\partial Z}(\Delta\ \overline{Z^2}) + \frac{\Delta}{r}(\overline{\Pi Z}) + \Delta\frac{\partial \Phi}{\partial z} = 0, \quad (4)$$

where the quantities $\overline{\Pi Z}$, $\overline{\Theta Z}$, and $\overline{Z^2}$ denote the average values of the products.

If we define the quantity

$$\frac{\partial \Phi}{\partial z} = -K_z \ ,$$

and assume rotational symmetry, which means that all derivatives with respect to θ are identically zero, equation 4 becomes

$$\frac{\partial}{\partial r} (\Delta \overline{\Pi Z}) + \frac{\partial}{\partial z} (\Delta \overline{Z^2}) + \frac{\Delta}{r} (\Pi Z) = \Delta K_z \ . \qquad (5)$$

In the galactic plane, where there is an ellipsoidal velocity destribution, there is an equal probability of positive and negative Z-velocities for each Π-velocity. The result is that the $\overline{\Pi Z}$ product is zero. Away from the galactic plane, where it is possible that the velocity ellipsoid is tilted toward the galactic center (due to the influence of the galactic center on the motions of the stars), the $\overline{\Pi Z}$ product may be greater than zero. White (private communication) has calculated that the $\overline{\Pi Z}$ term can become important for $z \geq 1$ kpc, but within this distance it is probably safe to assume $\overline{\Pi Z} = 0$. The equation governing the motions of stars, at least near the galactic plane, becomes

$$\frac{\partial}{\partial z} (\Delta \overline{Z^2}) = \Delta K_z(z) . \qquad (6)$$

This is the form of the hydrodynamical equation which is usually used in studies of the $K_z(z)$ force law.

Density and Velocity Distributions
Away from the Galactic Plane

It is of interest to ask, for a given density and velocity distribution in the galactic plane, what the density and velocity distribution will be at some height z. The relative density of stars in phase space having height z and velocity Z, f(z,Z), will be proportional to the length of time these stars spend in a volume element of phase space; that is,

$$f(z,Z)dz\ dZ = C\ dt$$
$$= C\ \frac{dz}{Z}\ .$$

If we assume

$$f(z,Z) = \Delta(z)\ \varphi\ (Z),$$

then

$$\Delta(z)\ \varphi\ (Z)dz\ dZ = C\ \frac{dz}{Z}\ . \qquad (7)$$

If we identify the values in the galactic plane with the subscript o, then

$$\Delta(o)\varphi_o\ (Z_o)dz_o\ dZ_o = \frac{dz_o}{Z_o}\ . \qquad (8)$$

Dividing (7) by (8) yields

$$\frac{\Delta(z)\ \varphi\ (Z)\ dz\ dZ}{\Delta(o)\ \varphi_o\ (Z)\ dz_o\ dZ_o} = \frac{dz}{Z}\ \frac{Z_o}{dz_o}\ .$$

Now

$$Z = \frac{dz}{dt}\ ,$$

and

$$K_z(z) = \frac{dZ}{dt} ;$$

therefore,

$$K_z(z)dz = ZdZ .$$

This integrates to

$$Z^2 - Z_o^2 = 2 \int_o^z K_z(z)dz = \text{Const.} ; \qquad (10)$$

therefore,

$$ZdZ = Z_o \, dZ_o . \qquad (11)$$

The substitution of (11) in (9) yields,

$$\Delta(z) \, \varphi \, (Z) = \Delta(o) \, \varphi_o \, (Z_o). \qquad (12)$$

If there is a Gaussian velocity distribution in the galactic plane, then

$$\varphi_o(Z_o)dZ_o = \frac{h}{\sqrt{\pi}} \exp \, (-h^2 Z_o^2)dZ_o, \qquad (13)$$

where

$$h^2 = \frac{1}{2\sigma^2} = \frac{1}{2Z_o^2} .$$

From (12) we obtain

$$\Delta(z) \, \varphi \, (Z) = \frac{\Delta(o)h}{\sqrt{\pi}} \exp \, (-h^2 Z_o^2). \qquad (14)$$

The substitution of (10) in (14) yields

$$\Delta(z) \, \varphi \, (Z) = \frac{\Delta(o)h}{\sqrt{\pi}} \exp \, [-h^2(Z^2 - 2 \int_o^z K_z(z)dz)], \qquad (15)$$

which when integrated over all Z becomes

$$\Delta(z) = \Delta(o) \exp \, (2h^2 \int_o^z K_z(z)dz) . \qquad (16)$$

Dividing (14) by (16) gives

$$\varphi(z) = \frac{h}{\sqrt{\pi}} \exp\left[-h^2(z_o^2 - 2\int_o^z K_z(z)dz)\right] .$$

With the substitution of (10), this simplifies to

$$\varphi(z) = \frac{h}{\sqrt{\pi}} \exp\left(-h^2 z^2\right) . \qquad (17)$$

This equation means that the velocity distribution at any height z is also Gaussian, with the same dispersion of velocities as in the galactic plane.

Comments on the Case of a Single Gaussian Velocity Distribution

If the velocities exhibit a single Gaussian distribution, the velocity dispersion is independent of z. It is possible to write

$$K_z(z) = \overline{z^2}\,\frac{d[\ln \Delta(z)]}{dz} . \qquad (18)$$

Now $\Delta(z)$ can be found from star counts at the galactic pole, and $\overline{z^2}$ can be found from nearby stars. This procedure simplifies the determination of $K_z(z)$ considerably.

When there is a single Gaussian distribution of velocities, the density at height z depends on the potential energy ($\int_o^z K_z(z)dz$), the velocity dispersion ($\overline{z^2}$), and the density in the galactic plane [$\Delta(o)$]. It can be seen from (16) that a high velocity dispersion (low h^2) implies a slow drop off in density away from the galactic plane; a low dispersion implies a rapid fall off in density.

Multiple Gaussian Velocity Distribution

If the sample of stars studied is a mixture of two or more kinematical groups, each with a different velocity dispersion, then the group with the greater dispersion in velocities will decrease more slowly in density. The ratio of the density of the high velocity group to that of the low velocity group will increase with increasing distance from the galactic plane. The result is that the velocity dispersion for the whole sample of stars will increase with increasing z. In this event, a solution for $K_z(z)$ must be made with the use of equation (6) instead of equation (18). In particular, $\overline{Z^2}(z)$ must be determined.

Poisson's Equation and the Determination of ρ_o

Poisson's equation in cylindrical coordinates takes the form

$$4\pi G\rho(z) = - \frac{\partial K_z}{\partial z} - \frac{\partial K_r}{\partial r} - \frac{K_r}{r} \quad ,$$

Where ρ is the total mass density, and K_z and K_r are the z- and r-accelerations; however,

$$K_r = -\Theta_c^2 / r \quad ,$$

where Θ_c is the velocity of an object in a circular orbit about the galactic center. We have

$$\frac{\partial K_r}{\partial r} = - \frac{2\Theta_c}{r} \frac{d\Theta_c}{dr} + \frac{\Theta_c^2}{r^2} \quad ,$$

so that

$$-\frac{\partial K_r}{\partial r} - \frac{K_r}{r} = \frac{2\Theta_c}{r}\ \frac{d\Theta_c}{dr} \quad .$$

It can be shown that in the solar neighborhood

$$\frac{\Theta_c}{r} = A-B \ ,$$

and that

$$\frac{d\Theta_c}{dr} = -(A+B) \ ,$$

where A and B are the Oort constants of galactic rotation. Poisson's equation then becomes

$$4\pi G\rho(z) = -\frac{\partial K_z}{\partial z} - 2(A^2-B^2) \ .$$

With the commonly accepted values for A, B and $\Delta(o)$ it is found that

$$4\pi G\rho(o) \approx 30(A^2-B^2) \ .$$

Because the K_r terms are relatively unimportant in the solar vicinity, Poisson's equation is usually used in the form

$$4\pi G\rho(z) = -\frac{\partial K_z}{\partial z} \ . \qquad (19)$$

If the $K_z(z)$ force law has been determined by (6) or (18), it is a simple matter to use the slope of $K_z(z)$ to determine the total mass density in the solar vicinity by the equation

$$\rho_o = -\frac{\partial K_z}{\partial z} \ / \ 4\pi G \ . \qquad (20)$$

APPENDIX II

CONSTRUCTION OF THE COMPOSITE GELATIN FILTERS

The method of cementing filters presented here is not the only one possible, nor is it necessarily the best method. It is simply a procedure arrived at by this writer after some experimentation; most important, it is a procedure which yielded good quality eight-inch square filters on more than half of the attempts.

The materials used were Eastman Kodak Wratten filters, glass from rejected photographic plates (the emulsion was stripped off with the aid of hot water), Eastman Kodak HE-S-1 optical cement, and acetone to clean away the excess cement. The HE-S-1 optical cement was used in preference to balsam because it sets to form a hard plastic layer over the entire face of the filter, resulting in a very sturdy, easily handled filter.

The actual construction was carried out under an exhaust hood kindly made available by Dr. A. K. Pierce of the Kitt Peak National Observatory. The use of an exhaust hood was necessary because of the presence of dangerous fumes, both from the cement and from the acetone.

Pegs were placed in a clean working surface to keep the parts being cemented from sliding over each

other. All surfaces to be cemented were thoroughly cleaned, and a piece of gelatin, cut to the correct size, was placed flat on the working surface.

A pool of cement was poured in the center of the gelatin. The cement was poured in an "X" pattern so that it could be more easily squeezed into the corners. Great care had to be taken while pouring the cement in order to keep bubbles from being trapped in the cement. The occasional bubbles which did form were fished out of the pool with a sharp knife point.

A piece of glass was then lowered slowly onto the pool of cement. One edge of the glass was set against the pegs on the working surface and the other edge was slowly lowered until the entire piece of glass lay flat on the pool of cement. When the glass was lowered too rapidly, bubbles would form in the layer of cement, and these were difficult to remove.

The glass was gently pressed down to spread the cement toward, but not up to, the edge of the filter. The gelatine and glass were then quickly but carefully picked up, as a unit, and placed flat between the pegs of the working surface with the glass on the bottom. Another pool of cement was poured on the now upward facing layer of gelatin, and another piece of glass was lowered onto the cement.

By carefully pushing near the center of the upper piece of glass, and slowly working toward the corners, the two pools of cement were spread out over the entire filter. The excess cement was allowed to run out the sides of the sandwich. Any bubbles which happened to be trapped between the layers were squeezed out the side by pushing behind them and letting the excess cement carry them away.

When most of the excess cement had been forced out, the sides of the filter were lightly clamped (using spring type clothespins), and a flat disk five inches in diameter was placed under the center of the filter in order to lift it off the working surface. A similar disk was placed on top of the filter. A 50 pound weight was then placed on the upper disk and left there for two hours, forcing out the remaining excess cement.

With the excess cement forced out, the sides and corners of the filter were securely clamped and the filter was baked for 48 hours at 120^{o}F. After 48 hours, the cement had become a hard plastic which was soluble in acetone. When the filter had cooled the excess cement was washed away with acetone, and the surfaces were thoroughly cleaned.

The filter was completed by cementing the second piece of gelatin between the half of the filter just

completed and a third piece of glass. The final result is a filter consisting of two layers of gelatin sandwiched between three layers of glass with four layers of cement. The combination is very sturdy, and, if carefully made, transmits light quite uniformly.

APPENDIX III

THE OBSERVED DATA

The observed data are listed in this appendix. Tables XXIII and XXIV contain the observed photoelectric magnitudes of the sequence stars in SA 56 and SA 27 respectively. Tables XXV and XXVI contain the photographic y-magnitudes and four-color indices of the program stars in SA 56 and SA 27 respectively. Figures 30 and 31 are finding charts for the stars in SA 56 and SA 27 respectively. Star number 50 in SA 56 is BD $+29^{\circ}2251$. Star number 144 in SA 27 is BD $+44^{\circ}1667$.

An explanation of the remarks in the last column of Tables XXV and XXVI is as follows.

Std. - A photoelectric sequence star

DD - Stars classified as disk dwarfs

HD - Stars classified as halo dwarfs

DG - Stars classified as disk giants

HG - Stars classified as halo giants

The spectral types are from the Bergedorfer Spektral-Durchmusterung.

Table XXIII. Photoelectric magnitudes of the sequence stars in SA 56.

Star	y	b	v	u
50	8.29	9.20	10.86	12.92
39	10.36	10.71	11.88	13.18
22	11.03	11.58	12.44	13.69
14	11.50	11.93	12.56	13.48
52	12.69	13.08	13.62	14.52
24	12.78	13.38	14.38	15.91
65	13.20	13.62	14.24	15.16
70	13.21	13.62	14.21	15.04
92	13.51	14.04	14.81	15.96
96	13.36	13.82	14.54	15.55
101	14.14	14.52	15.10	16.06
12	14.48	14.90	15.48	16.39
103	15.17	15.68	16.42	17.66
23	15.27	15.73	16.52	18.01
67	15.60	16.25	17.32	18.92
56	16.47	16.92	17.64	18.45
27	17.51	17.81	18.30	19.10
15	17.78	18.47	19.22	20.04
21	18.23	19.12	20.02	-
35	18.55	19.84	-	-

Table XXIV. Photoelectric magnitudes of the sequence stars in SA 27.

Star	y	b	v	u
144	9.07	9.86	11.29	13.14
168	10.84	11.14	11.58	12.55
82	11.30	11.69	12.18	13.09
170	11.42	11.77	12.24	13.14
180	11.80	12.46	13.49	14.86
160	12.66	13.05	13.64	14.58
110	13.32	13.68	14.46	15.56
73	13.82	14.40	15.24	16.53
101	14.05	14.36	14.82	15.62
112	14.10	14.58	15.19	16.28
148	14.15	14.66	15.47	16.66
48	14.59	14.99	15.50	16.41
143	14.68	15.08	15.54	16.40
189	14.75	15.37	16.35	17.65
75	14.92	15.23	15.62	16.63
106	16.03	16.36	16.90	17.90
142	16.38	16.90	17.42	18.49
68	17.41	17.95	18.54	19.24
169	17.82	18.94	20.32	-
116	17.92	18.66	19.09	19.54
81	18.07	18.74	19.54	20.26
150	18.17	19.27	-	-
157	18.23	18.76	19.72	19.98

Table XXV. The magnitudes and four-color indices of the program stars in SA 56.

Star	y	(b-y)	(u-b)	m_1	c_1	Remarks
1	17.95	0.33	1.19	0.08	0.37	HG
2	16.04	0.48	2.01	0.45	0.15	DD
3	17.13	0.51	1.72	0.22	0.26	HD
4	15.95	0.47	1.57	0.19	0.25	DD
5	15.48	0.51	1.81	0.19	0.41	DG
6	15.16	0.52	1.91	0.21	0.45	DG
7	18.15	0.40	0.96	-0.02	0.20	HD
8	17.20	0.95	2.44	0.31	-0.08	HD
9	13.02	0.47	1.64	0.22	0.26	DD, G0
10	15.35	0.98	2.69	0.36	0.01	HD
11	18.00	0.53	1.46	0.14	0.12	HD
12	14.53	0.37	1.72	0.23	0.52	DG
13	17.62	0.29	1.16	0.12	0.34	HD
14	11.50	0.43	1.55	0.20	0.29	DD, std, G2
15	17.93	0.53	1.59	0.09	0.35	HG, std
16	17.44	0.42	1.20	0.09	0.18	HD
17	16.92	0.33	1.12	0.13	0.20	HD
18	17.57	0.26	1.03	0.06	0.29	HD
19	15.20	0.39	1.44	0.12	0.42	DG
20	18.16	0.96	-	-0.27	-	DG
21	18.33	0.80	1.87	-0.13	0.53	HG, std
22	11.03	0.55	2.10	0.26	0.48	DG, std, G4
23	15.26	0.48	1.88	0.23	0.46	DG, std
24	12.74	0.60	2.53	0.33	0.-7	DG, std, K2
25	18.19	0.73	1.66	0.00	0.20	HD
26	17.05	0.44	1.93	0.35	0.35	DD
27	17.45	0.37	1.29	0.12	0.31	HD, std
28	17.39	0.44	1.09	-0.04	0.29	HD
29	17.31	0.34	1.07	0.07	0.25	HD
30	16.20	0.67	2.04	0.22	0.26	HD
31	15.94	0.27	1.22	0.01	0.66	HG
32	17.99	0.58	1.40	-0.02	0.28	HD
33	17.13	0.31	1.03	0.06	0.29	HD
34	13.32	1.04	3.06	0.22	0.54	
35	18.54	1.31	-	-	-	
36	15.74	0.40	1.43	0.11	0.41	DG
37	15.70	0.46	1.71	0.22	0.35	DD
38	15.49	0.65	2.36	0.35	0.36	DD
39	10.36	0.36	2.47	0.81	0.13	DD, std, K0
40	18.04	0.83	2.03	0.00	0.37	HD
41	17.56	0.31	0.87	-0.00	0.25	HD
42	17.65	0.34	1.21	0.00	0.53	HG

Table XXV. (Continued)

Star	y	(b-y)	(u-b)	m_1	c_1	Remarks
43	16.08	0.45	1.55	0.19	0.27	HD, std
44	14.34	0.49	2.20	0.26	0.70	DG
45	17.08	0.28	1.08	0.20	0.12	HD
46	17.50	1.08	2.32	-0.09	0.34	
47	16.22	0.46	1.58	0.16	0.34	HG
48	17.47	0.32	1.19	0.13	0.29	HD
49	13.56	0.54	1.79	0.13	0.45	HG, G0
50	8.29	0.91	3.72	0.35	0.80	HG, std, K3
51	17.16	1.12	2.28	-0.05	0.14	
52	12.73	0.37	1.43	0.15	0.39	DD, std
53	15.74	0.83	2.64	0.40	0.18	HD
54	16.33	0.69	2.30	0.36	0.20	HD
55	15.29	0.41	1.62	0.41	0.52	DG
56	16.47	0.45	1.53	0.24	0.15	DD, std
57	17.39	0.44	1.09	-0.04	0.29	HD
58	16.91	0.63	2.15	0.21	0.47	HG
59	14.24	0.42	1.46	0.07	0.48	HG
60	15.58	0.80	2.63	0.44	0.15	HD
61	18.36	0.79	1.25	-0.36	0.39	HD
62	18.19	0.73	1.66	0.00	0.20	HD
63	16.32	0.48	1.54	0.15	0.28	HD
64	15.31	0.38	1.48	0.09	0.54	DG
65	13.22	0.41	1.52	0.18	0.34	DD, std, G3
66	16.62	0.45	1.57	0.26	0.15	DD
67	15.62	0.64	2.29	0.32	0.37	DD, std
68	18.34	0.50	0.74	-0.39	0.52	HG
69	15.29	0.43	1.74	0.20	0.48	DG
70	13.32	0.37	1.35	0.17	0.27	DD, std, G1
71	17.80	1.14	-	-0.27	-	
72	15.29	0.46	1.70	0.13	0.52	DG
73	18.00	0.83	1.99	-0.02	0.37	HD
74	18.39	0.79	1.28	-0.13	0.10	HD
75	14.52	0.56	2.25	0.28	0.57	DG
76	15.25	0.53	1.89	0.15	0.53	HG
77	18.35	0.58	1.35	-0.02	0.23	HD
78	18.20	0.71	1.36	-0.11	0.16	HD
79	15.75	0.43	1.51	0.12	0.41	DG
80	13.69	0.49	1.93	0.19	0.57	DG, K2
81	18.03	0.99	1.98	-0.19	0.38	HD
82	17.22	0.91	2.13	0.06	0.19	HD
83	17.22	0.26	1.02	0.13	0.24	HD
84	17.90	0.53	1.21	-0.11	0.37	HG
85	15.95	0.44	1.44	0.15	0.26	DD

Table XXV. (Continued)

Star	y	(b-y)	(u-b)	m_1	c_1	Remarks
86	18.13	0.57	1.30	-0.01	0.18	HD
87	17.26	0.33	1.33	0.23	0.21	DD
88	16.55	0.52	1.69	0.26	0.13	HD
89	16.85	0.46	1.86	0.34	0.26	DD
90	17.14	0.36	1.17	0.17	0.11	HD
91	16.03	0.43	1.60	0.23	0.28	DD
92	13.47	0.56	1.98	0.19	0.48	HG, std
93	15.76	0.48	1.35	0.01	0.37	HG
94	18.00	0.92	2.07	-0.03	0.29	HD
95	17.49	0.80	2.25	0.35	-0.05	HD
96	13.36	0.48	1.81	0.23	0.39	DG, std
97	18.29	0.62	1.04	-0.21	0.22	HD
98	18.38	0.65	1.43	-0.04	0.21	HD
99	17.83	1.09	1.31	-0.29	-0.29	HD
100	18.32	0.43	0.77	-0.17	0.25	HD
101	14.12	0.41	1.48	0.15	0.36	DD, std
102	18.32	0.44	0.83	-0.25	0.45	HG
103	15.17	0.51	1.97	0.26	0.43	DG, std
104	13.48	0.41	1.32	0.09	0.32	HD
105	16.69	0.74	2.48	0.29	0.42	HG
106	16.94	0.51	2.05	0.37	0.29	DD
54a	17.06	0.36	1.19	0.17	0.13	HD

Table XXVI. The magnitudes and four-color indices of the program stars in SA 27.

Star	y	(b-y)	(u-b)	m_1	c_1	Remarks
1	13.52	0.06	1.48	-0.09	0.40	HG
2	14.08	0.97	2.60	0.01	0.64	HG
3	16.67	0.63	2.01	0.17	0.41	HG
4	17.05	0.53	1.61	0.09	0.37	HG
5	15.35	0.66	1.63	-0.13	0.57	HG
6	17.00	0.39	1.72	0.23	0.48	DG
7	17.30	0.68	1.90	0.26	0.02	HD
8	16.52	0.90	2.49	0.41	-0.13	HD
9	14.43	0.48	1.47	0.03	0.45	HD
10	16.65	0.45	1.70	0.11	0.58	HG
11	14.84	0.44	1.38	-0.02	0.54	HG
12	12.83	0.33	1.42	0.17	0.42	DD
13	16.33	0.46	1.76	0.05	0.74	HG
14	17.58	0.40	1.34	0.19	0.16	DD
15	15.78	0.59	2.03	0.15	0.55	HG
16	16.88	0.64	2.36	0.46	0.16	DD
17	15.16	0.54	1.58	-0.09	0.68	HG
18	16.50	0.72	2.11	0.16	0.35	HD
19	16.09	0.87	2.24	-0.03	0.56	HG
20	16.46	0.42	1.63	0.12	0.55	HG
21	12.70	0.35	1.47	0.21	0.35	DD
22	14.01	0.54	1.80	0.14	0.44	HG
23	16.67	0.47	1.86	0.17	0.58	HG
24	15.16	0.59	1.82	0.03	0.58	HG
25	15.44	0.56	1.45	-0.03	0.39	HD
26	15.32	0.51	1.43	0.03	0.35	HD
27	13.69	0.44	1.48	0.17	0.26	HD
28	14.74	0.59	1.75	0.00	0.57	HG
29	15.78	0.61	2.35	0.23	0.67	HG
30	17.23	0.56	1.65	0.18	0.17	HD
31	14.88	0.43	1.38	0.08	0.36	HG
32	15.64	0.72	1.78	-0.24	0.82	HG
33	17.40	0.63	1.87	0.20	0.21	HD
34	12.38	0.36	1.56	0.19	0.46	DG
35	17.58	0.52	1.15	-0.13	0.37	HG
36	16.12	0.43	1.54	0.06	0.56	HG
37	10.93	0.44	1.59	0.04	0.63	HG
38	14.45	0.53	1.44	-0.06	0.50	HG
39	16.51	0.33	1.54	0.16	0.56	DG
40	16.17	0.29	1.52	0.20	0.54	DG
41	12.83	0.33	1.42	0.17	0.42	DD
42	16.36	0.49	1.86	0.20	0.48	HG

Table XXVI. (Continued)

Star	y	(b-y)	(u-b)	m_1	c_1	Remarks
43	14.44	0.37	1.67	0.22	0.49	DG
44	14.90	0.31	1.44	0.16	0.50	DD
45	16.61	0.64	1.96	0.12	0.44	HG
46	16.08	0.47	1.71	0.17	0.43	HG
47	15.62	0.56	1.31	-0.18	0.55	HG
48	14.51	0.42	1.56	0.15	0.42	DG, Std
49	15.05	0.37	1.32	-0.05	0.68	HG
50	15.83	0.45	1.46	0.09	0.38	HD
51	13.74	0.53	1.49	0.02	0.39	HG
52	14.96	0.35	1.43	0.15	0.43	DD
53	14.77	0.58	2.05	0.22	0.45	HG
54	15.04	0.55	1.76	0.16	0.34	HD
55	17.40	0.74	1.47	-0.11	0.21	HD
56	17.39	0.54	1.78	0.26	0.18	HD
57	12.43	0.18	1.40	0.12	0.80	DD
58	17.55	0.35	1.40	0.31	0.08	DD
59	15.77	0.52	1.32	-0.13	0.54	HG
60	17.38	0.67	2.17	0.36	0.11	HD
61	16.69	0.87	2.43	0.37	-0.05	HD
62	15.56	0.65	2.75	0.38	0.69	DG
63	17.05	0.48	2.15	0.52	0.15	DD
64	13.60	0.33	1.60	0.33	0.28	DD
65	16.82	0.65	1.86	0.13	0.30	HD
66	15.01	0.45	1.41	0.02	0.47	HG
67	16.63	0.49	2.06	0.32	0.44	DG
68	17.53	0.43	1.28	0.11	0.20	HD, Std
69	15.23	0.35	1.34	0.13	0.38	DD
70	16.82	0.83	2.33	0.31	0.05	HD
71	16.06	0.44	1.58	0.06	0.58	HG
72	17.36	0.46	1.37	0.05	0.35	HG
73	13.79	0.59	2.11	0.24	0.45	HG, Std
74	13.91	0.56	1.97	0.19	0.47	HG
75	14.95	0.32	1.46	0.17	0.48	DD, Std
76	15.15	0.34	1.21	0.02	0.49	HG
77	16.21	0.40	1.59	0.13	0.53	HG
78	14.82	0.31	1.33	0.14	0.43	DD
79	17.25	0.62	1.82	0.22	0.14	HD
80	15.62	0.78	2.65	0.20	0.69	HG
81	18.14	0.67	1.57	0.09	0.05	HD, Std
82	11.35	0.35	1.44	0.01	0.72	HG, Std, F8
83	16.62	0.49	1.68	0.09	0.52	HG
84	17.02	0.53	1.73	0.19	0.29	HD
85	17.16	0.38	1.41	0.05	0.55	HG
86	16.14	0.57	1.50	-0.17	0.70	HG

Table XXVI. (Continued)

Star	y	(b-y)	(u-b)	m_1	c_1	Remarks
87	16.73	0.29	1.61	0.20	0.63	DG
88	17.43	0.42	1.74	0.35	0.20	DD
89	15.90	0.32	1.38	0.15	0.44	DD
90	15.45	0.38	1.70	0.20	0.54	DG
91	11.89	0.78	2.33	0.17	0.43	HG
92	17.33	0.59	1.72	0.25	0.04	HD
93	17.52	0.69	1.67	0.10	0.09	HD
94	11.98	0.33	1.60	0.15	0.64	DG, G2
95	17.57	0.38	1.29	-0.01	0.55	HG
96	16.96	0.68	2.22	0.34	0.18	HD
97	15.71	0.34	1.41	0.18	0.37	DD
98	13.19	0.32	1.67	0.32	0.39	DD
99	17.18	0.37	1.55	0.21	0.39	DD
100	16.49	0.31	1.47	0.16	0.53	DG
101	14.07	0.31	1.34	0.14	0.44	DD, Std
102	16.63	0.49	1.72	0.10	0.54	HG
103	16.31	0.42	1.97	0.32	0.49	DG
104	17.39	0.49	1.57	0.23	0.13	HD
105	14.46	0.50	1.91	0.26	0.39	DG
106	16.00	0.35	1.52	0.18	0.46	DG, Std
107	17.23	0.43	1.56	0.25	0.20	DD
108	15.39	0.42	1.47	0.11	0.41	HG
109	16.65	0.38	1.54	0.13	0.52	HG
110	13.33	0.38	1.75	0.34	0.31	DD, Std, G3
111	15.76	0.49	2.20	0.32	0.58	DG
112	14.16	0.48	1.71	0.12	0.51	HG, Std
113	16.39	0.43	2.24	0.40	0.58	DG
114	17.53	0.62	1.95	0.29	0.13	HD
115	14.13	0.29	1.41	0.14	0.55	DD
116	17.94	0.43	1.17	0.17	0.43	HG, Std
117	16.12	0.88	2.67	0.38	0.15	HD
118	17.55	0.36	1.40	0.20	0.28	DD
119	16.29	0.30	1.50	0.16	0.58	DG
120	16.85	0.61	2.45	0.57	0.09	DD
121	16.43	0.43	1.99	0.31	0.51	DG
122	17.39	0.60	1.87	0.35	-0.03	HD
123	16.94	0.51	2.07	0.41	0.23	DD
124	16.14	0.55	2.45	0.39	0.57	DG
125	16.25	0.49	2.34	0.40	0.56	DG
126	14.29	0.39	1.59	0.21	0.39	DD
127	16.10	0.45	1.66	0.14	0.48	HG
128	16.76	0.52	1.46	-0.10	0.62	HG
129	15.93	0.25	1.32	0.12	0.58	DD

Table XXVI. (Continued) The magnitudes and four-color indices of the program stars in SA 27.

Star	y	(b-y)	(u-b)	m_1	c_1	Remarks
130	16.16	0.66	2.30	0.23	0.52	HG
131	17.48	0.38	1.30	0.14	0.26	HD
132	16.04	0.78	2.81	0.52	0.21	HD
133	17.11	0.63	2.13	0.39	0.09	HD
134	17.19	0.45	1.75	0.38	0.09	DD
135	16.03	0.29	1.39	0.18	0.45	DD
136	17.59					
137	17.08	0.58	2.22	0.51	0.04	DD
138	17.38	0.62	1.35	-0.17	0.45	HG
139	16.41	0.49	2.18	0.35	0.50	DG
140	17.39	0.34	1.48	0.37	0.06	DD
141	16.16	0.50	2.21	0.40	0.41	DG
142	16.39	0.38	1.72	0.25	0.46	DG, Std
143	14.66	0.37	1.29	0.00	0.55	HG, Std
144	9.07	0.79	3.28	0.49	0.72	DG, Std, K2
145	17.10	0.27	1.54	0.27	0.46	DD
146	16.38	0.33	1.54	0.14	0.60	DG
147	16.33	0.87	2.56	0.38	0.06	HD
148	14.08	0.58	1.90	0.18	0.38	HD, Std
149	17.26	1.05	1.95	0.21	-0.56	
150	18.17	1.10	-	-	-	Std
151	15.91	0.51	1.83	0.16	0.49	HG
152	13.53	0.60	2.42	0.38	0.46	DG
153	15.39	0.96	2.82	0.27	0.36	HD
154	14.23	0.42	1.34	0.01	0.48	HG
155	17.29	0.53	2.04	0.41	0.16	DD
156	12.50	0.27	1.46	0.02	0.88	HG
157	18.19	0.53	1.22	0.39	-0.62	Std
158	17.52	0.51	1.65	0.24	0.15	HD
159	16.81	0.43	2.05	0.42	0.35	DD
160	12.66	0.35	1.58	0.26	0.36	DD
161	17.41	0.61	1.83	0.37	-0.13	HD
162	16.20	0.44	1.90	0.28	0.46	DD
163	16.67	0.65	2.50	0.57	0.06	DD
164	17.39	0.43	1.56	0.33	0.04	DD
165	14.67	0.53	1.37	-0.02	0.35	HD
166	16.71	0.37	1.73	0.24	0.51	DG
167	15.89	0.58	2.26	0.20	0.70	HG
168	10.84	0.30	1.41	0.14	0.53	DG, Std, F5
169	17.76	1.12	-	0.24	-	Std
170	11.43	0.33	1.43	0.02	0.73	HG, Std, G0
171	16.65	0.47	1.89	0.23	0.49	HG

Table XXVI. (Continued)

Star	y	(b-y)	(u-b)	m_1	c_1	Remarks
172	15.34	0.63	2.54	0.33	0.62	DG
173	17.21	0.82	2.07	0.28	-0.13	HD
174	13.40	0.37	1.62	0.28	0.32	DD
175	13.86	0.39	1.43	0.11	0.43	HG
176	15.68	0.49	1.56	0.02	0.54	HG
177	15.93	0.38	1.30	0.03	0.48	HG
178	16.63	0.39	1.42	0.06	0.52	HG
179	15.57	0.46	1.75	0.19	0.45	HG
180	11.79	0.65	2.41	0.31	0.49	DG, Std, G7
181	14.97	0.42	1.42	0.10	0.30	HG
182	15.97	0.45	1.76	0.18	0.50	HG
183	17.44	0.53	1.61	0.26	0.03	HD
184	16.51	0.91	2.49	0.44	-0.21	HD
185	15.93	0.41	1.60	0.17	0.44	HG
186	14.25	0.38	1.36	0.07	0.46	HG
187	16.27	0.46	2.01	0.28	0.53	DG
188	11.43	0.61	2.30	0.18	0.72	HG
189	14.79	0.55	2.33	0.39	0.45	DD, Std
190	17.53	0.31	1.33	0.32	0.07	DD
191	15.19	0.79	2.82	0.34	0.56	HG
192	13.75	0.74	2.98	0.39	0.72	DG
193	13.86	0.67	2.66	0.44	0.44	DD
194	17.33	0.63	1.99	0.40	-0.07	HD
195	17.30	0.47	1.98	0.44	0.16	DD
196	12.02	0.32	1.49	0.15	0.55	DG, G2
197	17.03	0.36	1.53	0.21	0.39	DD
198	15.51	0.47	1.68	0.18	0.38	HD
199	16.54	0.40	1.60	0.11	0.58	HG
200	16.41	1.08	2.44	0.28	-0.28	
201	15.03	0.43	1.70	0.20	0.44	DG
202	16.63	0.43	1.86	0.27	0.46	DG
203	16.81	0.91	2.50	0.37	-0.06	HD
204	15.77	0.55	2.07	0.21	0.55	HG
205	11.79	0.22	1.39	0.02	0.91	HG
206	12.80	0.33	1.49	0.26	0.31	DD
207	17.49	0.50	1.54	0.23	0.08	HD
208	15.42	0.44	1.64	0.09	0.58	HG
209	17.83	-	-	-	-	
210	16.45	0.43	1.94	0.27	0.54	DG
211	14.08	0.66	2.37	0.25	0.55	HG
212	17.34	0.50	1.68	0.32	0.04	HD
213	16.27	0.51	2.22	0.32	0.56	DG
214	14.01	0.55	1.71	0.07	0.47	HG

Table XXVI. (Continued)

Star	y	(b-y)	(u-b)	m_1	c_1	Remarks
215	16.53	0.44	1.80	0.21	0.50	HG
216	17.27	0.29	1.48	0.28	0.34	DD
217	15.41	0.42	1.40	0.04	0.48	HG
218	15.91	0.79	2.71	0.35	0.43	HD
219	15.23	0.45	1.42	0.06	0.40	HG
220	16.13	0.50	1.81	0.16	0.49	HG
221	17.01	0.70	2.20	0.51	-0.22	HD
222	16.98	0.42	1.82	0.37	0.24	DD
223	13.93	0.48	1.63	0.15	0.37	HG
224	15.17	0.42	1.63	0.14	0.51	DG
225	14.37	0.45	1.46	0.06	0.44	HG
226	17.12	0.47	1.77	0.33	0.17	DD
227	17.05	0.48	1.70	0.22	0.30	HD
228	16.78	0.40	1.27	-0.12	0.71	HG
229	16.80	0.89	2.41	0.33	-0.03	HD
230	15.23	0.56	1.88	0.13	0.50	HG
231	17.50	0.67	1.97	0.27	0.09	HD
232	11.65	0.34	1.46	0.06	0.66	HG
233	15.66	0.59	2.27	0.23	0.63	HG
234	15.50	0.43	1.46	0.11	0.38	HD
235	17.16	0.44	1.58	0.25	0.20	DD
236	15.08	0.46	1.50	0.13	0.32	HD
237	17.46	0.39	1.36	0.24	0.10	DD
238	16.23	0.36	1.51	0.10	0.59	HG
239	15.12	0.53	1.81	0.14	0.47	HG
240	14.19	0.45	1.35	-0.01	0.47	HG
241	14.39	0.34	1.28	0.05	0.50	HG
242	16.72	0.55	2.18	0.33	0.42	DG
243	16.95	0.41	1.51	0.07	0.55	HG
244	16.14	0.72	2.60	0.40	0.36	HD
245	16.54	0.37	1.56	0.13	0.56	HG
246	17.41	0.50	1.90	0.40	0.10	DD
247	17.15	0.62	2.12	2.45	-0.02	HD
248	16.08	0.48	1.84	0.24	0.40	HG
249	16.19	0.76	2.59	0.39	0.29	HD
250	16.75	0.36	1.61	0.20	0.49	DG
251	14.22	0.44	1.44	0.06	0.44	HG
252	17.25	0.51	1.61	0.28	0.03	HD
253	15.82	0.46	1.60	0.06	0.56	HG
254	15.31	0.52	1.97	0.15	0.63	HG
255	15.66	0.51	1.95	0.20	0.53	HG
256	16.39	0.29	1.48	0.25	0.40	DD
257	13.64	0.42	1.59	0.22	0.31	DD

Table XXVI. (Continued).

Star	y	(b-y)	(u-b)	m_1	c_1	Remarks
258	16.09	0.58	2.28	0.31	0.50	HG
259	17.02	0.56	2.05	0.38	0.17	HD
260	14.76	0.47	1.62	-0.14	0.96	HG
261	15.02	0.43	1.39	0.06	0.41	HG
262	17.03	0.39	1.58	0.22	0.36	DD
263	17.13	0.45	1.72	0.34	0.14	DD
264	17.35	0.61	2.10	0.53	-0.18	HD

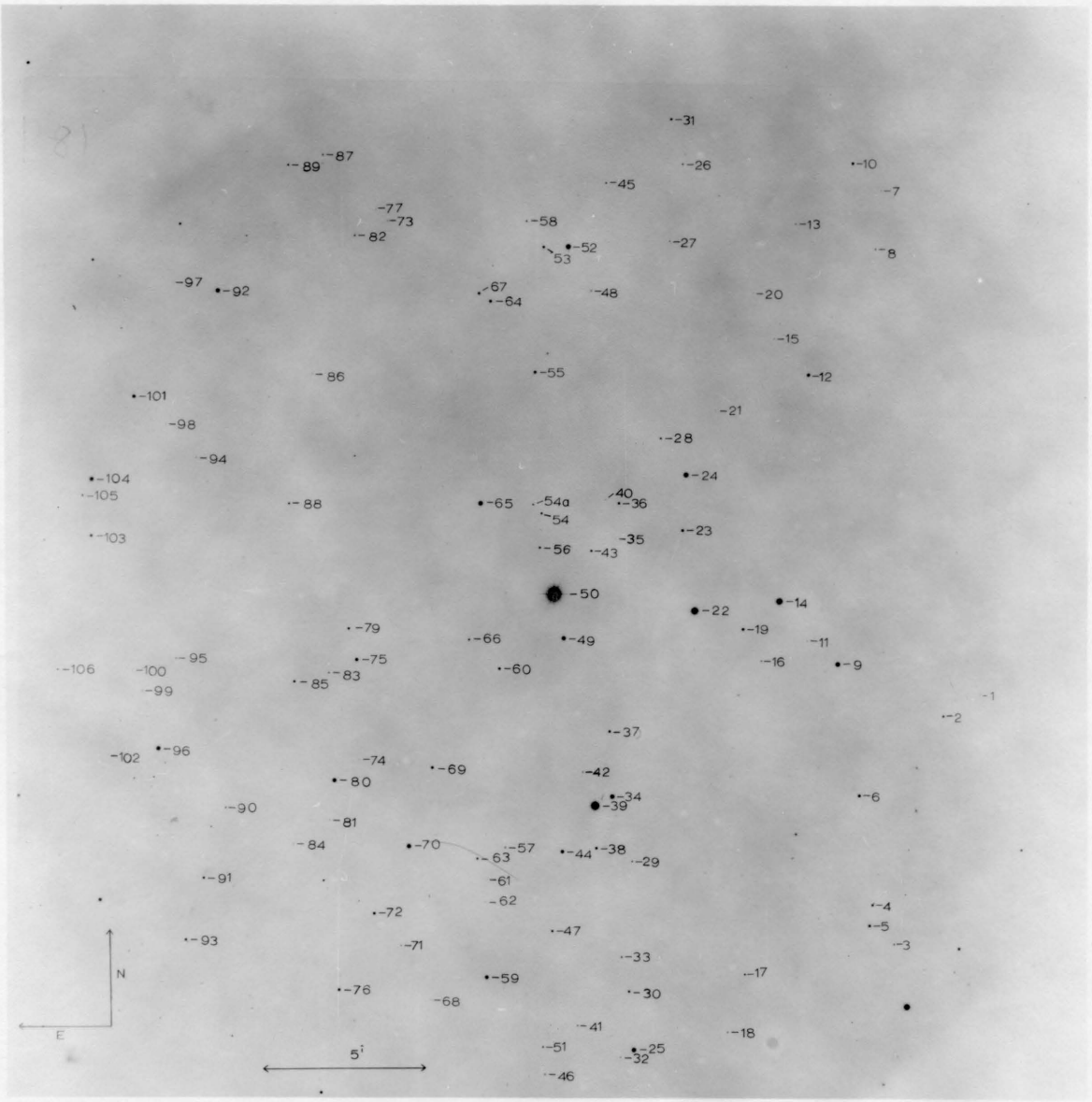

Figure 30. The finding chart for SA 56 ($\alpha = 12^h01^m$, $\delta = +29^o23'$).

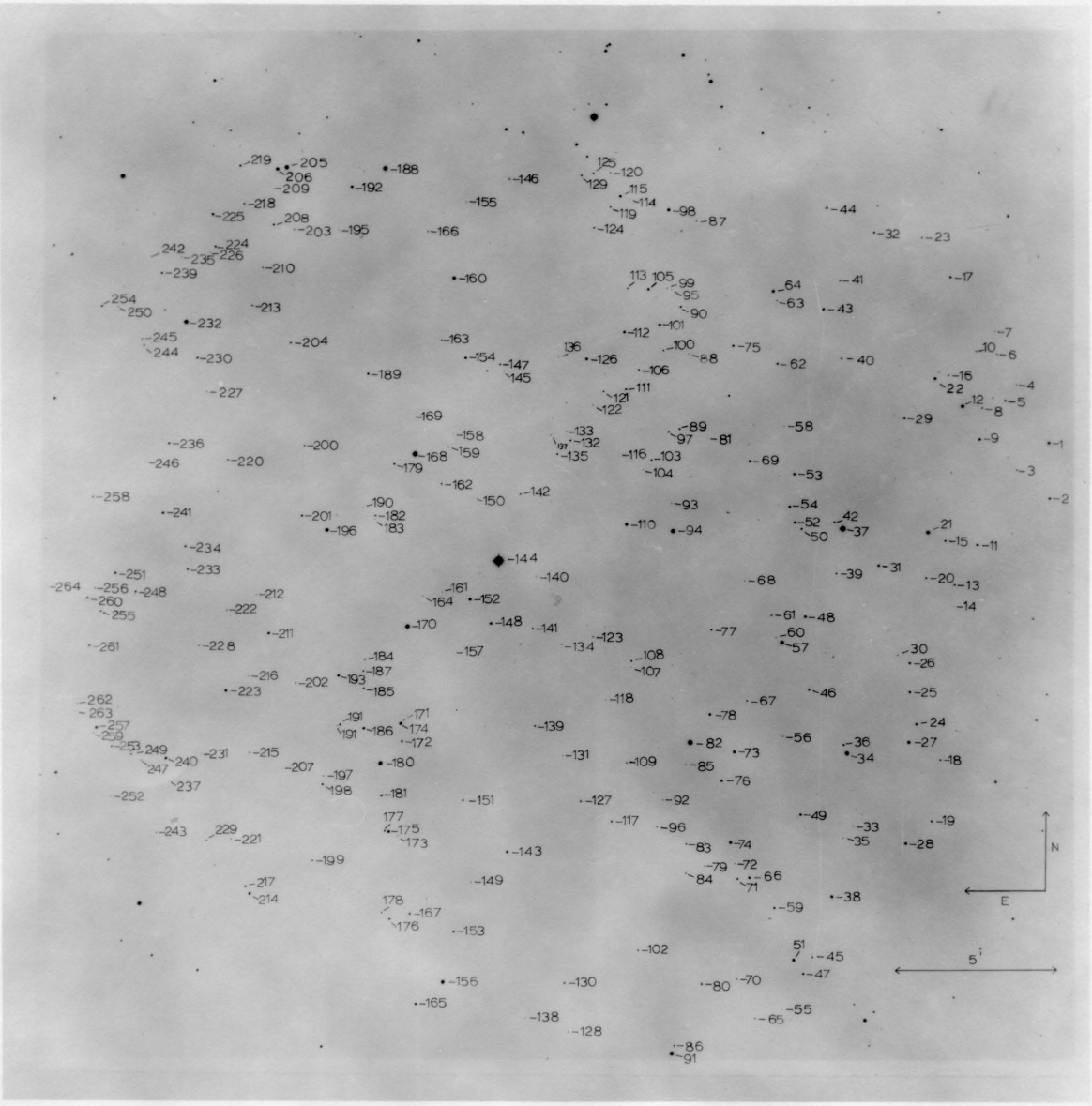

Figure 31. The finding chart for SA 27 ($\alpha = 7^h42^m$, $\delta = +44^o43'$).

REFERENCES

Arp, H. C. 1965, Stars and Stellar Systems, A. Blaauw and M. Schmidt Eds. (University of Chicago Press, Chicago), Vol. 5, Chapt. 19.

Becker, W. 1963, Stars and Stellar Systems, K. Aa. Strand Ed. (University of Chicago Press, Chicago), Vol. 3, Chapt. 13.

Becker, W. 1965, Z. Astrophys. 62, 54.

Becker, W. 1967, Z. Astrophys. 66, 404.

Bidelman, W. P. and Westerlund, B. E. 1960, Astron. J. 65, 483.

Blaauw, A. 1965, Stars and Stellar Systems, A. Blaauw and M. Schmidt Eds. (University of Chicago Press, Chicago), Vol. 5, Chapt. 20.

Blaauw, A. and Elvius, T. 1965, Stars and Stellar Systems, A. Blaauw and M. Schmidt Eds. (University of Chicago Press, Chicago), Vol. 5, Appendix.

Blaauw, A., Gum, C. S., Pawsey, J. L., and Westerhout, G. 1960, Mon. Not. Roy. Astr. Soc. 121, 123.

Blanco, V. M., Demers, S., Douglass, G. G. and FitzGerald, M. P. 1968, Publ. U.S. Nav. Obs. (Second Series), XXI.

Bok, B. J. 1970, Galactic Astronomy, H. Chiu and A. Muriel Eds. (Gordon and Breach, New York), Vol. 1.

Bok, B. J. and Basinski, J. 1964, Mem. Mt. Stromlo Obs. 4, 3.

Bok, B. J. and MacRae, D. A. 1941, Ann. New York Acad. Sci. 42, 219.

Bond, H. E. 1970, Unpublished Dissertation, University of Michigan.

Cayrel, R. 1968, Astrophys. J. 151, 997.

Crawford, D. L. and Barnes, J. V. 1969a, Astron. J. 74, 407.

Crawford, D. L. and Barnes, J. V. 1969b, Astron. J. 74, 818.

Crawford, D. L. and Barnes, J. V. 1969c, Astron. J. 74, 1008.

Crawford, D. L. and Barnes, J. V. 1970, Astron. J., In Press.

Crawford, D. L., Barnes, J. V. and Golson, J. C. 1970, Astron. J. 75, 624.

Crawford, D. L. and Perry, C. L. 1966, Astron. J. 71, 206.

Cuffey, J. 1956, Sky and Tel. 15, 258.

Eggen, O. J., Lynden-Bell, D., and Sandage, A. R. 1962, Astrophys. J. 136, 748.

Elvius, T. 1955, Stockholm Obs. Ann. 18, No. 7.

Elvius, T. 1964, Trans. IAU 12A, 549.

Elvius, T. 1965, Stars and Stellar Systems, A. Blaauw and M. Schmidt Eds. (University of Chicago Press, Chicago), Vol. 5, Chapt. 3.

Feige, J. 1958, Astrophys. J. 128, 267.

Fenkart, R. P. 1967, Z. Astrophys. 66, 390.

Fenkart, R. P. 1968, Z. Astrophys. 68, 87.

FitzGerald, M. P. 1968, Astron. J. 73, 983.

Gottlieb, D. M. and Upson, W. L., II. 1969, Astrophys. J. 157, 611.

Graham, J. A. 1966, Publ. Astr. Soc. Pac. 78, 433.

Haro, G. and Luyten, W. J. 1962, Bol. Obs. Ton. y Tac. No. 22, 37.

Hill, E. R. 1960, Bull. Ast. Inst. Neth. 15, 1.

Hoffleit, D. 1964, Catalogue of Bright Stars (Yale University Observatory, New Haven).

Hubble, E. P. 1934, Astrophys. J. 79, 8.

Humason, M. L. 1932, Astrophys. J. 76, 224.

Humason, M. L. and Zwicky, F. 1947, Astrophys. J. 105, 85.

Iriarte, B. and Chavira, E. 1957, Bol. Ton. y Tac. No. 16, 3.

Jeans, J. H. 1915, Mon. Not. Roy. Astr. Soc. 76, 70.

Johnson, H. L. and Harris, D. L. 1954, Astrophys. J. 120, 196.

Johnson, H. L., Mitchell, R. I., Iriarte, B., and Wisniewski, W. Z. 1966, Commun. Lunar and Planetary Laboratory No. 63.

Jones, D. H. P. 1962, Roy Obs. Bull. 52.

King, I. R. 1965, Astron. J. 70, 296.

Kinman, T. D. 1965, Astrophys. J. 142, 1241.

Kinman, T. D., Wirtanen, C. A., and Janes, K. A. 1966, Astrophys. J. Suppl. 13, 379.

Kodaira, K. 1964, Z. Astrophys. 59, 139.

Kodiara, K., Greenstein, J. L., and Oke, J. B. 1969, Astrophys. J. 155, 525.

Luyten, W. J. 1968, Mon. Not. Roy. Astr. Soc. 139, 221.

Luyten, W. J., Anderson, J. H., and Sandage, A. R. 1967, A Search for Faint Blue Stars (University of Minnesota Observatory, Minneapolis), Vol. 47.

McClure, R. D. and Racine, R. 1969, Astron. J. 74, 1000.

McNamara, D. H. and Langford, W. R. 1969. Publ. Astr. Soc. Pac. 81, 141.

Mihalas, D. and Routley, P. M. 1968, Galactic Astronomy (W. H. Freeman, San Francisco).

Nahon, F. 1957, Bull. Astr. 21, 55.

Oort, J. H. 1932, Bull. Astr. Inst. Neth. 6, 249.

Oort, J. H. 1938, Bull. Astr. Inst. Neth. 8, 233.

Oort, J. H. 1960, Bull. Astr. Inst. Neth. 15, 45.

Oort, J. H. 1965, Stars and Stellar Systems, A. Blaauw and M. Schmidt Eds. (University of Chicago Press, Chicago), Vol. 5, Chapt. 21.

Oort, J. H. and van Woerkom, A. J. J. 1941, Bull. Astr. Inst. Neth. 9, 185.

Parenago, P. P. 1952, Astron. Zh. 29, 245.

Parenago, P. P. 1958, Astron. Zh. 35, 182.

Perry, C. L. 1969a, Astron. J. 74, 139.

Perry, C. L. 1969b, Astron. J. 74, 705.

Peterson, B. A. 1970, Astron. J. 75, 695.

Philip, A. G. D. 1968, Astrophys. J. 152, 1107.

Philip, A. G. D. 1969a, Astron. J. 74, 209.

Philip, A. G. D. 1969b, Astron. J. 74, 812.

Philip, A. G. D. 1970, Astrophys. J. Lett. 160, L61.

Pickering, E. C., Kapteyn, J. C., and Rhijn, P. J. van 1918, Harvard Annals 101.

Plaut, L. 1966, Bull. Astr. Inst. Neth. Suppl. 1, 105.

Rhijn, P. J. van. 1936, Publ. Groningen No. 47.

Roman, N. G. 1955, Astrophys. J. Suppl. 2, 195.

Sandage, A. R. 1957, Astrophys. J. 125, 422.

Sandage, A. R. 1962, Astrophys. J. 135, 333.

Sandage, A. R. and Luyten, W. J. 1969, Astrophys. J. 155, 913.

Schmidt, M. 1956, Bull. Astr. Inst. Neth. 13, 15.

Schmidt-Kaler, Th. 1965, Astronomy and Astrophysics, H. Voigt Ed. (Springer-Verlag, Berlin).

Schwassman, A. and Rhijn, P. J. van. 1935, Bergedorfer Spektral-Durchmusterung der 115 nordlichen Kapteynschen Eichfelder (Hamburger Sternwarte, Bergedorf).

Seares, F. H., Kapteyn, J. C., and Rhijn, P. J. van. 1930, Carnegie Inst. Publ. No. 402.

Slettebak, A. and Stock, J. 1959, Astron. Abh. Hamburg No. 5.

Slettebak, A., Bahner, K., and Stock, J. 1961, Astrophys. J. 134, 195.

Slettebak, A., Wright, R. R., and Graham, J. A. 1968, Astron. J. 73, 152.

Strömgren, B. 1963a, Stars and Stellar Systems, K. Strand Ed. (University of Chicago Press, Chicago), Vol. 3, Chapt. 9.

Strömgren, B. 1963b, Quart. J. Roy. Astr. Soc. 4, 8.

Strömgren, B. 1964, Astrophys. Norweg. 9, 333.

Strömgren, B. 1966, Ann. Rev. Astron. and Astrophys. L. Goldberg Ed. (Annual Reviews Inc., Palo Alto), Vol. 4, 433.

Stothers, R. and Tech, J. L. 1963, Mon. Not. Roy. Astr. Soc. 137, 287.

Tifft, W. G., Fannin, B. B., Hanzi, R. A., and Bowers, V. A. 1969, Space Astronomy at the Steward Observatory, Technical Report No. T69-14.

Turon-Lacarrieu, C. 1968, Unpublished Doctoral Thesis, University of Paris.

Upgren, A. R., Jr. 1963, Astron. J. 68, 475.

Urassin, I. 1969, Izv. Astr. Obs. V. P. Engel'gardta No. 37.

Wallerstein, G. and Carlson, M. 1960, Astrophys. J. 132, 276.

Wallerstein, G. and Hunziker, W. 1964, Astrophys. J. 140, 214.

Weidemann, V. 1967, Z. Astrophys. 67, 286.

Westerlund, B. E. 1963, Mon. Not. Roy. Astr. Soc. 127, 83.

White, R. E. 1967, Unpublished Dissertation, University of Illinois.

Woolley, R. 1957, Mon. Not. Roy. Astr. Soc. 117, 198.

Woolley, R. and Stewart, J. M. 1967, Mon. Not. Roy. Astr. Soc. 136, 329.

Wurm, K. 1963, Air Force Cambridge Research Laboratory-63-679, Technical Report No. 2.

Yasuda, H. 1961, Ann. Tokyo Astr. Obs. 7, 47.